INFORMATION TO USERS

This manuscript has been reproduced from the microfilm master. UMI films the text directly from the original or copy submitted. Thus, some thesis and dissertation copies are in typewriter face, while others may be from any type of computer printer.

The quality of this reproduction is dependent upon the quality of the copy submitted. Broken or indistinct print, colored or poor quality illustrations and photographs, print bleedthrough, substandard margins, and improper alignment can adversely affect reproduction.

In the unlikely event that the author did not send UMI a complete manuscript and there are missing pages, these will be noted. Also, if unauthorized copyright material had to be removed, a note will indicate the deletion.

Oversize materials (e.g., maps, drawings, charts) are reproduced by sectioning the original, beginning at the upper left-hand corner and continuing from left to right in equal sections with small overlaps. Each original is also photographed in one exposure and is included in reduced form at the back of the book.

Photographs included in the original manuscript have been reproduced xerographically in this copy. Higher quality 6" x 9" black and white photographic prints are available for any photographs or illustrations appearing in this copy for an additional charge. Contact UMI directly to order.

UMI

A Bell & Howell Information Company
300 North Zeeb Road, Ann Arbor MI 48106-1346 USA
313/761-4700 800/521-0600

Université d'Ottawa · University of Ottawa

Abstract

Chain reaction mechanisms have been the focus of this thesis. Two systems, dehydrobromination of ring-substituted α-bromoacetophenones in alcohols and 1,5-hydrogen atom transfer reactions involved with *o*-bromo-*p*-methoxy ethers, have been studied using different approaches.

Ring substituted α-bromoacetophenones react with alcohols in a chain reaction leading to the corresponding acetophenone, HBr, and the carbonyl compound from oxidation of the alcohol. Two different mechanisms, involving hydrogen or electron transfer by ketyl radicals, have been proposed in order to accommodate the unusual selectivities of these reactions. By studying the efficiency of isotope incorporation from deuterated alcohols, it has been possible to determine the relative contributions from both mechanisms. For example, electron transfer dominates in the case of 2-propanol, while hydrogen transfer is most important for methanol. The results demonstrate that ring substitution in the starting ketone is not a main contributing factor in the discrimination between the two mechanisms. The only parameter that seems to be playing a major role is the nature (reducing strength) of the alcohol-derived ketyl radicals.

Intramolecular hydrogen transfer reactions (radical translocations) have been receiving considerable attention recently in synthetic applications since they offer a fast and selective alternative for carbon-carbon bond-forming reactions. This approach has taken a new turn with the advent of protecting groups serving as initial radical precursors and where, via translocation, an unactivated carbon-hydrogen bond indirectly serves as a second radical precursor in standard radical procedures such as the tin hydride method. However, this radical translocation strategy has been limited in its applicability by the lack of reported information regarding kinetics and selectivity of intramolecular hydrogen transfer reactions from carbon-

hydrogen bonds to reactive carbon radicals. A mechanistic study involving 1,5-hydrogen atom transfer for a newly introduced protecting/radical translocating group is described. The absolute rate constant for the radical translocation (1,5-hydrogen atom transfer) following halogen abstraction of 2-bromo-4-methoxy-1-(2-phenylethoxy) benzene (**27**) by $Et_3Si^{\bullet}$ radicals has been examined using laser flash photolysis techniques. The protocol was first to generate aryl radicals from halogen abstraction by $Et_3Si^{\bullet}$ radicals which were subsequently translocated to a new carbon center by a 1,5-hydrogen atom transfer process. The rate constant measured at 300 K with the help of concentration dependence studies is $1.1 \times 10^7\ s^{-1}$. The absolute rate constant for the dehalogenation reaction of $Et_3Si^{\bullet}$ radicals with 2-bromo-4-methoxy-1-(2-phenylethoxy) benzene (**27**) and 1-bromo-2,5-dimethoxy benzene (**31**) has also been investigated using laser flash photolysis techniques. The rate constants at 300 K are $2.4 \times 10^8\ M^{-1}\ s^{-1}$ and $4.6 \times 10^8\ M^{-1}\ s^{-1}$, respectively.

Acknowledgments

First and foremost, I would very much like to thank Dr. J. C. (Tito) Scaiano, my research supervisor, for all his support, guidance and encouragement over these last few years. Not only was he a superb supervisor filled with precious comments and insights but he was also a mentor. His patience, advice and understanding were greatly appreciated and his professional help will always be remembered.

I would like to thank all my fellow colleagues in Dr. Scaiano's lab and in the chemistry department whom I had the pleasure of working with during my time at the University of Ottawa. In particular, I would like to thank Dr. David Avila, Dean Weldon, Nadareh Mohtat, Sonia Corrent, Claudette Pliva, Serge Meunier and Denis Carrière for their friendship, assistance, helpful discussions and memorable moments. Many thanks to Dr. Monica Barra for her help regarding chain reaction mechanisms. I would also like to thank Dr. Terry Connolly for his advice relating to synthesis, for his help in analyzing NMR spectra and simplifying them for me and for letting me use some of his NMR time. Thanks also to Sarah Monahan whom I had the opportunity to supervise during "the summer of 1995". Thanks to André Simard for helping me out with the laser system in moments of despair and for keeping it operational. And finally, special thanks also go to a dear friend and a fantastic individual that I had the privilege of collaborating with, Dr. Alain Berinstain. My experience at Ottawa U. would not have been the same without him.

I would like to thank Raj Capoor for the NMR analysis and Dr. Clem Kazakoff for his prompt mass spectral services. I would also like to thank Lise Maisonneuve for helping me out with all the red tape involved with graduate studies.

Thanks are also due to Dr. A Houmam and Dr. D.D.M. Wayner for their expertise and assistance regarding the cyclic voltammetry measurements.

I would also like to thank the National Sciences and Engineering Research Council (NSERC), the Canadian Networks of Centres of Excellence, DuPont and the University of Ottawa for their financial support during my Master's studies.

Finally, I would like to acknowledge my family for their encouragement throughout my studies, especially my mother, Claudette, for her unconditional love and support. She is one of my many mentors that I will always look up to. It is to her that I dedicate this thesis.

Table of Contents

Chapter 1

Chapter 2

Chapter 1

Chapter 2

List of Tables

Chapter 1

Ac	acetyl
CH_3CN	acetonitrile
AIBN	2,2'-azo-bis-isobutyronitrile
calcd	calculated
c-C_6H_6	cyclohexane
CTMP	chemithermomechanical pulp
δ	chemical shift in parts per million downfield
d	doublet (NMR)
DEAD	diethyl azodicarboxylate
ΔOD	change in optical density
EI	electron impact (in mass spectrometry)
eq.	equivalent(s)
ESR	electron spin resonance
%et	percentage of electron transfer
eV	electron volt
FID	flame ionization detection
GC	gas chromatography
GC-MS	gas chromatography-mass spectrometry
GPIB	general purpose interface bus
%Ht	percentage of hydrogen transfer
HRMS	high resolution mass spectrum
Hz	hertz
J	coupling constant (given in Hertz)
k	rate constant
LFP	laser flash photolysis
m	multiplet (NMR)
M	moles per liter
M_{150}	molecular ion peak of 150
M_{151}	molecular ion peak of 151

MHz	megahertz
mp	melting point
MS	mass spectrometry
m/z	mass to charge ratio
NMR	nuclear magnetic resonance
ppm	parts per million
PRT	protecting radical translocating
s	singlet (NMR); second(s)
SCE	saturated calomel electrode
t	triplet (NMR)
TBAP	tetrabutylammonium perchlorate
TBS	*tert*-butyldimethylsilyl
THF	tetrahydrofuran
%TIC	percentage of total ion count (GC-MS)
TLC	thin layer chromatography
TMP	thermomechanical pulp
TMS	trimethylsilane
TS	transition state
V	volt(s)
UV	ultraviolet
YAG	yttrium:aluminium:germanium

1. Hydrogen vs. Electron Transfer Mechanisms in the Chain Decomposition of Phenacyl Bromides

1.1. Introduction

1.1.1. Pulp and Paper Background

Production of thermomechanical pulp (TMP) and chemithermomechanical pulp (CTMP), two types of high-yield mechanical pulps, has more than tripled in Canada in the last decade.[1] These processes consist of mechanical defribrification of wood chips at high temperatures and require little or no chemical treatment, making them popular choices from an environmental point of view. In the case of CTMP, there is only a single chemical treatment using Na_2SO_3 that precedes the thermal step. However, photoinduced yellowing of paper manufactured from ultra-high yield pulps limits their use to low-grade paper products, such as newsprint, catalog and advertising products. They can be further bleached chemically and be used in higher quality papers but their aging (yellowing) process still creates a limitation to the application of these lignin-rich papers.

Woody plants are made of strong, relatively thick-walled long cells that make good fibers. The cell wall in these types of plants are complex mixtures of natural polymers that varies in composition. However it can roughly be divided into 70% polysaccharides (cellulose and hemicellulose) and 28% lignin; which has been described as being the "adhesive material of wood" because it cements the fibers together for strength.

Fifty years of "yellowing research" were necessary in order to come to the conclusion that it was the photooxidation of ill-defined lignin chromophores,

absorbing near-UV light (300-400 nm), that is responsible for the aging of mechanical pulps.

There are presently two main types of bleached pulps available: chemical and high-yield pulps.

Chemical pulps are obtained by delignification of wood following chemical treatments, either in an acidic (bisulfite treatment: HSO_3^-/H_2SO_3) or a basic ("Kraft" treatment: $NaOH/Na_2S$) medium. The manufacturing process is then followed by a multistep bleaching process yielding pulps which are almost "lignin-free". These pulps have the distinct advantages of being strong, having a high brightness level and being relatively stable to UV irradiation. However, they have the major drawbacks of being produced only with ~50% efficiency and generating environmentally hazardous materials during fabrication.

High-yield pulps are made from mechanical defribrification of woods chips. They therefore still contain all the initial components of wood, including lignin. They are bleached by either oxidation (peroxide/OH^-) or reduction ($Na_2S_2O_4$) of lignin chromophores. Their advantages include high-yield of production from wood (yield > 90%) and since few chemical treatments are needed during fabrication, they generate less pollution. Disadvantages are their weaker mechanical resistance and lower brightness levels but more importantly, they are relatively unstable to sunlight.

The yellowing process results largely from photoinduced reactions involving the chromophores in lignin; among these, mono- and dimethoxyphenols, methoxyacetophenones, and aryloxyanisoles are believed to play an important role.[2] The absorption of light leads to various unstable intermediates, such as aromatic ketone singlets and triplets, phenoxyl, phenacyl, and peroxyl radicals, and presumably singlet oxygen. Ultimately,

yellow products such as quinones, oligomers and other degradation products are formed.[2] A variety of radical mechanisms are believed to play a role in the photodegradation of lignin. These include the direct photodecomposition of phenols to yield phenoxyl radicals, the abstraction of phenolic hydrogens to yield also phenoxyl radicals, the cleavage of excited states of substituted α-phenoxyacetophenones to produce phenacyl and phenoxyl radicals, and the cleavage of aromatic ketyl radicals.[2-4]

The ever increasing demand for paper products combined with the depletion of forest reserves have urged the paper industry to try to find a cure in order to prevent the aging of paper. Such improvements would therefore increase the usefulness of high-yield pulps and having an eventual goal of replacing chemical pulps. Since it is the photostability that is the major concern in using mechanical pulps, countless efforts are made in order to understand the chemical and photochemical behavior of lignin-containing papers. The knowledge of the kinetics and mechanisms of the reactions of unstable intermediates should advance our understanding of lignin photochemistry in general and lead to rational strategies to inhibit the photoyellowing of paper.

The complexity of lignin (Figure 1.1) is such that studies on native lignin are difficult and their interpretation is frequently inconclusive. Several research groups have employed "designer" model compounds in their studies. These molecules tend to include some of the key features of lignin, and therefore, their behavior can be taken to represent a modest fraction of the reactions that may occur in native lignin. Among these model compounds, α-guaiacoxyacetoveratrone (**1**) has been the subject of numerous studies (Figure 1.2).[3, 5-10]

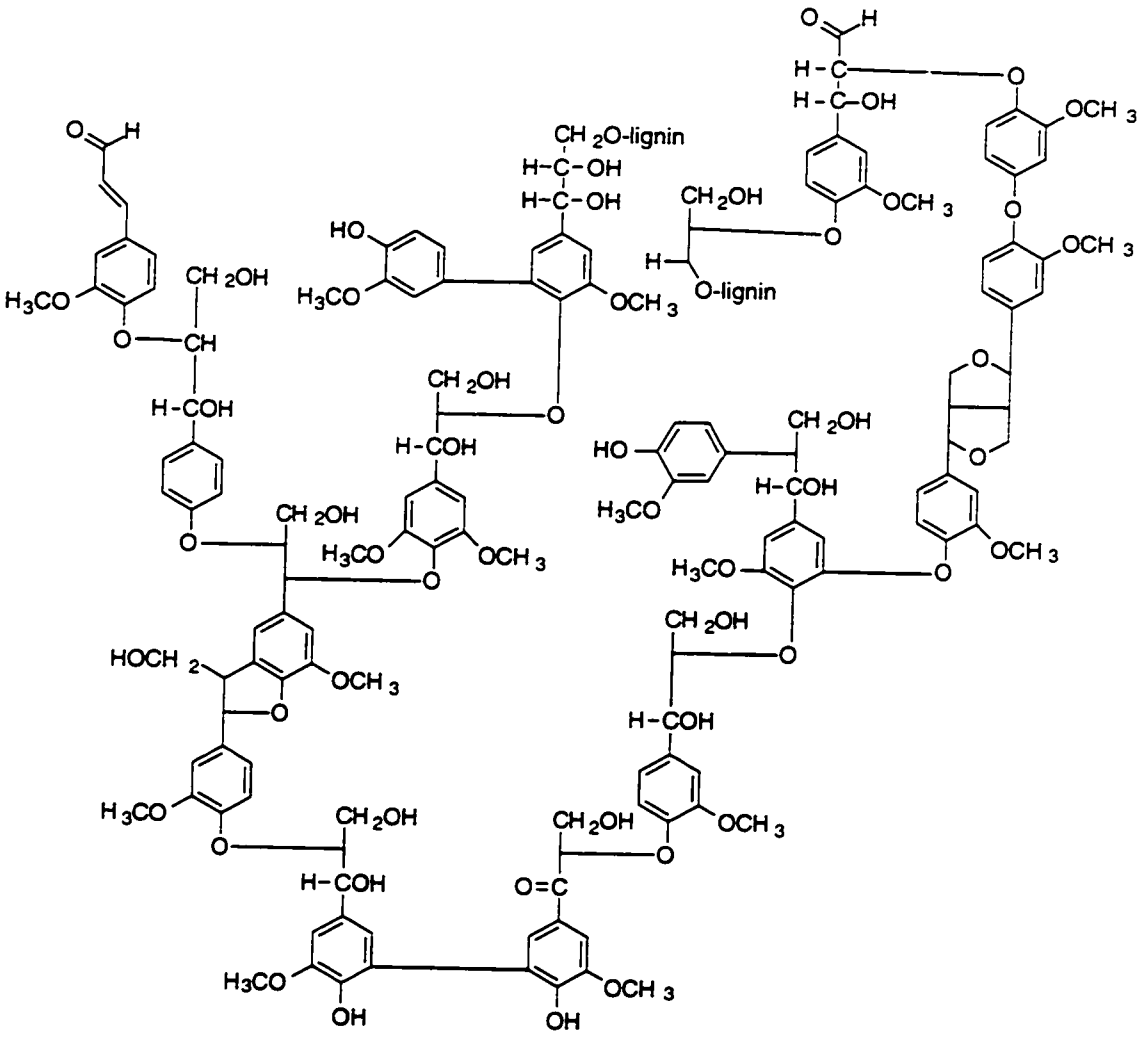

Figure 1.1 A proposed structure for lignin.[11]

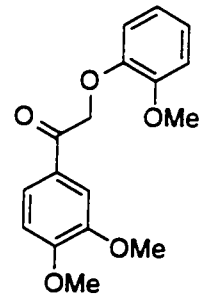

1

Figure 1.2 Chemical structure of α-guaiacoxyacetoveratrone (**1**).

Of the various radicals mentioned above, phenacyl radicals are probably the least understood; yet, they may be very important species in the chain of events leading to the oxidative degradation of lignin. In pulp, phenacyl radicals are probably produced by photoinduced cleavage of β-ether bonds in a process resembling the mechanism of decomposition of **1**, Equation 1.[12]

Equation 1.

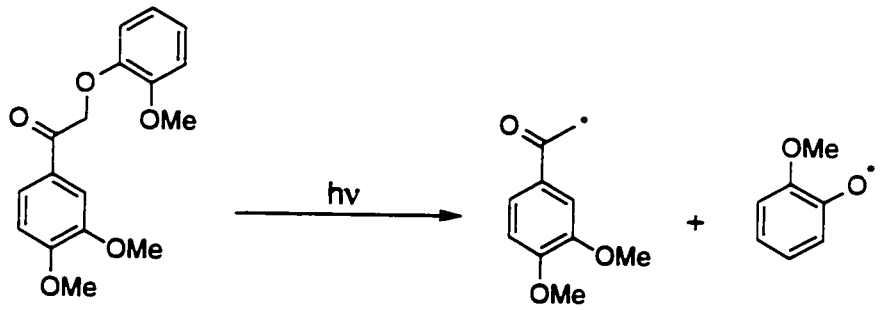

1 **2** **3**

1.1.2. Previous Studies Conducted with Ring-Substituted α-Bromoacetophenones

In order to study the behavior of the phenacyl radical (**2**) without the spectral and chemical interferences of the phenoxyl radical (**3**), ring-substituted derivatives of α-bromoacetophenones (**4**) can be used as phenacyl precursors, where the primary photoprocess involves cleavage of the α-C-Br bond to yield the phenacyl radical (**5**) and a bromine atom, Equation 2.[13-15]

Equation 2.

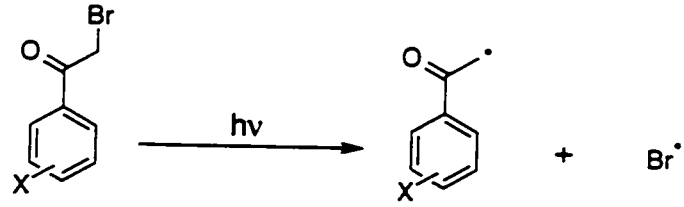

4 **5**

These radicals are readily detectable because they have a characteristic absorption band in the 500 nm region.[16] Bromine atoms, the other intermediates produced in this photoreaction, are invisible in laser photolysis experiments, but their presence can be confirmed by adding complexing reagents such as benzene or bromide ions.[17, 18]

While the phenacyl radical (**5**) has been written as a carbon-centered species, it can also be written in its canonical form, as an oxygen-centered radical (**6**) (Figure 1.3).

5 6

Figure 1.3 Canonical structures of phenacyl radical (5).

Recent work has suggested that the "oxy" form of this radical may account for its absorption properties,[19] which are reminiscent of those recently reported for cumyloxyl radicals.[20, 21] While *p*-methoxyphenacyl radical may have a spin density as a high as 0.3 at the carbonyl oxygen, its reactivity is dominated by the radical character at the carbon site.[13]

Product studies on the addition of phenacyl radicals to olefins show that these reactions lead to C-C bond formation, thus showing carbon-centered radical behavior.[22, 23] Methoxyphenacyl radicals have modest reactivity, for example, the addition of the *p*–methoxyphenacyl radical to the highly reactive double bond in 1,1-diphenylethylene occurs with a rate constant of 9.4×10^7 $M^{-1}s^{-1}$.[13] In addition, they are also modest hydrogen abstractors, an example showing their low reactivity towards hydrogen abstraction is observed in various alcohol solvents and acetonitrile as solvents. Typical half-lives for the *p*-methoxyphenacyl radical in solvents such as methanol, ethanol, 2-propanol, and acetonitrile are in the neighborhood of 10 μs.[13]

Although these carbon centered radicals seem to be rather unreactive, our work with α-bromoacetophenones shows that steady-state irradiation in alcohol solvents leads to remarkably rapid consumption of the starting material with concomitant formation of the corresponding acetophenone. Typically, irradiation times for significant conversions are 20-50 times shorter

in alcohols as compared to acetonitrile, thus suggesting the involvement of a chain reaction mechanism.[15]

It should be noted that other bromo compounds are known to be able to carry similar chains. Chain lengths greater than 10 at temperatures between 30 and 60 °C, have been measured for systems studying the radical chain reaction of primary and secondary α-bromo esters by 2-propanol and 2-methyldioxolane.[24] Also, using vicinal dibromides as starting materials, one can generate two bromine atoms per chain propagation step.[25]

The purpose of this research is to report an exploratory study of the chain reaction mechanisms for the dehydrobromination of ring-substituted α-bromoacetophenones in alcohols. Ketones **7-11** (Figure 1.4) are the subject of this work.

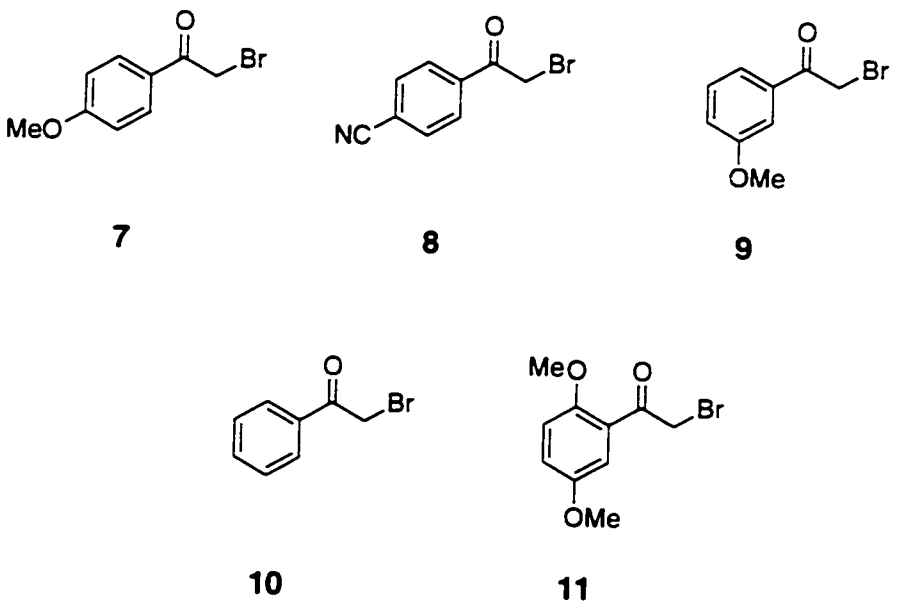

Figure 1.4 Structures of the α-bromoacetophenones studied during this work.

1.2. Results and Discussion

1.2.1. Chain Length Studies

Ketones **7-11** undergo decomposition readily upon broadband irradiation centered at 350 nm. The irradiation times required for significant conversion to take place are 20-50 times shorter in alcohols, as compared with non-hydrogen donating solvents, such as acetonitrile. For example, in the case of **7** the relative yields of *p*-methoxyacetophenone (**12**) in various solvents are 1:4:97 for cyclohexane, methanol and 2-propanol. Taking the quantum yield for the primary photocleavage of the C-Br bond in cyclohexane as 0.35,[14] then the overall quantum yields are 1.4 and 34 for methanol and 2-propanol, respectively, showing a long chain in 2-propanol and a short one in methanol. Figure 1.5 shows the results obtained when compound **7** is irradiated with six UV lamps centered at 350 nm using *n*-dodecane as an internal standard.

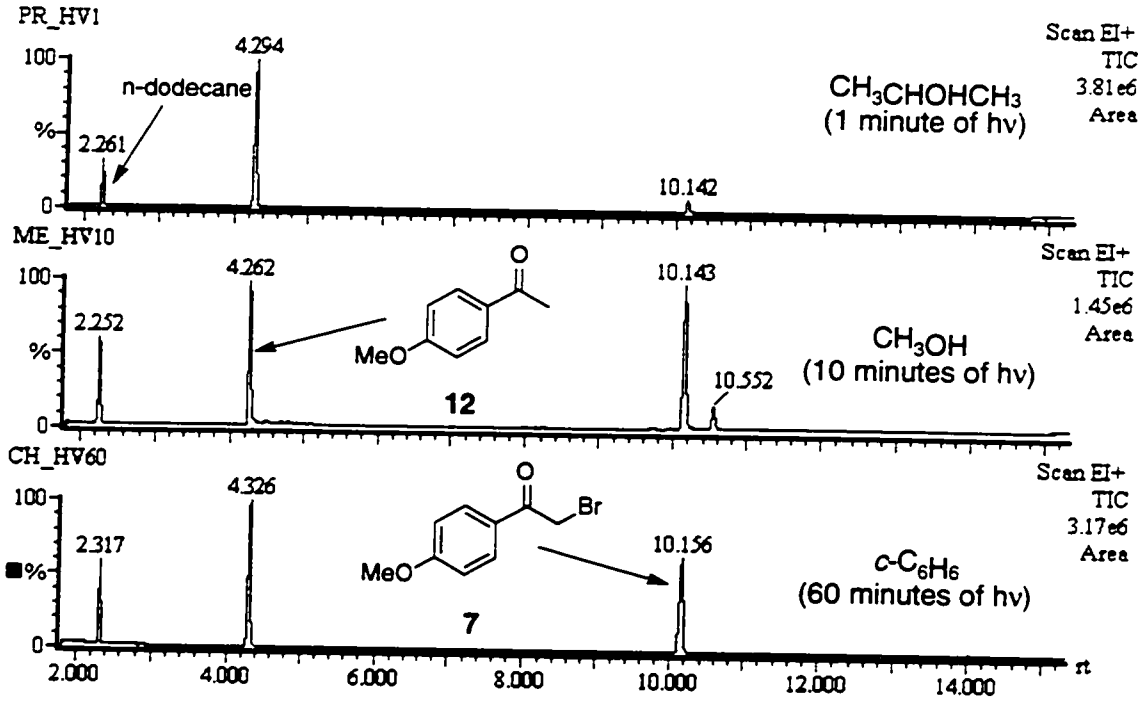

Figure 1.5 GC-MS traces showing the results obtained during irradiation of compound **7** in various deoxygenated solvents with *n*-dodecane as an internal standard using six RPR-3500 lamps.

To achieve a better understanding of the chain lengths involved in these systems, valerophenone (**13**) in benzene was chosen as an actinometer,[26] since it gave the same photoproduct, acetophenone (**14**), as our compound **10** in the alcohol systems of interest. Figure 1.6 summarizes the approach employed in the chain length experiments for both the reference system and compound **10**. Figure 1.7 shows the results obtained in three alcohol solvents using six UV lamps centered at 350 nm.

α-Bromoacetophenone (**10**)

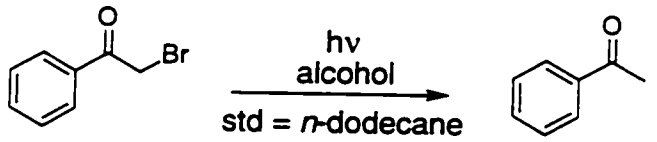

10 **14**

Valerophenone (**13**)

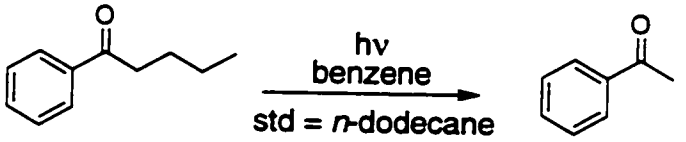

13 chain length = 1 Φ = 0.30 **14**

Figure 1.6 Chain length experiment approach for valerophenone (**13**) as an actinometer in deoxygenated benzene and for compound **10** in deoxygenated alcohols with *n*-dodecane as an internal standard using six RPR-3500 lamps.

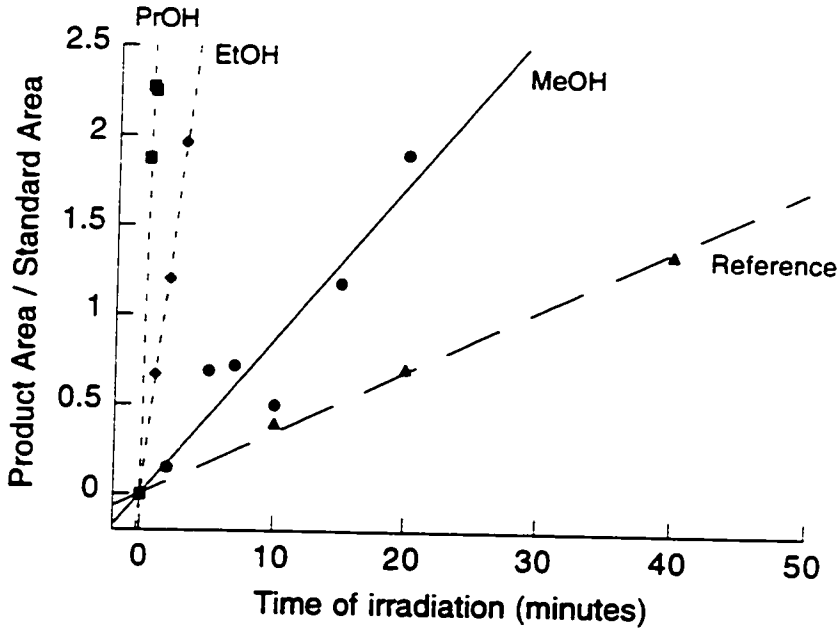

Figure 1.7 Acetophenone (**14**) yield ratios as a function of time of irradiation for valerophenone (100 mM) in deoxygenated benzene as a reference and for compound **10** (25 mM) in deoxygenated methanol, ethanol, 2-propanol irradiated using six RPR-3500 lamps.

When comparing slopes for any given experiment with that for valerophenone (**13**) one obtains relative chain lengths of 2.5 and 19 for methanol and ethanol respectively, and a lower limit of ≥ 116 for 2-propanol. In 2-propanol, the conversion was so high that very short irradiation times had to be employed in order to minimize any interference from the photoproducts; exposure times were of the order of seconds as opposed to minutes for the other two solvents. Depletion of the starting material led to non-linear production of acetophenone even after 30 seconds (Figure 1.8). Taking into consideration the quantum yield of acetophenone formation of 0.30 for 100 mM valerophenone in benzene,[26] values of 0.75, 5.7 and a lower limit of ≥ 35 were obtained as overall quantum yields of product formation.

Again, short (or non-existent) chain lengths in methanol and increasing chain lengths for ethanol and 2-propanol were shown.

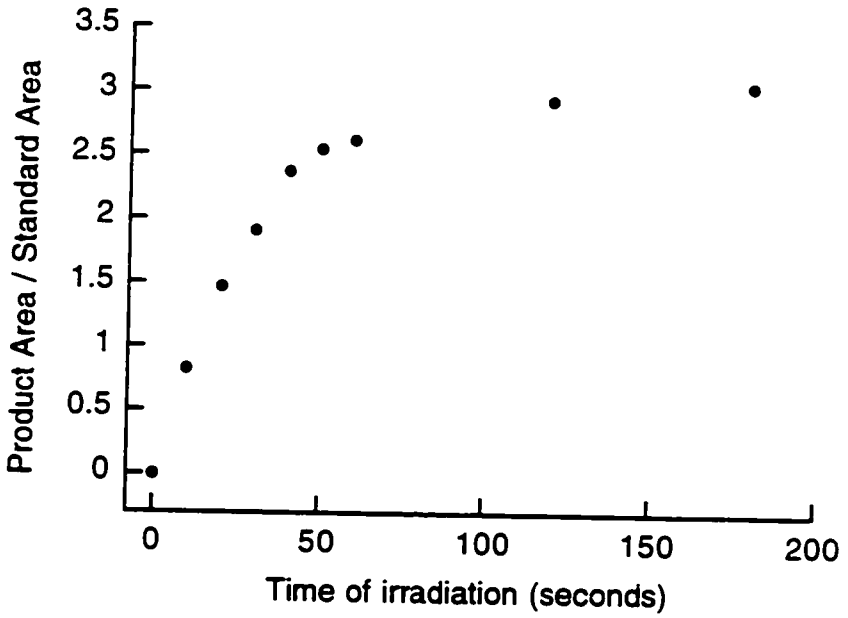

Figure 1.8 Acetophenone (**14**) yield ratios as a function of time of irradiation for compound **10** in deoxygenated 2-propanol irradiated with two RPR-3500 lamps.

In a chain reaction mechanism involving photochemical initiation, the chain length is inversionally proportional to the square root of the light absorbed, i.e.,

$$\text{Rate}_p \propto (\text{Rate}_i / k_t)^{1/2} \bullet k_p \bullet (\text{conc. term})$$

where the "concentration term" will usually contain one of the reactants. Rate_i is the rate of initiation. The chain length, λ, is given by:

$$\lambda = (\text{Rate}_p / \text{Rate}_i) = k_p / (\text{Rate}_i \bullet k_t)^{1/2} \bullet (\text{conc. term})$$

For a reaction initiated photochemically, the rate of initiation will be directly proportional to the light intensity absorbed (I_a) by the photoinitiator,

$$\text{Rate}_i \propto I_a$$

thus,

$$\lambda \propto 1 / I_a^{1/2}$$

In a first, rather rough, approximation, I_a is proportional to the number of lamps used in the photoreactor, leading to:

$$\lambda \propto 1 / (\#\,\text{lamps})^{1/2}$$

To verify this mathematical relationship, the number of lamps was varied in a series of experiments. Table 1.1 shows the results obtained in methanol and 2-propanol. These results are in agreement with the mathematical relationship derived above, and therefore the chain length increased when fewer lamps were used in the photoreactor. Table 1.1 also includes results obtained in ethanol using six UV lamps centered at 350 nm.

Table 1.1 Chain lengths of compound **10** in various alcohol solvents.

Solvent	UV lamps	Slope ratio	Chain length
MeOH	1	5.3	1.6
i-PrOH	2	263	79
MeOH	6	2.5	0.75
EtOH	6	19	5.7
i-PrOH	6	> 116	> 35

1.2.2. Complexation with Bromide Studies

The bromine atoms produced in the cleavage of the C-Br bond, as shown in Equation 2, abstract hydrogen readily from alcohols and can initiate chain reactions by two distinct mechanisms.[24] Scheme 1.1 and Scheme 1.2 illustrate the mechanisms in the case of methanol.

Scheme 1.1 Bromine atom mechanism (hydrogen transfer).

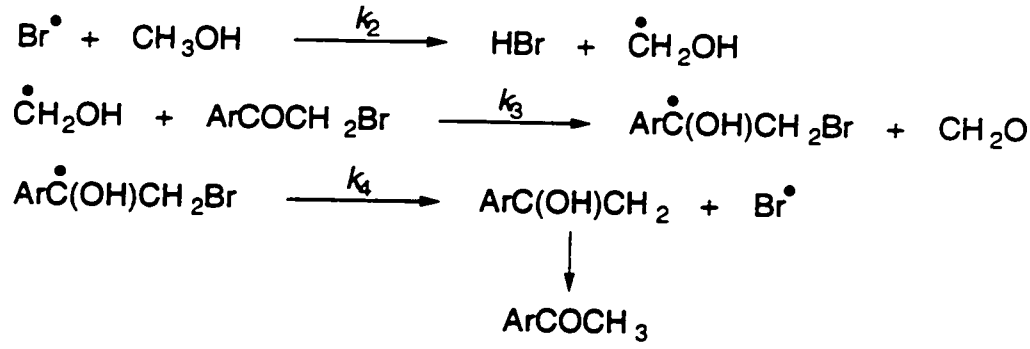

Scheme 1.2 Phenacyl radical mechanism (electron transfer).

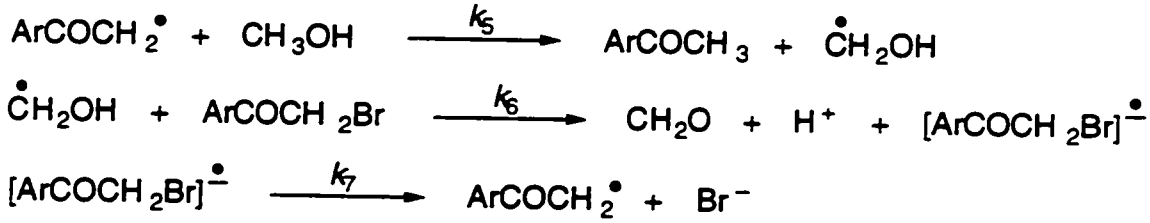

Since both mechanisms involve the intermediacy of a common radical ($^{\bullet}CH_2OH$), they cannot function as independent chains and we presume one of them will normally dominate. The final products from both reactions should be the same. Scheme 1.2 represents an electron transfer mechanism which we anticipated to be favored in the case of electron deficient molecules, such as 8. At low conversions, the reactions are quite clean, giving only the expected products. We noted however, that upon prolonged, high conversion conditions, a characteristic, heavier product was systematically

formed. Figure 1.9 shows the results obtained for the case of compound **8** in a (acetonitrile/1 M methanol) solvent mixture. In the case of **8**, this product has been characterized as the acetal **15**, on the basis of its mass spectral and NMR characteristics (Figure 1.10).

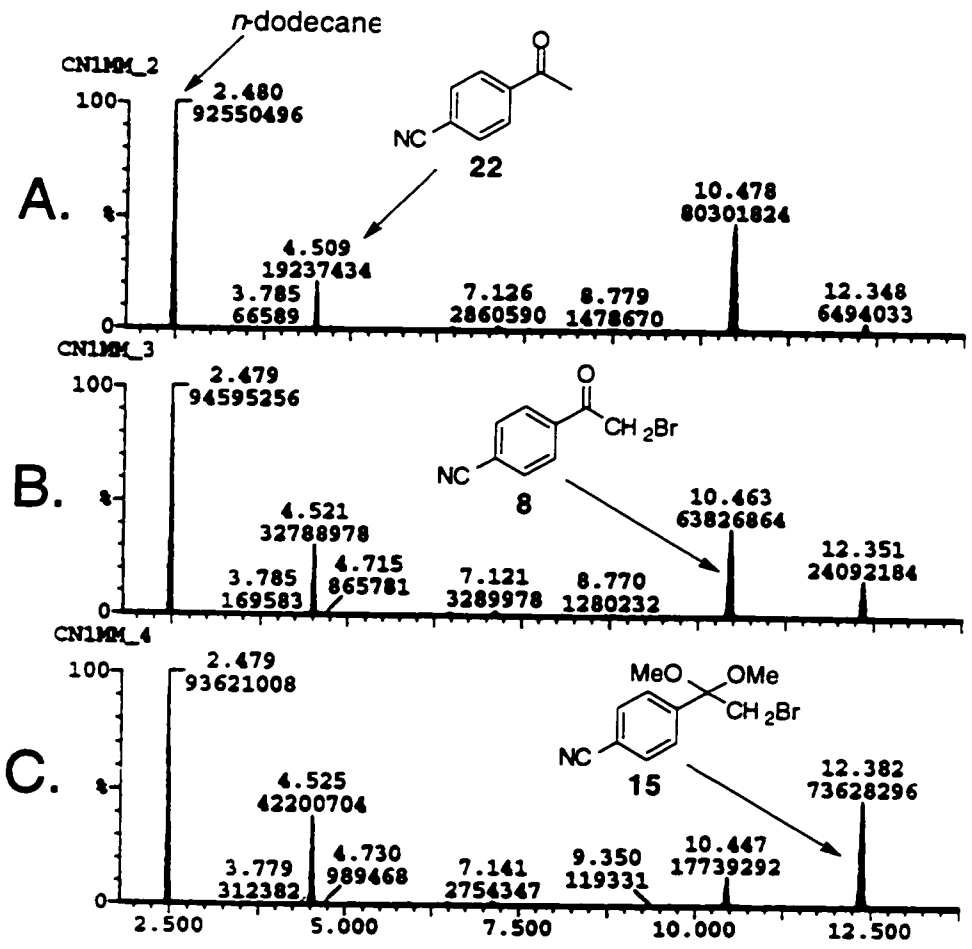

Figure 1.9 GC-MS traces showing the results obtained during prolonged irradiation times of compound **8** in a deoxygenated (acetonitrile/1 M methanol) solvent mixture with *n*-dodecane as an internal standard using six RPR-3500 lamps. A: 30 minutes of hv; B: 60 minutes of hv; C: 120 minutes of hv.

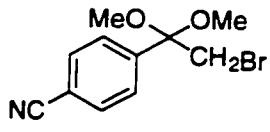

15

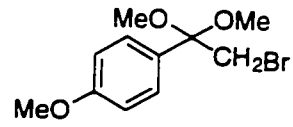

16

Figure 1.10 Structures of ketals **15** and **16**.

In the case of **7** the yield of the heavier product was lower, but mass spectral analysis is fully consistent with the corresponding acetal (**16**). We note that the formation of these acetals can also be promoted by addition of HBr to the solutions. In this case **15** and **16** are produced in both dark and illuminated samples. On the other hand, the formation of these products could be readily prevented by carrying out the photolysis in the presence of a small amount of calcium carbonate that removes HBr as it is formed (Figure 1.11).

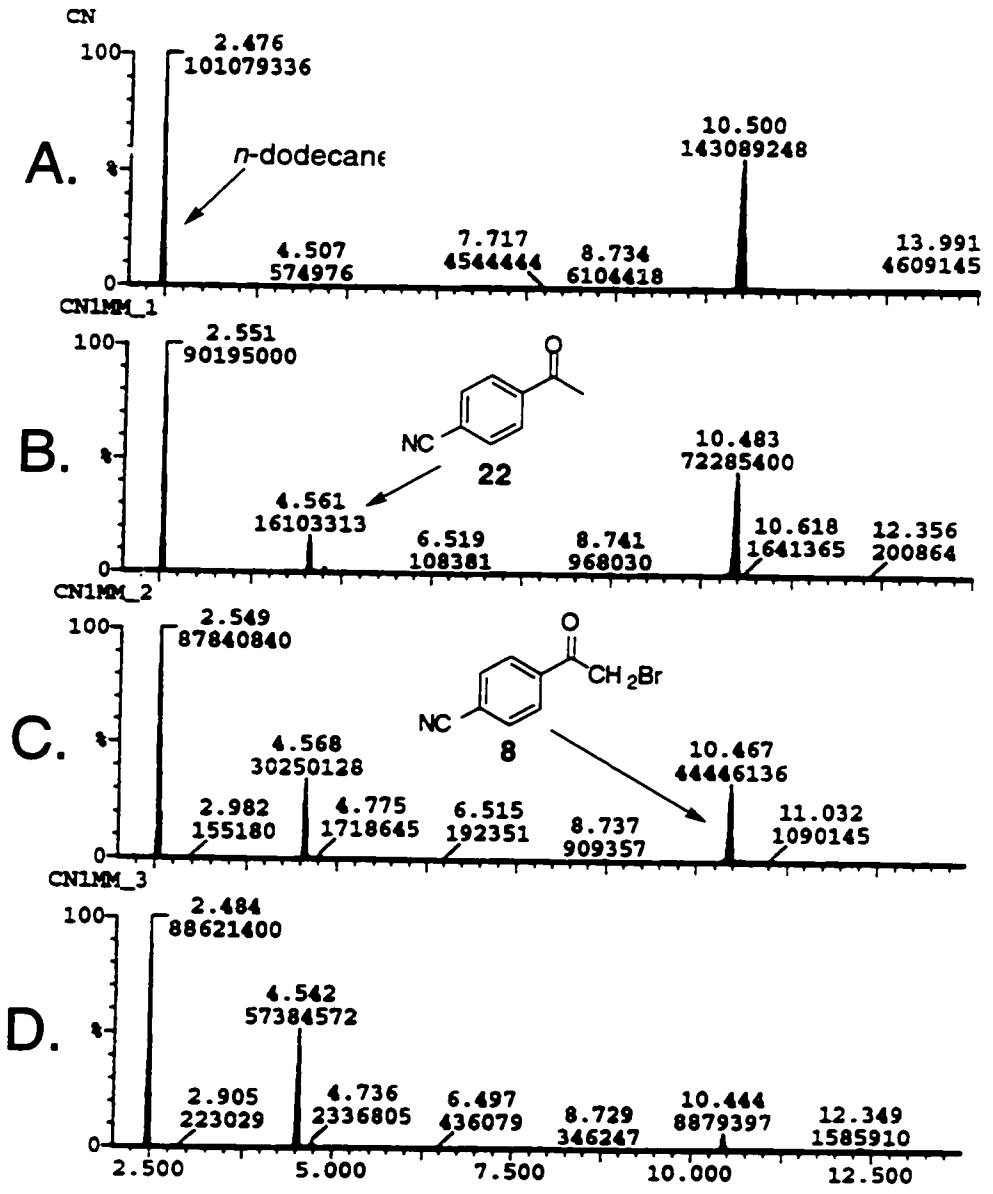

Figure 1.11 GC-MS traces showing the results obtained during prolonged irradiation times of compound 8 in a deoxygenated (acetonitrile/1 M methanol) solvent mixture with *n*-dodecane as an internal standard in the presence of $CaCO_3$ using six RPR-3500 lamps. A: before irradiation; B: 30 minutes of hν; C: 60 minutes of hν; D: 120 minutes of hν.

To distinguish between the mechanisms of Scheme 1.1 and Scheme 1.2, experiments were carried out in the presence of 10 mM bromide ions, added as Bu_4NBr. We assumed that the mechanism of Scheme 1.1 would be heavily influenced, since bromine atoms form the less reactive intermediate $Br_2^{\bullet-}$ by complexation with bromide (Equation 3).[18, 25, 27]

Equation 3.

$$Br^{\bullet} + Br^{-} \rightleftharpoons Br_2^{-\bullet}$$

We found that in methanol solvent, addition of bromide ion caused a 4.5 times decrease in product formation in the case of **7**, but only a factor of 2.0 in the case of **8**. These results suggest that the bromine atom mechanism must be dominant for **7** and possibly plays a role even in the case of the electron-deficient cyano-substituted compound **8**.

1.2.3. Neophyl Rearrangement Study

In contrast with earlier studies in benzene, where toluene was detected from the neophyl rearrangement of the phenacyl radical[28], no decarbonylation products were detected in our experiments. This is not entirely unexpected, since the neophyl rearrangement occurs with a rate constant of only 10 s^{-1} (for the parent radical at 25 °C)[28, 29] and could not compete with abstraction reactions of phenacyl radicals.[13] Scheme 1.3 shows the neophyl rearrangement for the case of the phenacyl radical (**17**). The rearrangement of radical **17**, first to a 1-keto spiro[2.5]octadienyl radical (**18**), then to a phenylacetyl radical (**19**), which undergoes α-scission to yield a benzylic radical (**20**) and carbon monoxide ultimately generates toluene (**21**) after hydrogen abstraction. Figure 1.12 shows the results obtained for the case of compound **10**.

Scheme 1.3 Neophyl rearrangement of phenacyl radical (**17**).[28]

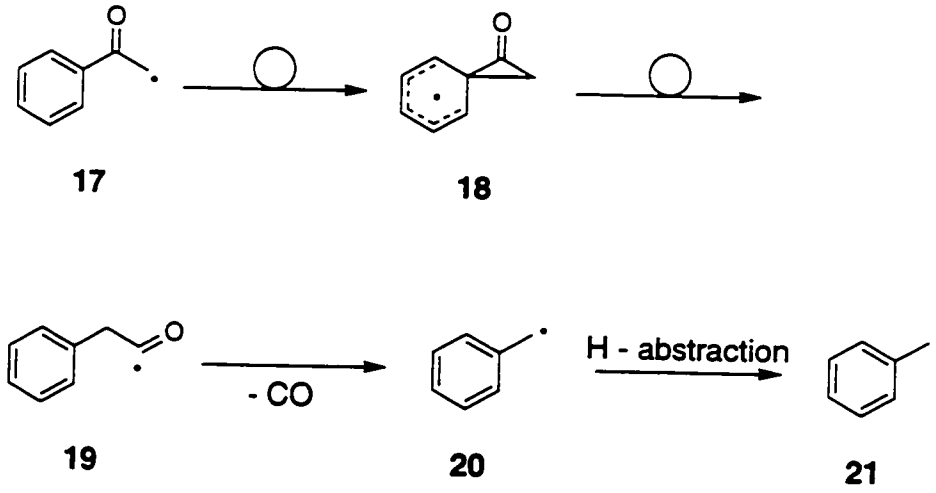

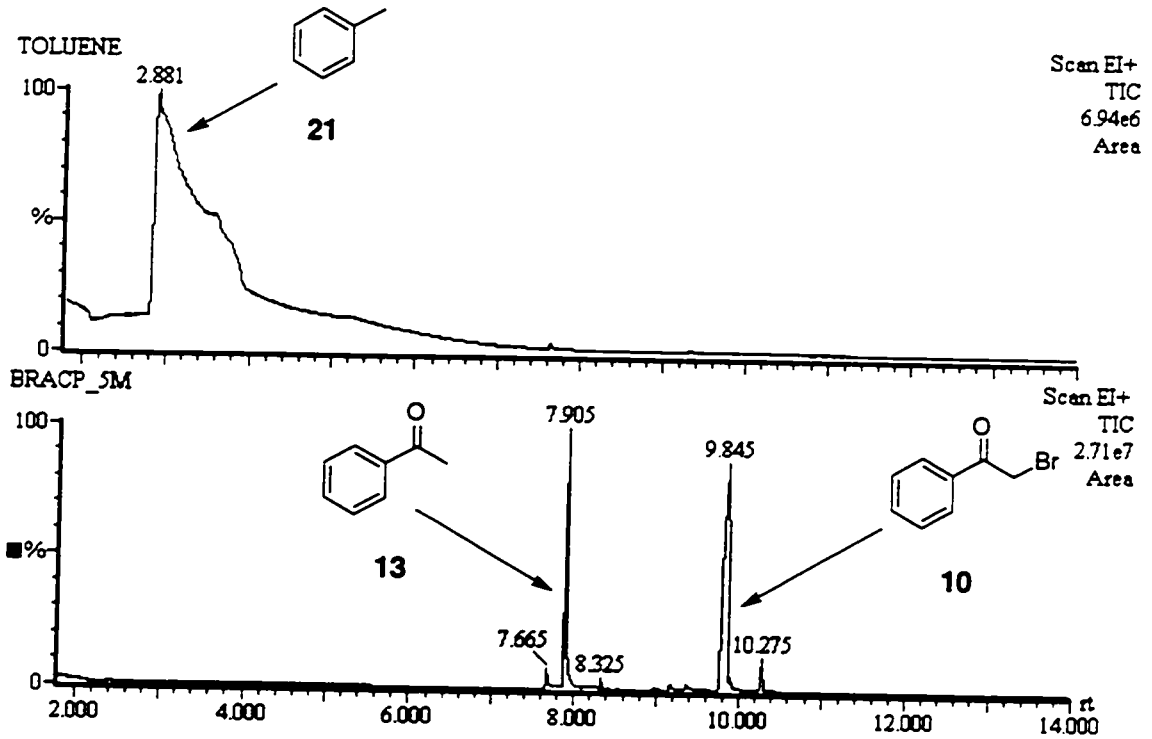

Figure 1.12 GC-MS traces comparing the results obtained during irradiation of compound **10** in deoxygenated methanol with toluene using six RPR-3500 lamps.

1.2.4. Competitive Studies

To determine the relative reactivity of ketones **7-11** towards ketyl radicals, we carried out a series of competitive experiments in which ketones **7-11** were irradiated in pairs, and the ratio of products examined for various ratios of starting materials. The product ratio for ketones **A** and **B** is related to the ratio of precursors according to Equation 4:

Equation 4.

$$\frac{\phi_A}{\phi_B} = \frac{k_r^A}{k_r^B} \frac{[A]}{[B]}$$

where k_r^A and k_r^B represent the values of k_3 and k_6, since these are the only steps in which the two ketones compete for reaction with the ketyl radical (Equation 5).

Equation 5.

$$k_r^A = k_3^A + k_6^A$$

Clearly, product formation in both reaction schemes is determined by reaction of the ketyl radicals with the α-bromoacetophenones, regardless of which one is the predominant mechanism.

Figure 1.13 shows plots according to Equation 4 for representative pairs of ketones in methanol, while Figure 1.14 shows the corresponding plots for **7** and **8** in methanol, ethanol and 2-propanol. The values of k_r^A / k_r^B obtained from these studies have been summarized in Table 1.2. The para-substituted ketones follow the anticipated order of reactivity according to their electron accepting ability, i.e. *p*-CN > *p*-H > *p*-MeO.

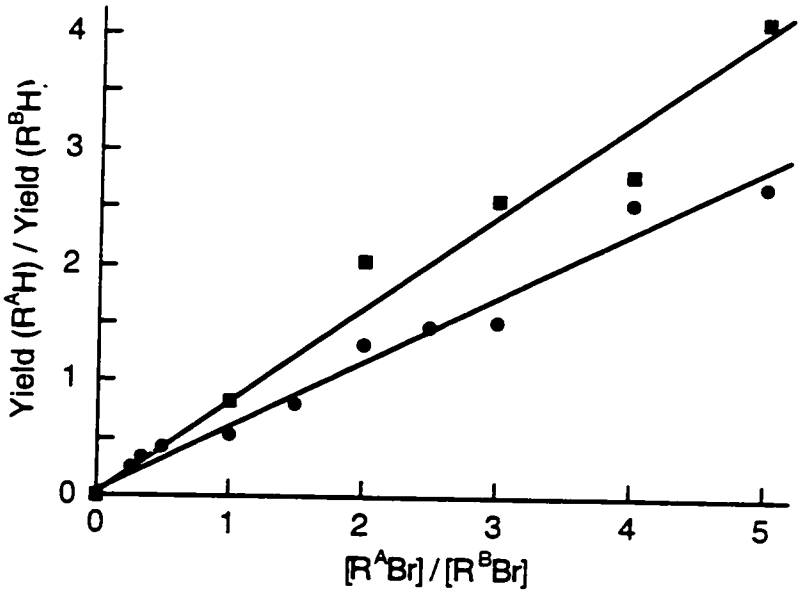

Figure 1.13 Dependence of product ratios following 350 nm irradiation of **7**/**8** (●) and **10**/**8** (■) mixtures in methanol.

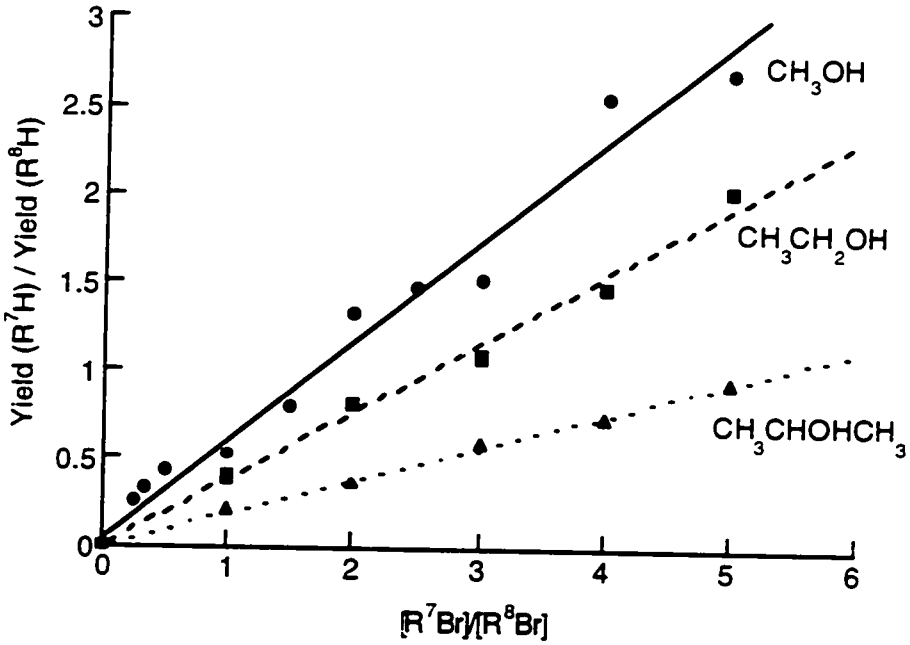

Figure 1.14 Dependence of the product ratios following 350 nm irradiation of 7/8 mixtures in methanol, ethanol, and 2-propanol.

Table 1.2 Competitive studies of ketone photodecomposition in deoxygenated alcohol solvents at 30 °C.

Substrates			
A	B	Solvent	k_r^A / k_r^B
7	**8**	Methanol	0.56
7	**9**	Methanol	1.22
10	**8**	Methanol	0.80
9	**11**	Methanol	0.70
7	**8**	Ethanol	0.39
7	**8**	2-Propanol	0.19
10	**8**	Ethanol	0.67
10	**8**	2-Propanol	0.35

We were surprised by the results for 7/8 mixtures in the different alcohols. These results (see Table 1.2) show that the selectivity order is 2-propanol > ethanol > methanol. Assuming that the better reducing agent (2-propanol) will react faster, one would have anticipated the lowest selectivity in this case.

The fact that 7 is less reactive than 8 suggests that the reaction is not in the Marcus inverted region since the kinetics follow the normal dependence on driving force.[30, 31] A more likely explanation for the unusual selectivity-structure dependence is that the hydrogen transfer mechanism of Scheme 1.1 is intrinsically less selective than the electron transfer process of Scheme 1.2. Further, we anticipate that the mechanism of Scheme 1.1 will be more likely to be favored over Scheme 1.2 in the case of methanol than for 2-propanol. This rationale is based on our analysis of bond energy data for the various ketyl radicals, where Equation 6 is not very sensitive to the detailed substitution pattern.

Equation 6.

$$R^1R^2\dot{C}OH \longrightarrow R^1R^2CO + H^{\bullet}$$

The ΔH_r for reactions are 30.3, 27.7 and 27.2 kcal/mol for the radicals from methanol, ethanol and 2-propanol, respectively.[32]

1.2.5. Isotope Labeling Studies used as a Mechanistic Probe

A quantitative approach in order to discriminate between these two schemes is to utilize deuterium labeled alcohols, since both reaction pathways should give a distinct isotopic pattern. Under such isotopic labeling conditions, Scheme 1.1 and Scheme 1.2 would yield the same product acetophenone with one unit mass difference, i.e., for the case of compound 7 in CD_3OH Scheme 1.4 and Scheme 1.5 show the reaction products:

Scheme 1.4 Bromine atom mechanism (hydrogen transfer).

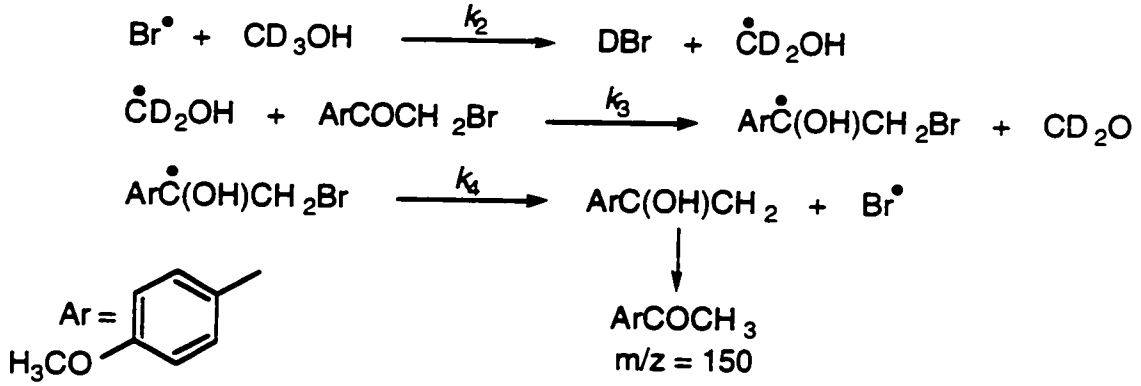

Scheme 1.5 Phenacyl radical mechanism (electron transfer).

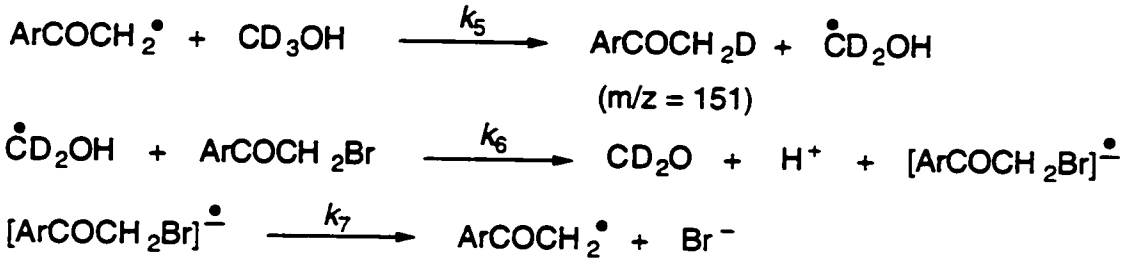

Table 1.3 shows the percentage of electron transfer measured for compounds 7 and 8 in three different deuterated alcohol solvents. The choice of substrates permitted to study both extremes of electron accepting capability of the para-substituted family, and the choice of alcohols permitted to study both extremes of electron donating capability of the ketyl radicals.

Table 1.3 Percent of electron transfer measured for compounds **7** and **8** in various deuterated alcohol solvents (^{13}C corrected).

Compound	CD_3OH	$CH_3CDOHCH_3$	$CH_3CHODCH_3$
	21	81	96
7	23	85	98
	22	77	96
Average	**22**	**81**	**97**
	23	88	96
8		89	94
		87	93
		82	
Average	**23**	**86**	**94**

The percentage of electron transfer was determined by measuring and comparing the intensity (%TIC) of the molecular ion peaks corresponding to the parent and the mono-deuterated acetophenones. A measured natural abundance of ^{13}C of 9.5% was taken as the correction factor for adjusting these peaks. For example, the system studying the photochemistry of compound 7 in CD_3OH was analyzed as follow:

Product formation resulting from Scheme 1.4 gives a molecular ion peak of 150. Correcting for the ^{13}C content, the molecular ion peak now corresponds to:

$$M_{150} = M_{150\ (exp.)} \bullet (1 + 9.5\%)$$

Product formation resulting from Scheme 1.5 gives a molecular ion peak of 151. Correction of this peak corresponds to:

$$M_{151} = \{M_{151\ (exp.)} \bullet (1 - (M_{150\ (exp.)} \bullet 9.5\%))\} \bullet (1 + 9.5\%)$$

were the last multiplying factor takes into consideration the ^{13}C abundance present in the mono-deuterated peak.

Therefore the percentage of electron transfer (% et) is given by the following relationship:

$$\%\ et = M_{151} / (M_{150} + M_{151}) \bullet 100\%$$

and consequently the percentage of hydrogen transfer (% Ht) is given by:

$$\%\ Ht = 100\ \% - \%\ et$$

Figure 1.15 shows a typical GC-MS trace for compound 8 in $CH_3CHODCH_3$. Figure 1.16 gives the m/z ratio in the molecular ion peak region for the *p*-cyanoacetophenone (**22**) formed during irradiation of compound 8 in $CH_3CHODCH_3$.

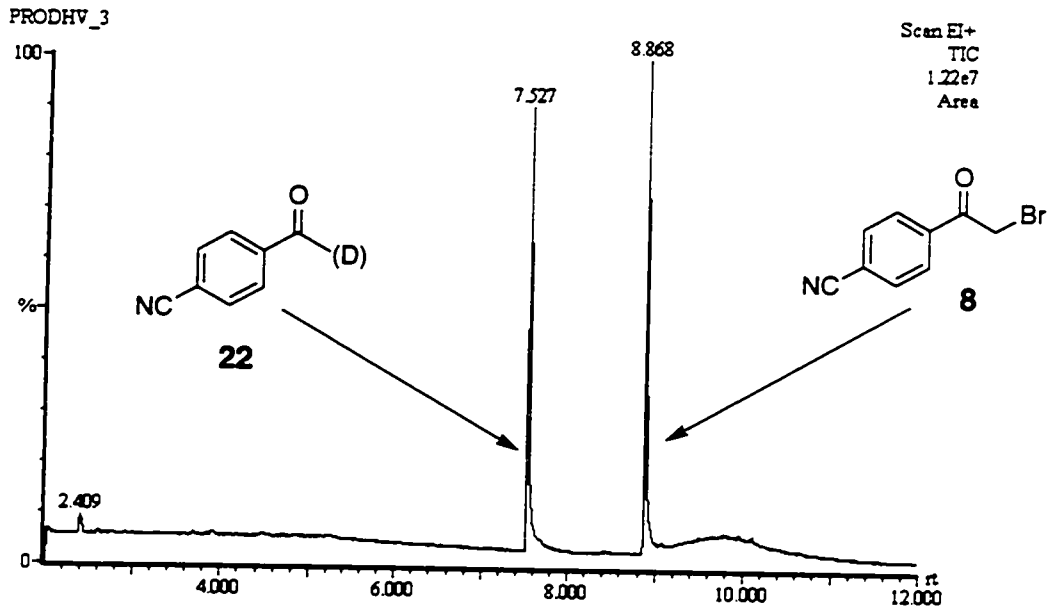

Figure 1.15 GC-MS trace of compound **8** in deoxygenated $CH_3CHODCH_3$ in the presence of Na_2CO_3 after 1 minute of irradiation using two RPR-3500 lamps.

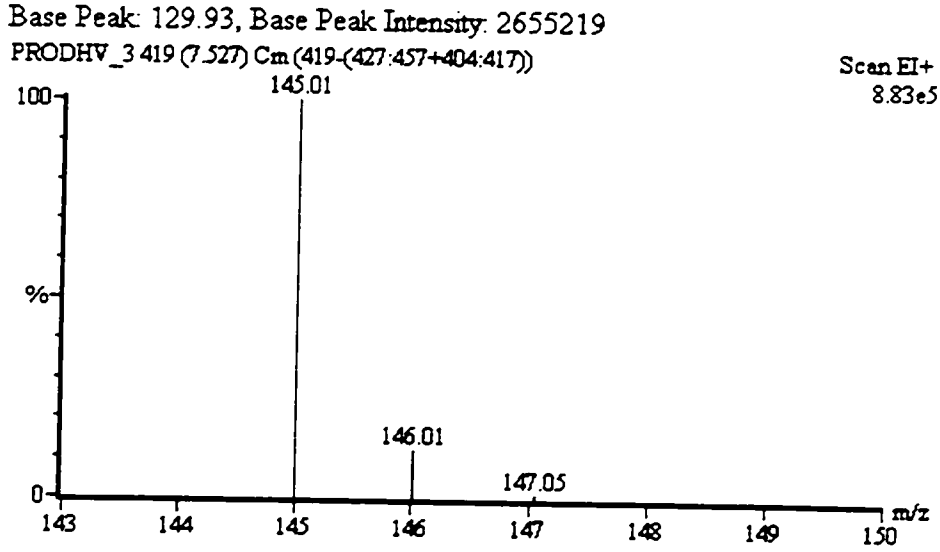

Figure 1.16 Mass spectral data of the molecular ion peak region for *p*-cyanoacetophenone (**22**) in deoxygenated $CH_3CHODCH_3$ in the presence of Na_2CO_3 after 1 minute of irradiation of compound 8 using two RPR-3500 lamps.

Clearly, these results demonstrate that the nature of the starting material is not a main contributing factor in the discrimination between the two schemes. The only parameter that seems to be playing a major role is the nature (reducing strength) of the ketyl radicals.

Because of isotope effects, one can anticipate that the hydrogen transfer step in the overall mechanism (k_3) will be the one that is going to be influenced the most by the nature of the deuterated solvent. This effect will explain the differences in percentage of electron transfer between the two isopropanol solvents. In the case of $CH_3CHODCH_3$, that step is slowed down to the degree of being unable to compete anymore with the electron transfer step (k_6) and therefore we observe near-quantitative electron transfer for that system.

1.2.6. Control Experiments

A few control experiments were done in order to validate the results presented. Since the photolysis of these systems generates an acidic medium, we were concerned whether the corresponding acetophenones could experience isotopic scrambling through a thermal exchange mechanism (Scheme 1.6).

Scheme 1.6 Possible thermal exchange mechanism for *p*-methoxyacetophenone (**12**) in an acidic CH_3OD medium showing deuterium incorporation.

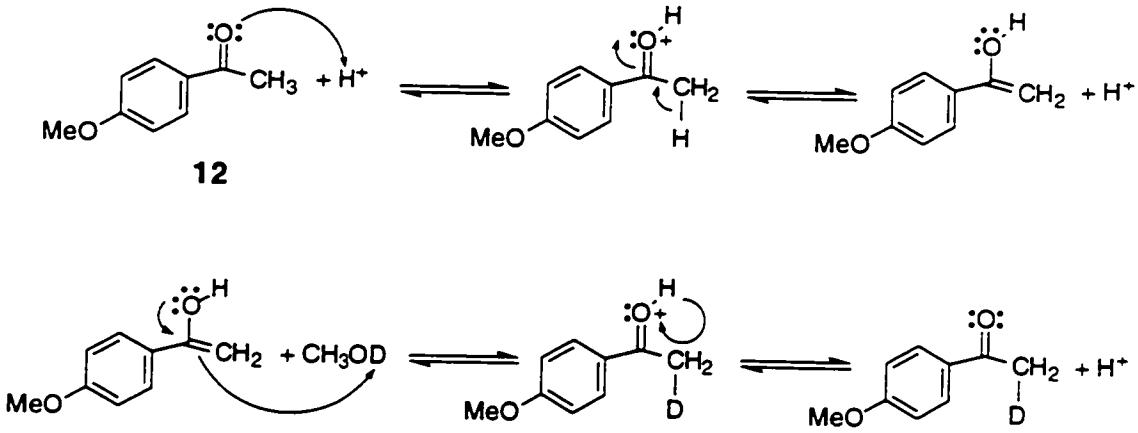

Irradiation at 350 nm of 2 mM solutions of *p*-methoxyacetophenone (**12**) in deoxygenated CH_3OD, CD_3OH, and $CH_3CHODCH_3$ in the presence of 1 mM of HBr were analyzed by GC-MS. The only system that did show deuterium incorporation was the one involving CH_3OD as the solvent. Irradiation experiments where sodium carbonate was added to the solution of compound 7 were also conducted with CH_3OD but the substitution pattern in the molecular ion peak region still showed deuterium incorporation caused by thermal exchange. For this reason studies with CH_3OD were not included in Table 1.3. Figure 1.17 shows the molecular ion peak regions of *p*-methoxyacetophenone (**12**) obtained after photolysis for the systems employing CH_3OD with HBr and Na_2CO_3 added. Figure 1.18 shows the mass spectral data obtained for *p*-methoxyacetophenone (**12**).

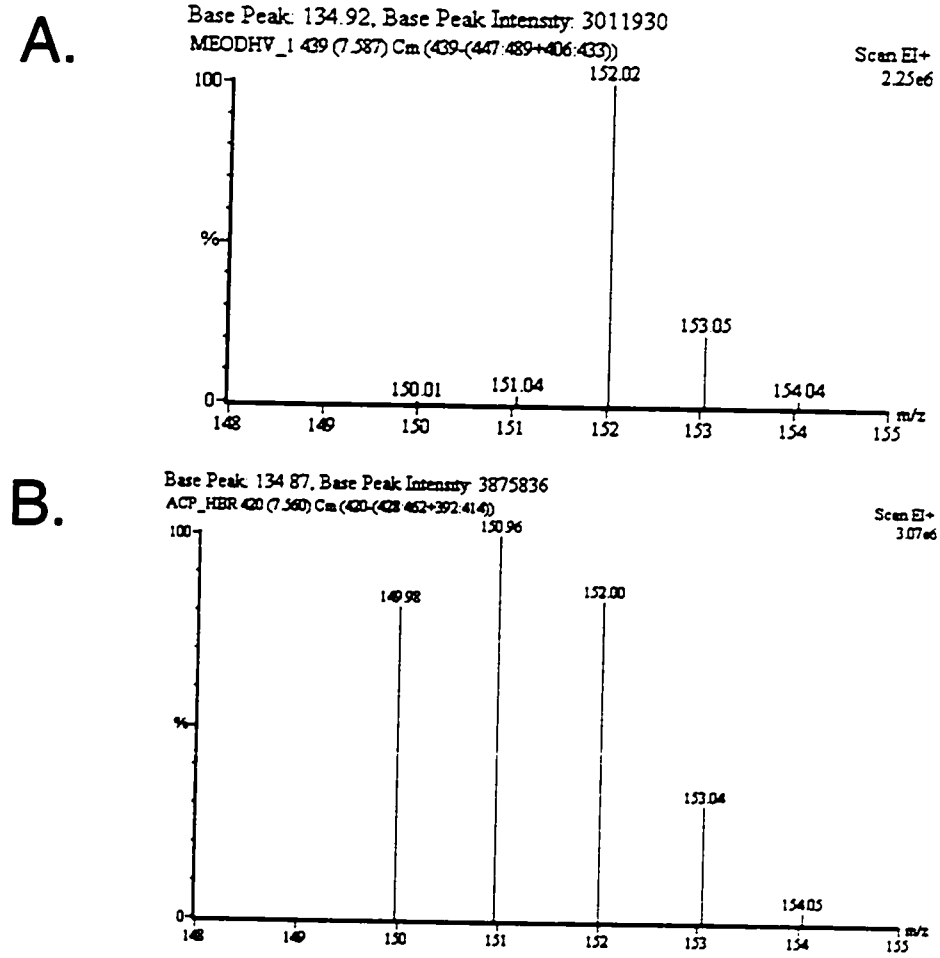

Figure 1.17 Molecular ion peak regions for *p*-methoxyacetophenone (**12**) in CH_3OD with A: Na_2CO_3 and irradiation of compound **7**; B: HBr and irradiation of compound **12**; after 2 minutes of irradiation using two RPR-3500 lamps.

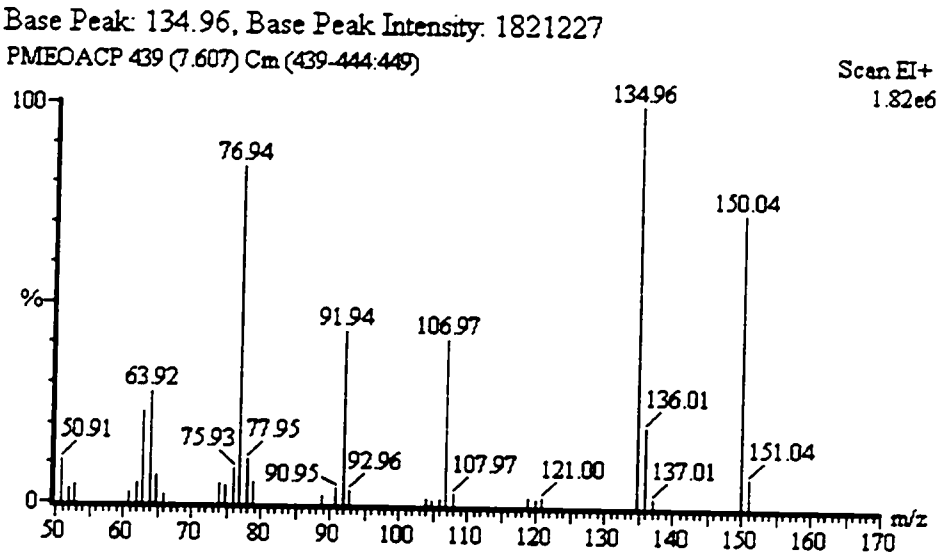

Figure 1.18 Mass spectral data of *p*-methoxyacetophenone (**12**).

CD_3OH and $CH_3CDOHCH_3$ were considered "clean" systems since any exchange with the solvent would not alter the substitution pattern. To verify this assumption, *p*-methoxyacetophenone (**12**) was irradiated in CD_3OH with HBr present and then analyzed by GC-MS. Figure 1.19 shows the results obtained after 2 minutes of irradiation using two UV lamps centered at 350 nm.

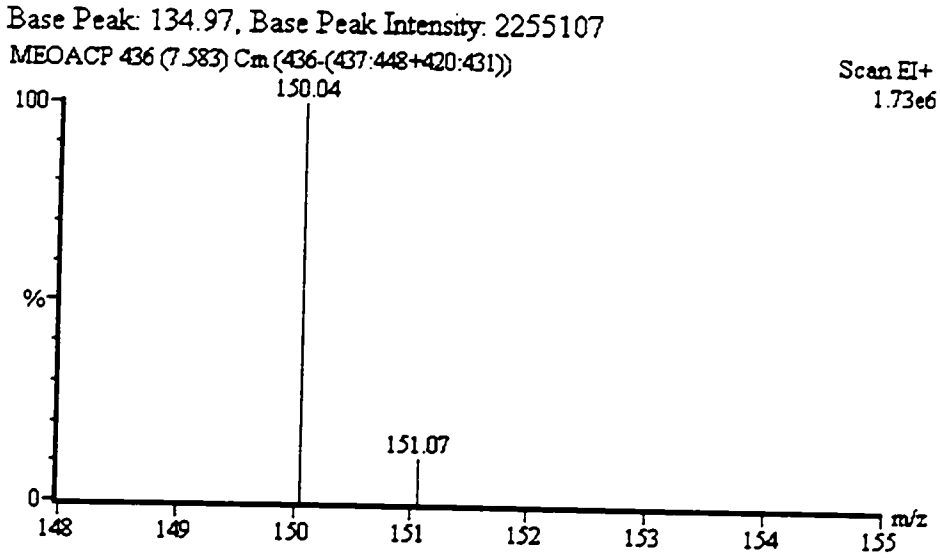

Figure 1.19 Mass spectral data of the molecular ion peak region for *p*-methoxyacetophenone (**12**) in deoxygenated CD_3OH with HBr (1 mM) added after 2 minutes of irradiation using two RPR-3500 lamps.

Control experiments using $CD_3CHOHCD_3$ were also carried out to verify that no atom transfer involving loss of hydrogen atom from the methyl group of the ketyl radical to form CD_2=C(OH)CD_3 would interfere in the deuteration pattern of the final ketone (step k_{c3} in Scheme 1.7). This was done with compounds **7** and **8** and, for both systems, the M+1 peak was measured to be ~10%, as expected from the ^{13}C abundance. Figure 1.20 and Figure 1.21 show the molecular ion peak region for both compounds.

Scheme 1.7 Bromine atom mechanism showing competing hydrogen transfer steps (k_3 and k_{c3}) for compound **7** in $CD_3CHOHCD_3$.

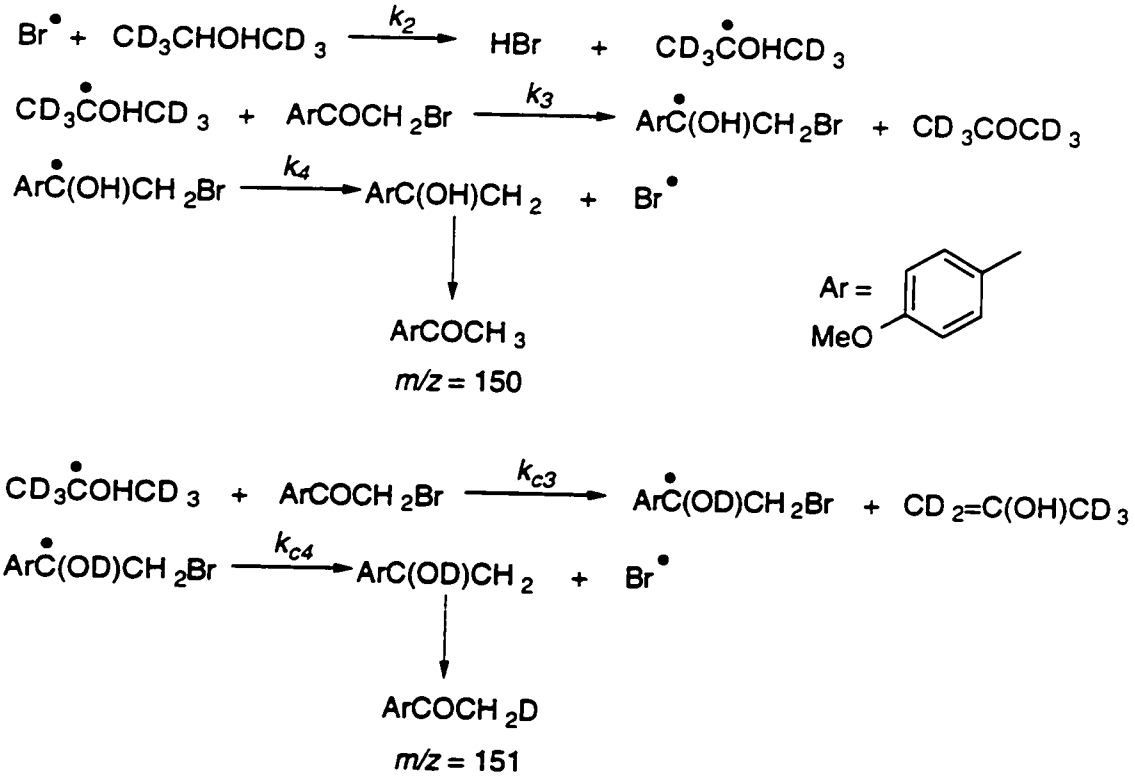

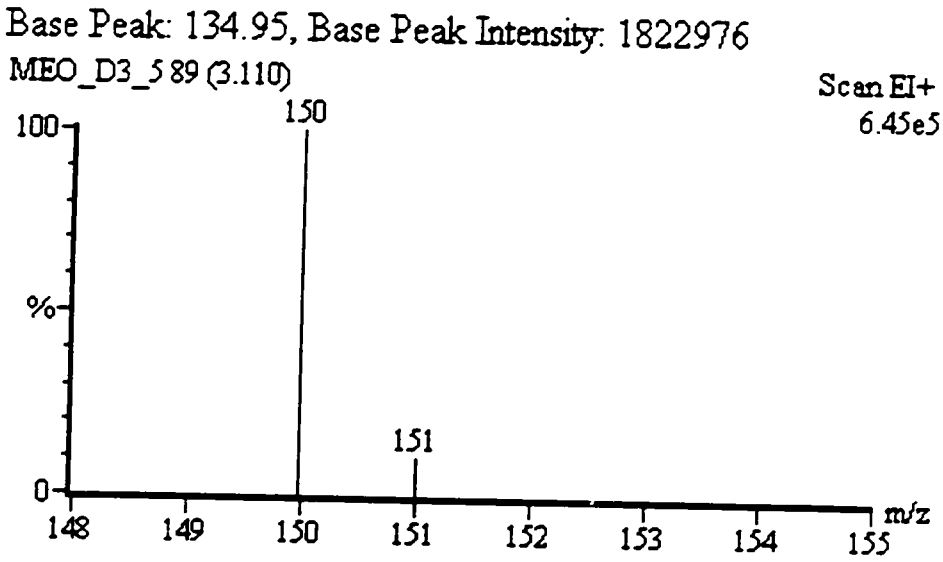

Figure 1.20 Mass spectral data of the molecular ion peak region for *p*-methoxyacetophenone (**12**) in deoxygenated $CD_3CHOHCD_3$ with Na_2CO_3 added after 1 minute of irradiation of compound **7** using two RPR-3500 lamps.

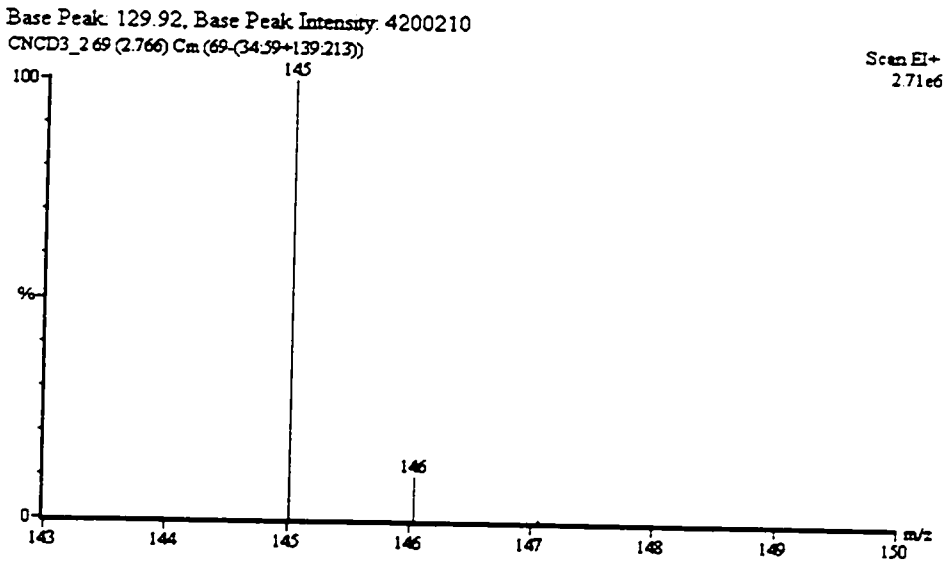

Figure 1.21 Mass spectral data of the molecular ion peak region for *p*-cyanoacetophenone (**22**) in deoxygenated $CD_3CHOHCD_3$ with Na_2CO_3 added after 1 minute of irradiation of compound **8** using two RPR-3500 lamps.

1.2.7. Cyclic Voltammetry Studies

Cyclic voltammetry experiments were performed on the para-substituted family of acetophenones in order to verify that the electrochemical properties of the starting material were an unimportant parameter in the overall chain reaction mechanism. Table 1.4 summarizes the results obtained for the reduction potentials measured in acetonitrile. These results are in agreement with the previous statement that the nature of the substrate is of little consequence in determining the reaction pathway chosen during the photodecomposition.

Table 1.4 Reduction potentials[a] for compounds **7**, **8** and **10** in acetonitrile/0.1 M TBAP at 25 °C, reported with respect to the saturated calomel electrode (SCE).

Compound	E ($RBr/R^{\bullet}Br^{-}$) V vs. SCE
7	-0.78 V
8	-0.68 V
10	-0.78 V

[a]Estimated irreversible reduction potentials, see experimental section.

1.3. Conclusion

In conclusion, the photoinitiated reaction of ring substituted α-bromoacetophenones with alcohols involves an efficient chain reaction leading to the corresponding acetophenone, HBr, and the carbonyl compound from oxidation of the alcohol. Two different mechanisms, involving hydrogen or electron transfer by ketyl radicals, have been proposed in order to accommodate the unusual selectivities of these reactions. Studies of isotope incorporation from deuterated alcohols lead to the conclusion that electron transfer (Scheme 1.2) dominates in the case of 2-propanol, while hydrogen transfer (Scheme 1.1) is most important for methanol. The results demonstrate that ring substitution in the starting ketone is not a main contributing factor in the discrimination between the two mechanisms; the observation is further corroborated by the relatively minor variations observed (see Table 1.4) in the reduction potentials. The only parameter that seems to be playing a major role is the nature (reducing strength) of the ketyl radicals.

1.4. Experimental

1.4.1. Materials

The various substituted α-bromoacetophenones were obtained from either Lancaster or Aldrich and were recrystallized from hexane before use. Bromide ions were added as $(C_4H_9)_4NBr$ from Aldrich which had suitable solubility in the alcohol solvents used. *n*–Dodecane (used as a chromatographic standard) was a BDH product, hydrogen bromide, valerophenone, *p*-methoxyacetophenone and *p*-cyanoacetophenone where purchased from Aldrich and used as received. Solvents were OmniSolv grade from BDH. Deuterated alcohol solvents were obtained from either Aldrich or Cambridge Isotope Laboratories.

1.4.2. General Techniques

1.4.2.1. Competitive Studies

Typical samples were 3 mL, containing 2 mM to 10 mM concentration of a ketone (**7-11**) in alcohol solvents. The samples were contained in Pyrex tubes and were deaerated (15 minutes) by bubbling with oxygen-free nitrogen. The samples were irradiated with 2 to 6 RPR-3500 lamps; irradiations were carried out in a "merry-go-round" apparatus to ensure that all samples received the same irradiation dose. Irradiation times varied between 30 seconds and 5 minutes and were adjusted in order to obtain around 20% conversion of the starting material. Calculations of conversions were done using *n*-dodecane as an internal standard. The temperature of the irradiation chamber was in the 30-35 °C range. The products ratio were analyzed by GC and/or GC-MS. Product identification was achieved by comparison of GC retention times with authentic samples and/or GC-MS analysis.

1.4.2.2. Characterization of Ketal 15

A solution containing 0.23 g of **8** in 50 mL of 1 M methanol in acetonitrile was purged with nitrogen and irradiated for two days with six RPR-3500 lamps. CH_2Cl_2 was then added and the solution washed with a saturated solution of $NaHCO_3$, then water and aqueous sodium chloride. The organic phase was evaporated and then co-evaporated three times with $CDCl_3$ in order to prepare for ^{1}H-NMR [δ=3.21 (s, 6H); 3.57 (s, 2H)]; mass spectra (see GC-MS below), *m/z* 102 (23), 116 (22), 128 (10), 130 (35), 158 (11), 176 (100), 177 (10), 238 (15), 240 (15).

1.4.2.3. Deuterium Labeled Product Studies

Typical samples were 1 mL, containing 2 mM of para-substituted α-bromoacetophenones in deuterated alcohol solvent. The samples were

contained in Pyrex tubes and were deaerated (15 minutes) by bubbling with oxygen-free nitrogen. The samples were irradiated as described above. Sodium carbonate was added to each sample in order to prevent any acid-catalyzed isotopic exchange between the ketone product and the solvent. Substitution patterns were analyzed by GC-MS. Control samples were prepared to ensure that isotopic substitution remained intact throughout the experiment. This was done using a 2 mM solution of *p*-methoxyacetophenone (**12**) in CH_3OD, CD_3OH or $CH_3CHODCH_3$, adding 1 mM HBr, purging for 15 minutes with oxygen-free nitrogen and irradiating at 350 nm with two lamps for 2 minutes. Control experiments using deoxygenated $CD_3CHOHCD_3$ were also carried out in order to verify that no atom transfer involving loss of hydrogen atom from the methyl group of the ketyl radical to form CD_2=C(OH)CD_3 would interfere in the deuteration pattern of the final ketone. This was done by irradiating for 1 minute with two RPR-3500 lamps compounds **7** and **8** in the presence of Na_2CO_3. For both systems, the M+1 peak was measured to be ~10%, as expected from the ^{13}C abundance. All calculations of percentage electron transfer took into consideration the natural abundance of ^{13}C, which was measured to be 9.5% (expected 9.9% for **7-9**) using authentic samples of the corresponding acetophenones. Furthermore, no M-1 contribution were observed for any mass spectra during this analysis.

1.4.2.4. Quantum Yields

These were determined by two different experiments. In a first experiment, compound **7** was used as a starting material and the quantum yields were measured by comparing the acetophenone yields in cyclohexane with those obtained in alcohols. Irradiations were carried out at 350 nm and product concentrations determined as indicated below. The quantum yield for the primary photocleavage of the C-Br bond in cyclohexane was taken as 0.35, the same value determined earlier in methanol solvent.[14] The second

experiment involved using a reference system as an actinometer. Valerophenone in benzene yields acetophenone by Norrish Type II photofragmentation with a quantum yield of 0.30.[26] Compound **10** was used as a starting material and the quantum yields were measured in methanol, ethanol and 2-propanol. Both systems had concentrations adjusted in order to have an absorption of 1.5 at 350 nm. Concentrations of 25 mM for the α-bromoacetophenone system and 100 mM for the reference system were used throughout these experiments. Deaerated samples were irradiated side by side with one to six RPR-3500 lamps as described above. Irradiation times were varied between 10 seconds and 70 minutes. Calculations of conversions were done using *n*-dodecane as an internal standard. The ratios between acetophenone formation and internal standard were analyzed by GC and then plotted as a function of time. Comparing slopes between the two systems permitted to measure chain lengths.

1.4.2.5. Gas Chromatography

The competitive studies of ketone photodecomposition in alcohol solvents and quantum yields experiments using valerophenone as a reference system were quantitatively analyzed on a Perkin Elmer Model 8320 capillary gas chromatograph equipped with a flame ionization detector (FID) and a DB-5 bonded-phase column of 15 m length (from J & W Scientific).

1.4.2.6. GC-MS

Analysis of samples including those containing Bu_4NBr were quantitatively performed on a Fisons Instruments 8000 series gas chromatograph with a capillary (DB-5, 15 m, 0.25 mm) column coupled with a MD-800 series mass spectrometer equipped with an EI ion source and a Dynolite detector, and controlled by a DEC/486 PC operating with Masslab software, release 1.12.

1.4.2.7. Cyclic Voltammetry

Cyclic voltammetry measurements were carried out using a standard three electrode cell with a glassy carbon working electrode having 3 mm in diameter, a platinum coil counter electrode, and a platinum wire reference electrode in a Bu_4NBF_4 (0.1 M) acetonitrile solution. The solvent for all measurements was distilled acetonitrile (EM Science) containing 0.1 M tetrabutylammonium perchlorate (TBAP/Fluka) as the supporting electrolyte, which was recrystallyzed twice from a CH_2Cl_2/ether mixture. Solutions were deoxygenated with a stream of dry argon. Measurements were made using a PAR Model 173 potentiostat equipped with a PAR Model 175 universal cell programmer. Voltammograms were recorded on a HP 7045B X-Y recorder. All potentials are reported with respect to the saturated calomel electrode (SCE). The voltammogram obtained for α-bromoacetophenone (**10**) at 200 mVs^{-1} showed two reduction peaks. The first cathodic peak, located at -0.78V with respect to the saturated calomel electrode, is relevant to the irreversible reduction of compound **10**, and its height (measured with respect to the monoelectronic wave of ferrocene) corresponds to the consumption of one electron per molecule. The second peak that was observed corresponds to the reduction of acetophenone as shown by comparison with an authentic sample. The same cyclic voltammetric behavior was observed with compounds **7** and **8**. The results obtained by these experiments are summarized in Table 1.4 and were done at the National Council of Research under the supervision of Drs. A. Houmam and D.D.M. Wayner.

1.4.2.8. Bond Energy Data Analysis

Bond energies for the various ketyl radicals were calculated using the NIST Structures and Properties Database and Estimation Program software version 1.1.[32]

1.5. References

[1] C. Heitner, "Light-Induced Yellowing of Wood-Containing Papers," in *Photochemistry of Lignocellulosic Materials*, vol. 531, C. Heitner and J. C. Scaiano, Eds. Washington: ACS Symposium Series, **1993**, pp. 2-25.

[2] G. J. Leary, "Recent Progress in Understanding and Inhibiting the Light-Induced Yellowing of Mechanical Pulps," *J. Pulp Paper Sci.*, **20** (6) , J154-160, **1994**.

[3] A. B. Berinstain, M. K. Whittlesey, and J. C. Scaiano, "Laser Techniques in the Study of the Photochemistry of Carbonyl Compounds Containing Lignin-Like Moieties," in *Photochemistry of Lignocellulosic Materials*, vol. 531, C. Heitner and J. C. Scaiano, Eds. Washington: ACS Symposium Series, **1993**, pp. 111-121.

[4] J. A. Schmidt and C. Heitner, "Light-Induced Yellowing of Mechanical and Ultrahigh Yield Pulps. Part 1. Effect of Methylation, Sodium Borohydride Reduction and Ascorbic Acid on Chromophore Formation," *J. Wood Chem. Technol.*, **11** (4) , 397-418, **1991**.

[5] J. A. Schmidt, E. Goldsmidt, C. Heitner, J. C. Scaiano, A. B. Berinstain, and L. J. Johnston, "Photodegradation of α-Guaiacoxyacetoveratrone. Triplet State Reactivity Induced by Protic Solvents," in *Photochemistry of Lignocellulosic Materials*, vol. 531, C. Heitner and J. C. Scaiano, Eds. Washington: ACS Symposium Series, **1993**, pp. 122-128.

[6] J. C. Scaiano, A. B. Berinstain, M. K. Whittlesey, P. R. L. Malenfant, and C. Bensimon, "Lignin-Like Molecules: Structure and Photophysics of Crystalline α-Guaiacoxyacetoveratrone," *Chem. Mater.*, **5** (5) , 700-704, **1993**.

[7] A. Castellan, N. Colombo, C. Vanucci, P. Fornier de Violet, and H. Bouas-Laurent, "A Photochemical Study of an o-Methylated α-Carbonyl β-1 Lignin Model Dimer: 1,2-Di(3',4'-dimethoxyphenyl)ethanone (Deoxyveratroin)," *J. Photochem. Photobiol., A: Chem.*, **51** , 451-467, **1990**.

[8] W. U. Palm and H. Dreeskamp, "Evidence for Singlet State β Cleavage in the Photoreaction of α-(2,6-Dimethoxyphenoxy)-acetophenone Inferred from Time-Resolved CIDNP Spectroscopy," *J. Photochem. Photobiol., A: Chem.*, **52** , 439-450, **1990**.

[9] W. U. Palm, H. Dreeskamp, H. Bouas-Laurent, and A. Castellan, "The Photochemistry of α-Phenoxyacetophenones Investigated by Flash-CINDP-Spectroscopy," *Ber. Bunsenges. Phys. Chem.*, **96** (1) , 50-61, **1992**.

[10] J. A. Schmidt, A. B. Berinstain, F. de Rege, C. Heitner, L. J. Johnston, and J. C. Scaiano, "Photodegradation of the Lignin Model α-Guaiacoxyacetoverathrone, Unusual Effects of Solvent, Oxygen, and Singlet State Participation," *Can. J. Chem.*, **69** (1) , 104-107, **1991**.

[11] K. Freudenberg, "Lignin: Its Constitution and Formation from *p*-Hydroxycinnamyl Alcohols," *Science*, **148** (30 April) , 595-600, **1965**.

[12] A. B. Berinstain, M. K. Whittlesey, and J. C. Scaiano, "Laser Techniques in the Study of the Photochemistry of Carbonyl Compounds Containing Ligninlike Moieties," in *Photochemistry of Lignocellulosic Materials*, vol. 531, C. Heitner and J. C. Scaiano, Eds. Washington: ACS Symposium Series, **1993**, pp. 111-121.

[13] S. V. Jovanovic, J. Renaud, A. B. Berinstain, and J. C. Scaiano, "Kinetic Study of the Reactions of Methoxy-Substituted Phenacyl Radicals," *Can. J. Chem.*, **73** (2) , 223-231, **1995**.

[14] W. G. McGimpsey and J. C. Scaiano, "Photochemistry of α-Chloro and α–Bromoacetophenone. Determination of Extinction Coefficients for Halogen Benzene Complexes," *Can. J. Chem.*, **66** , 1474-1478, **1988**.

[15] J. Renaud and J. C. Scaiano, "Chain Mechanisms for the Dehydrobromination of Ring-Substituted α-Bromoacetophenones in Alcohols," *Res. Chem. Intermed.*, **21** (Special issue in honor of Professor Henry L. Bolker) , 457-465, **1995**.

[16] F. L. Cozens, H. Garcia, and J. C. Scaiano, "Intrazeolite Photochemistry. 9. Laser Flash Photolysis of Xanthenium Ion Generated by Adsorption of 9-Xanthenol within Acid Zeolites," *Langmuir*, **10** (7) , 2246-2249, **1994**.

[17] G. L. Hug, *Optical Spectra of Nonmetallic Inorganic Transient Species in Aqueous Solution*, vol. NSRDS-NBS 69. Washington: National Bureau of Standards, **1981**.

[18] J. C. Scaiano, M. Barra, G. Calabrese, and R. Sinta, "Photochemistry of 1,2-Dibromoethane in Solution. A Model for the Generation of Hydrogen Bromide," *J. Chem. Soc., Chem. Commun.* (19) , 1418-1419, **1992**.

[19] J. C. Scaiano, M. K. Whittlesey, A. B. Berinstain, P. R. L. Malenfant, and R. H. Schuler, "Pulse Radiolysis and Laser Flash Photolysis Studies of the Lignin Model α-(*p*-Methoxyphenoxy)-*p*-methoxyacetophenone and Related Compounds," *Chem. Mater.*, **6** (6) , 836-843, **1994**.

[20] J. T. Banks and J. C. Scaiano, "The Laser-Drop Method: A New Approach To Induce Multiple Photon Chemistry with Pulsed Lasers. Examples Involving Reactions of Diphenylmethyl and Cumyloxyl Radicals," *J. Am. Chem. Soc.*, **115** (14) , 6409-6413, **1993**.

[21] D. V. Avila, J. Lusztyk, and U. Ingold, "Color Benzyloxyl, Cumyloxyl Orange, and 4-Methoxycumyloxyl Blue. Unexpected Discovery that Arylcarbinyloxyl Radicals Have Strong Absorptions in the Visible," *J. Am. Chem. Soc.*, **114** (16) , 6576-6577, **1992**.

[22] G. A. Russell, S. V. Kulkarni, and R. K. Khanna, "Radical and Ionic Reactions of (Benzoylmethyl)mercurials," *J. Org. Chem.*, **55** , 1080-1086, **1990**.

[23] G. A. Russell and S. V. Kulkarni, "Three-Component Radical Condensations Involving Benzoylmethyl Radicals, Alkenes, and Diphenyl Disulfide," *J. Org. Chem.*, **58** , 2678-2685, **1993**.

[24] F. Fontana, R. J. Kolt, Y. Huang, and D. D. M. Wayner, "Organic Reducing Agents: Some Radical Chain Reactions of Ketyl and 1,3-Dioxolanyl Radicals with Activated Bromides," *J. Org. Chem.*, **59** , 4671-4676, **1994**.

[25] J. C. Scaiano, M. Barra, M. Krzywinski, T. Hancock, G. Calabrese, and R. Sinta, "Photoreaction of Vicinal Dibromides with Alcohols: Chain-Amplified Generation of Hydrogen Bromide," *Chem. Mater.*, **7** (5) , 936-940, **1995**.

[26] P. J. Wagner, P. A. Kelso, A. E. Kemppainen, J. M. McGrath, H. N. Schott, and R. G. Zepp, "Type II Photoprocesses of Phenyl Ketones. A Glimpse at the Behavior of 1,4-Biradicals," *J. Am. Chem. Soc.*, **94** (21) , 7506-7512, **1972**.

[27] V. Nagarajan and R. W. Fessenden, "Flash Photolysis of Transient Radicals. 1. X_2^- with X = Cl, Br, I, and SCN," *J. Phys. Chem.*, **89** , 2330-2335, **1985**.

[28] G. Brunton, H. C. McBay, and K. U. Ingold, "Kinetic Applications of Electron Paramagnetic Resonance Spectroscopy. 30. Rearrangement of the Benzoylmethyl Radical," *J. Am. Chem. Soc.*, **99** (13) , 4447-4450, **1977**.

[29] D. Griller and K. U. Ingold, "Free-Radical Clocks," *Acc. Chem. Res.*, **13** , 317-323, **1980**.

[30] R. A. Marcus, "On the Theory of Electrochemical and Chemical Electron Transfer Processes," *Can. J. Chem.*, **37** , 155-163, **1959**.

[31] R. A. Marcus, "On the Theory of Oxidation-Reduction Reactions Involving Electron Transfer. I," *J. Chem. Phys.*, **24** , 966-978, **1956**.

[32] S. E. Stein, J. M. Rukkers, and R. L. Brown, *NIST Structures & Properties Database and Estimation Program: Ver. 1.1.* Gaithersburg: NIST, U.S. Department of Commerce, **1991**.

2. A Kinetic Investigation of the Chain Reaction Mechanism of *o*-Bromo-*p*-methoxy Ethers

2.1. Introduction

2.1.1. The Tin Hydride Method as an Application for Free Radical Chain Reactions in Organic Synthesis

Free radicals are highly reactive intermediates of considerable importance in the design and development of organic synthesis. They are known to react with themselves by combination or disproportionation in the diffusion control range of kinetics. Desirable experimental conditions usually require a low radical concentration during the course of a given reaction. It is for this reason that chain reactions are ideal systems, since they meet the aforementioned requirement. To be useful in synthetic applications, a chain reaction must generate radical-sites selectively, and furthermore, these radicals must be sufficiently long-lived in order to undergo desired chemical reactions. However, special care must be taken not to allow for them to live too long since this would engage in destructive chain-termination steps. The lifetime of these radicals is controlled by the nature of the chain-transfer steps. Since the rate of the chain-transfer steps determines what reactions will (or will not) be permitted to occur on intermediate radicals, the knowledge of their absolute value is an essential element in synthetic planning.

A reaction that meets the above requirements is the trialkyltin hydride mediated reduction of various organic functional groups, most of which are halides,[1-4] however there exist a wide variety of carbon-heteroatom bonds serving as radical precursors (Equation 1).[5]

Equation 1.

$$R\text{-}X + Bu_3Sn^{\bullet} \longrightarrow R^{\bullet} + Bu_3SnX$$

X = halogen, thiophenyl, selenophenyl, xanthate, etc. $X \neq H$

Modern free radical-based synthetic methods often apply trialkyltin hydrides to mediate chain reactions. Scheme 2.1 shows the salient features of this method.

Scheme 2.1 Trialkyltin hydride mediated radical reaction.[6]

$$RX + Bu_3Sn^{\bullet} \xrightarrow{k_X} R^{\bullet} + Bu_3SnX \qquad \text{step1}$$

$$R^{\bullet} \xrightarrow{k_R} R'^{\bullet} \qquad \text{step 2}$$

$$R^{\bullet} + Bu_3SnH \xrightarrow{k_H} RH + Bu_3Sn^{\bullet} \qquad \text{step 3}$$

$$R'^{\bullet} + Bu_3SnH \xrightarrow{k_{H'}} R'H + Bu_3Sn^{\bullet} \qquad \text{step 4}$$

$$R'^{\bullet} \xrightarrow{k_D} \text{non-radical products} \qquad \text{step 5}$$

When a tri-*n*-butyltin radical reacts with an organic halide, halogen atom abstraction (step 1) yields the organic radical R$^{\bullet}$. The site of the initial radical is determined by the location of the halogen moiety. This newly formed radical has then the opportunity to undergo a series of intra- and intermolecular reactions (step 2) to form the subsequent radical R'$^{\bullet}$. Both of these radical lifetimes are determined by the bimolecular rate of the chain-transfer steps 3 and 4. These rates are controlled by both the rate constants for hydrogen abstraction (k_H, $k_{H'}$) and by the trialkyltin hydride concentration. The application of the tin hydride reagent is useful from an organic synthetic point of view since it generates site-selective radicals from a given substrate and allows these radicals to have a sufficiently long lifetime to undergo

chemical reaction, but not a sufficient time to decompose by chain termination processes (step 5). The knowledge of relevant rate constants implicated in a chain reaction sequence can become a powerful tool in the ability to design synthetic strategies employing radical chemistry.

2.1.2. Translocation of Radical Sites by Intramolecular 1,5-Hydrogen Atom Transfer

Although the carbon-hydrogen bond is the simplest conceivable radical precursor, it can never be used directly for the tin hydride method since hydrogen abstraction from a C-H bond by a tin-centered radical is usually an endothermic process (Figure 2.1).

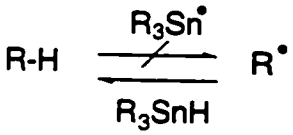

Figure 2.1 Direct use of a C-H bond as a radical precursor in the tin hydride method (not possible).

In the late 1980's, Curran and coworkers[5] introduced a collection of related reactions in which a free radical is produced indirectly from a carbon-hydrogen bond following initial generation of a radical at a remote site. They termed this concept of remote functionalization, "radical translocation". In this concept, radicals are generated at favorable sites and then "translocated" to new sites prior to the desired radical-derived reactions.

A reaction that has been extensively used for remote functionalization is the hydrogen atom transfer reaction, a fundamental reaction in organic free radical chemistry. From a preparative standpoint, intramolecular 1,5-hydrogen atom transfer reactions are prime candidates for such functionalization because they permit the indirect use of a carbon-hydrogen

bond as a radical precursor. They possess the interesting feature of introducing a six-membered transition state (TS) structure and therefore displaying a rather strain free process. This "radical translocation" is illustrated with the help of Figure 2.2.

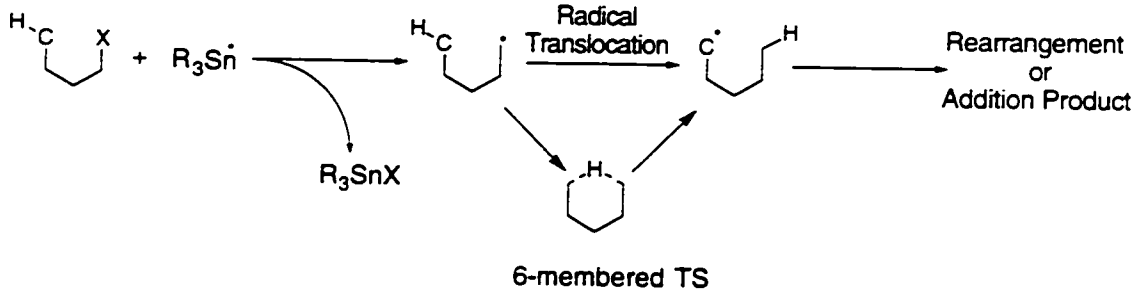

Figure 2.2 Indirect use of a C-H bond as a radical precursor in the tin hydride method.[7]

Two variations have been proposed using this approach. In one, the radical is first generated on the alkene that is destined to become the hydrogen acceptor for the subsequent cyclization. Scheme 2.2 provides a detailed description of the propagation steps anticipated for this variation.

Scheme 2.2 Propagation steps for the cyclization of vinyl halide (**1**) mediated by tri-*n*-butyltin hydride.[5]

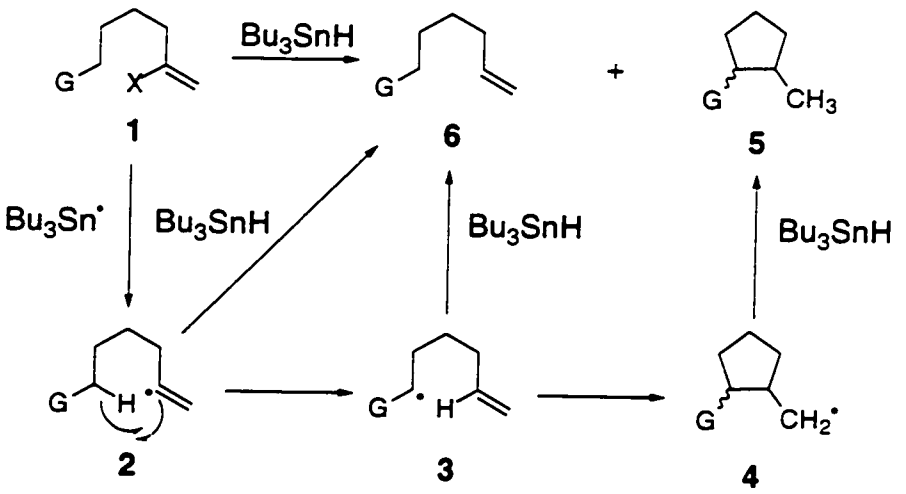

G = radical stabilizing group

When a vinyl halide such as compound **1** is treated with tri-*n*-butyltin hydride, it leads to the formation of the vinyl radical **2**. 1,5-Hydrogen atom transfer then produces the stabilized radical **3**. Hexenyl radical cyclization (**3** → **4**) is then followed by the standard tri-*n*-butyltin hydride reduction to give the end product **5**. This reaction sequence can be bypassed to give the directly reduced compound **6** if the 1,5-hydrogen atom transfer reaction or the cyclization step is slower than the bimolecular trapping reaction. In order to prevent this side reaction, experimental conditions usually operate under minimum tri-*n*-butyltin hydride concentrations therefore favoring the formation of **5** over **6** by slowing down sufficiently the rate of all bimolecular reactions involving tin. Furthermore, in order to ensure that the 1,5-hydrogen atom transfer is sufficiently rapid to propagate chain reactions, a radical stabilizing group (**G**) is introduced in order to weaken the C-H bond.

A representative example of this process is outlined in Equation 2. Addition of a 0.02 M benzene solution of tri-*n*-butyltin hydride (containing 5 mol % of 2,2′-azobisisobutyronitrile (AIBN)) to a 0.02 M benzene solution of vinyl iodide (**7**) gave cyclic ketal (**8**) in 67% yield after standard chromatographic purification. Furthermore, there was no evidence for the formation of the directly reduced (uncyclized) product under these conditions.[5]

Equation 2.[5]

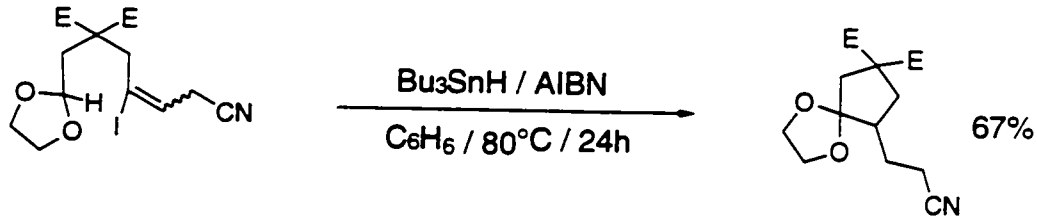

7 **8**

E = CO_2CH_3

The recent renaissance in synthetic applications of radical reactions is founded largely on carbon-carbon bond forming reactions.[8] The methodologies using this approach must respect the following three requirements. The carbon radicals must: 1) be generated rapidly and selectively; 2) have a sufficient lifetime in order to yield the proper reaction; and, 3) be trapped by tin hydride prior to radical-radical or radical-solvent reactions. Cases regarding procedures that generate carbon-centered radicals with the help of 1,5-hydrogen atom transfer reactions have played a small role in the radical renaissance. This is mainly due to very short lifetimes which are often associated with such radicals. Therefore, only the sufficiently fast carbon-carbon bond forming reactions can compete with reactions of the intermediate carbon-centered radicals with the efficient radical traps that may be present during these procedures. In essence, requirements 1 and 3 are met, but requirement 2 is not.

In the second variation, the radical is first generated in a strategically selected protecting group. Having a goal of developing radical translocation reactions that could be used under standard radical conditions, such as tin hydride reduction conditions, Curran and coworkers have focused their attention on 1,5-hydrogen atom transfer reactions from C-H bonds to reactive carbon-centered radicals. These types of hydrogen transfers had been observed over the years, most of which were accidental.[9] They were considered on many occasions as been nuisance from a synthetic standpoint, often competing with desired transformations (especially 6-exo cyclizations). They have recently harnessed the features of 1,5-hydrogen atom transfer reactions and introduced a variety of new synthetic methods.[10-12] In many of these, a radical is initially generated in a "protecting group" and then translocated by 1,5-hydrogen atom transfer prior to cyclization, addition, isotopic labeling, or oxidative self-removal of the protecting group.

2.1.3. Protecting/Radical Translocating (PRT) Groups

Recently Curran and coworkers[13] introduced an extension of the "remote functionalization" concept: the protecting/radical translocating concept. Using this approach, a functional group is added to a molecule and serves a dual function during the synthesis of a target molecule. In addition to serving as a protecting group both before and after the radical reaction, this modified "protecting group" serves as a site for generation of the initial radical that then "translocates" to a new site within the molecule prior to a carbon-carbon bond-forming reaction. These protecting groups, like standard synthetic protecting groups, should be designed with ease of introduction and removal, and they should resist common experimental conditions. Furthermore, they must function rapidly and selectively in the radical translocation which is often an intramolecular hydrogen atom transfer reaction.

A certain amount of research has been done by Curran and coworkers over the years in order to introduce a number of PRT groups. These groups vary both in the nature of the protecting group and in the functional group that is protected. Figure 2.3 shows a few PRT groups designed for alcohols,[14] amides, amines[14] and carboxylates.[10] The target hydrogen atom that is to be abstracted via "translocation" has been marked for each structure.

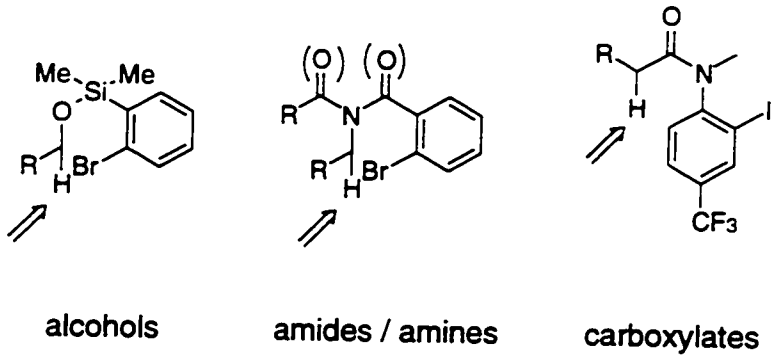

Figure 2.3 Examples of protecting radical translocating (PRT) groups.

The protecting group, which contains a halogen atom, is converted to its reduced form during the radical reaction. An example of this strategy is shown in Figure 2.4.[5]

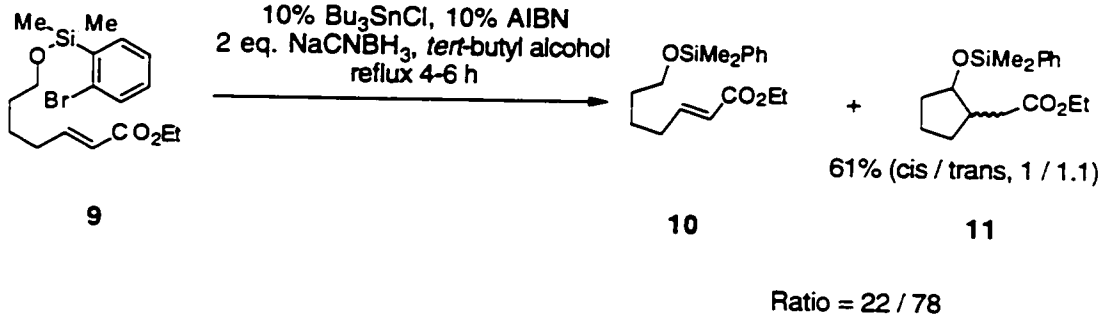

Figure 2.4 Example of the protecting radical translocating strategy using the catalytic tin hydride method of Stork.[15]

2.1.4. *o*-Bromo-*p*-methoxyphenyl Ethers. Protecting/Radical Translocating Groups That Generate Radicals from C-H Bonds β to Oxygen Atoms

Until very recently, all of these PRT groups shared a common denominator: the targeted C-H bond to be abstracted was located α to the protected functional group. Curran extended this idea and introduced the first class of PRT group that generates radicals β to the protected functional group. The *p*-methoxy-*o*-bromophenyl group protects alcohols before and after its use as a translocating group. Figure 2.5 shows the general structure of this β-translocating compound and its synthetic equivalent after the 1,5-hydrogen atom transfer reaction has taken place.

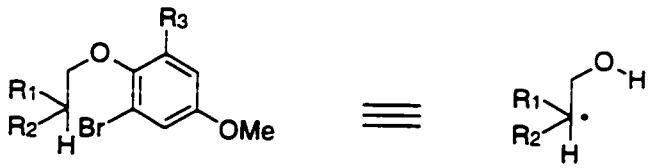

12 **13**

R_1 = alkyl
R_2 = H, alkyl
R_3 = H, Br, Me

Figure 2.5 Structure of the *o*-bromo-*p*-methoxyphenyl ether and its synthetic equivalent after 1,5-hydrogen atom transfer.

Curran's detailed study of substituent effects on intramolecular 1,5-hydrogen atom transfer reactions for a model system provided some guidelines for the design of this new type of PRT group.[7] From their work, they suggested that there was an analogy between 5-exo-cyclizations and 1,5-hydrogen atom transfer reactions; i.e., systems where rapid and selective 5-exo-cyclizations were occurring could also undergo rapid and selective 1,5-hydrogen atom

transfer reactions. Based on this suggestion, locating the target C-H bond α to the functional group may not be as important as the nature and geometry of the connecting chain between the target C-H bond and the initial radical site formed on the PRT group when promoting rapid 1,5-hydrogen atom transfer reactions. Simply stated, the nature and geometry of the transition structure may overshadow the bond dissociation energy of the targeted C-H bond when it comes to rapid 1,5-hydrogen atom transfer reactions.

The design of this newly introduced β-translocating group was aided by the proposed analogy between 5-exo-cyclizations and 1,5-hydrogen atom transfer reactions made by Beckwith.[16-19] From Beckwith's research, it was found that the cyclizations of aryl allyl ether radicals such as **14** (Figure 2.6) are exceptionally rapid and selective. This behavior is believed to be the result of the high reactivity of the aryl radicals coupled with the favorable geometry of the substrate during cyclization.

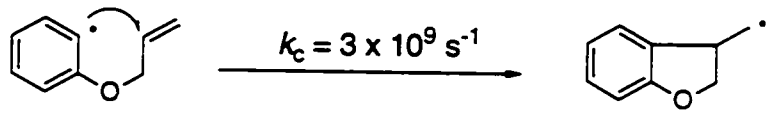

14 **15**

Figure 2.6 Cyclization of aryl allyl ether radical (**14**).[18]

Curran and coworkers thus suggested that 1,5-hydrogen atom transfer reactions of radicals similar to **16** could also be sufficiently rapid and selective for their use as PRT groups. This last proposition was based on Beckwith's observations that 1,5-hydrogen atom transfer reactions of the type depicted in Figure 2.7 were competitive with 6-exo-cyclization when R = vinyl. What Curran set out to investigate was if this type of hydrogen transfer could occur when the vinyl group was replaced by an alkyl group.

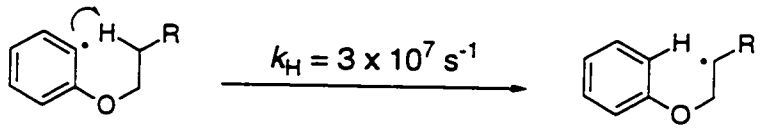

16 **17**

R = $CH{=}CH_2$

Figure 2.7 1,5-Hydrogen atom transfer reaction of aryl allyl ether radicals (**16**).[19]

What they concluded from their results was that hydrogen transfer reactions of aryl radicals were sufficiently rapid to be useful for synthetic applications. They even estimated a value for the rate constants (@ 50 °C) for the transfer of secondary hydrogens to be in the range of (1-5) x $10^6\ s^{-1}$, and those of tertiary hydrogens to be > $10^7\ s^{-1}$. The *p*-methoxy-*o*-bromophenyl group did protect the alcohol moiety during the radical chemistry, and it generated secondary alkyl radicals from C-H bonds β to the oxygen atom with 50-55% efficiency and tertiary alkyl radicals with 80-85% efficiency. These efficiencies could be augmented to values greater than 80% for secondary radicals and greater than 90% for tertiary radicals if a second *o*-bromine atom or an *o*-methyl group was introduced in the PRT group.

Four different *p*-methoxyphenyl ether protecting groups for alcohols were studied during their research: monobromides **18a** (R = H), **18c** (R = Me) and **18d** (R = CMe_2OTBS); and dibromide **18b** (R = Br). (Figure 2.8)

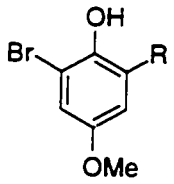

18a R = H
b R = Br
c R = Me
d R = CMe_2OTBS

Figure 2.8 Structures of the *p*-methoxyphenyl ether protecting groups for alcohols used during Curran's recent research.[13]

They reduced several substrates under fixed concentration conditions with deuterated tributyltin hydride in order to explore and compare the efficiency of 1,5-hydrogen atom transfer reactions versus 1,6-hydrogen atom transfer reactions and direct reduction of the aryl radical. Scheme 2.3 illustrates their proposed mechanism for the chain reaction with one of the substrates investigated during tin hydride reduction. Bromine abstraction mediated by a tin radical to generate the aryl radical (**20**) is followed by a competition between direct reduction (yielding compound **21**), 1,5-hydrogen atom transfer (leading to **23** after 5-exo-cyclization of **22** and deuterium transfer), and 1,6-hydrogen atom transfer (resulting in **25** after deuterium transfer).

Scheme 2.3 Proposed mechanism for the chain reaction for substrate **19** under tin hydride reduction condition.[13]

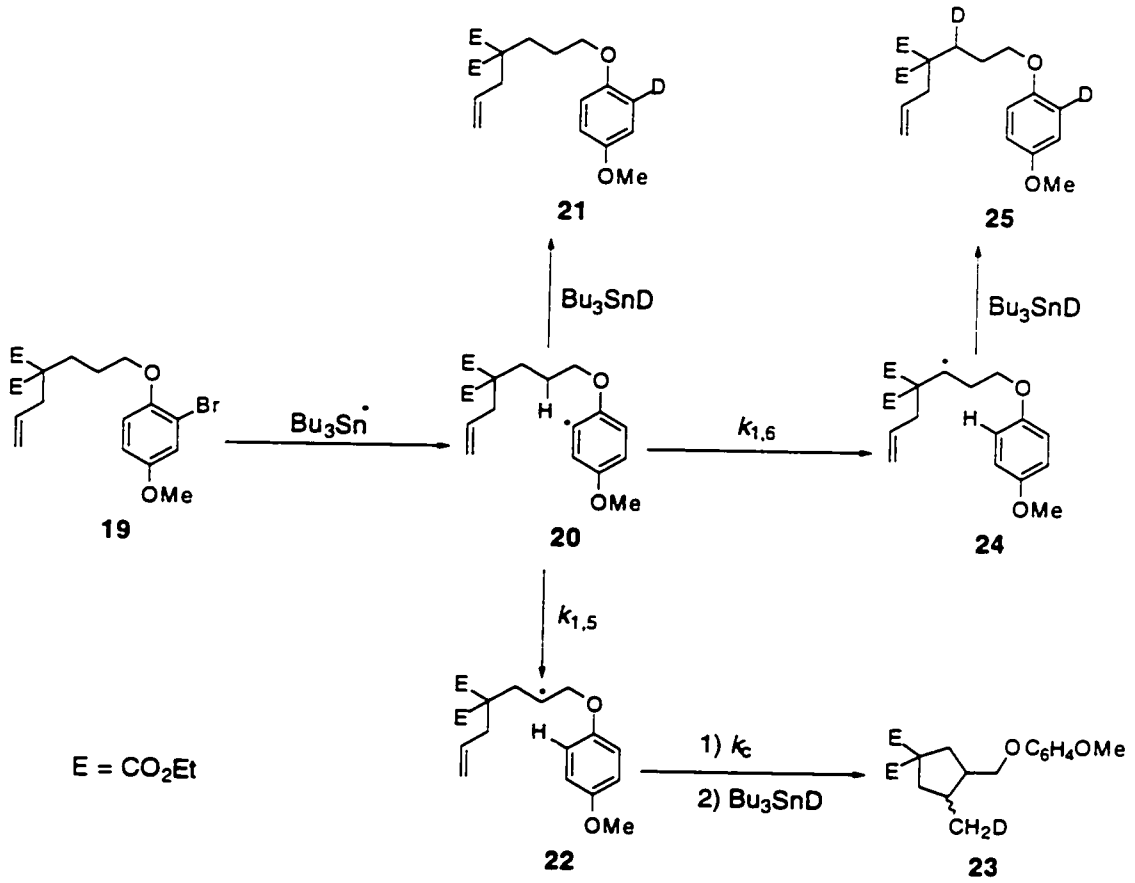

The purpose of this work is to investigate quantitatively the kinetics of the 1,5-hydrogen atom transfer reaction under study with the help of laser flash photolysis technology. Compound **27** (Figure 2.9) was used as a lead compound since it enabled us to isolate and study solely the 1,5-hydrogen atom transfer reaction.

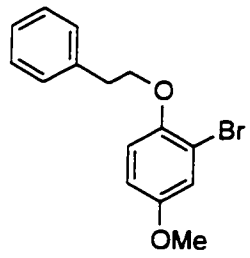

27

Figure 2.9 Structure of 2-bromo-4-methoxy-1-(2-phenylethoxy) benzene (**27**).

2.2. Results and Discussion

2.2.1. Preliminary Studies

Laser excitation of compound **27** was anticipated to generate the spectroscopically visible benzylic radical (**29**) after 1,5-hydrogen atom transfer reaction. The initial strategy involved looking for a growth signal around 320 nm that would be indicative of our desired radical. Furthermore, oxygen quenching experiments were expected to generate the corresponding arylperoxyl radical (**30**) that is expected to absorb in the 480 nm spectral range.[20] Scheme 2.4 illustrates the original strategy behind this research. Figure 2.10 and Figure 2.11 show typical kinetic traces obtained under nitrogen and oxygen atmospheres respectively, using acetonitrile as the solvent.

Scheme 2.4 Original laser flash photolysis strategy for the study of compound **27**.

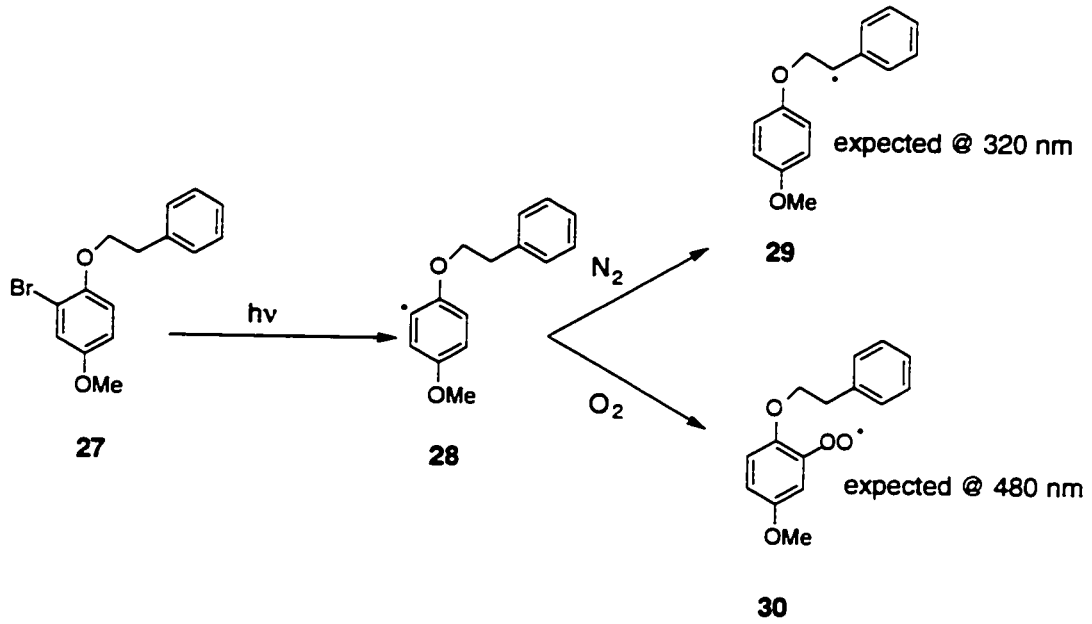

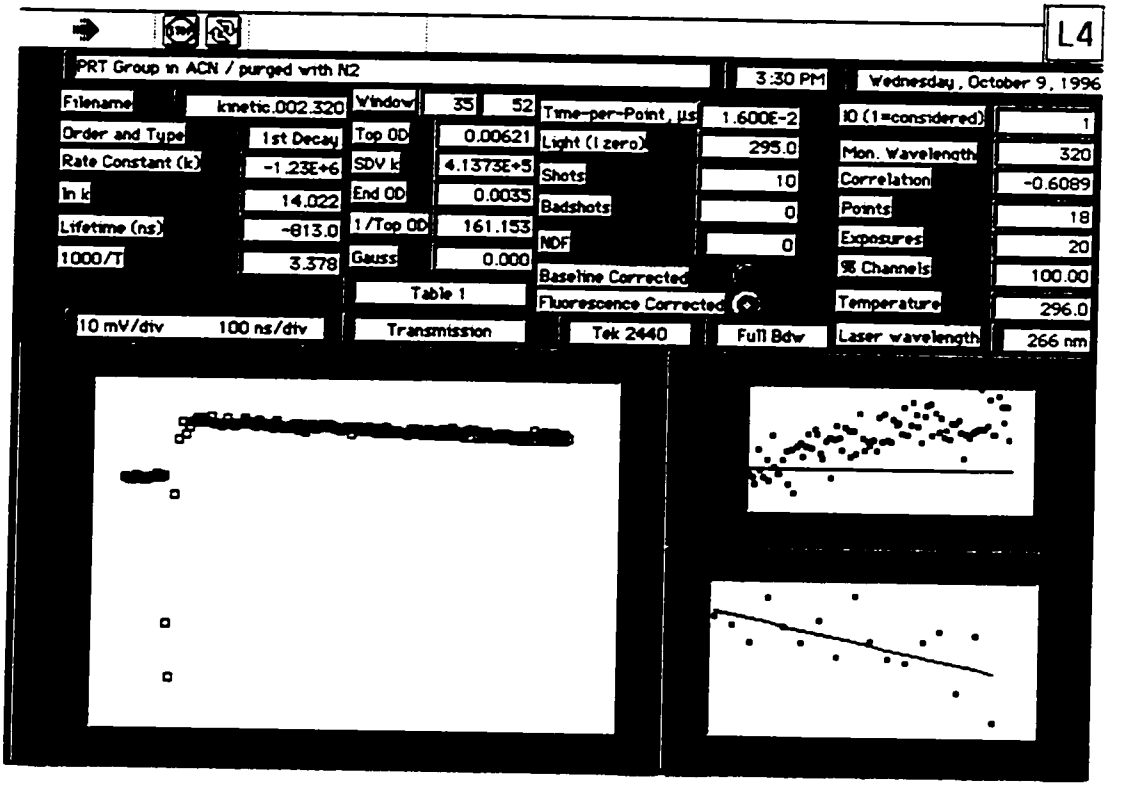

Figure 2.10 Transient kinetic trace recorded following 266 nm laser excitation of compound **27** (0.5 mM) in deoxygenated acetonitrile monitored at 320 nm.

Unfortunately, the traces obtained for both experiments gave uninformative results. Based on spectral evidence, the signals obtained under these two atmospheres did not correspond to that of a benzylic radical. The presence of a peak at 320 nm in oxygen saturated acetonitrile confirmed that the signal observed wasn't coming from such a radical because of their known reactivity towards oxygen. A benzylic radical would therefore be quenched under such conditions and the spectral data would be devoid of a peak in that region. Figure 2.12 and Figure 2.13 compare spectral data for our two conditions with that of the benzyl radical (

Figure 2.14) recorded earlier in our laboratory and that agrees with literature data.[21] Following these results, the conclusion was reached that we were probably observing a system where heterolytic rather than homolytic cleavage was the preferred route of photodegradation. This possible heterolytic route was not explored any further.

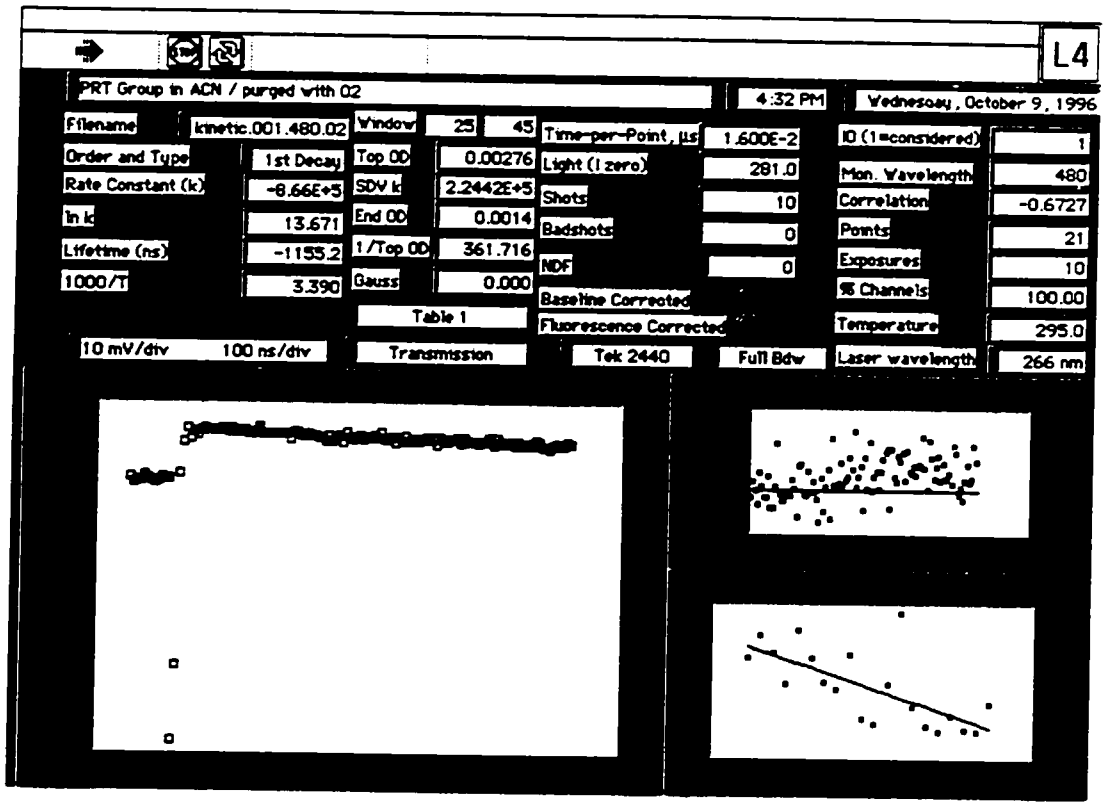

Figure 2.11 Transient kinetic trace recorded following 266 nm laser excitation of compound **27** (0.5 mM) in oxygen saturated acetonitrile monitored at 480 nm.

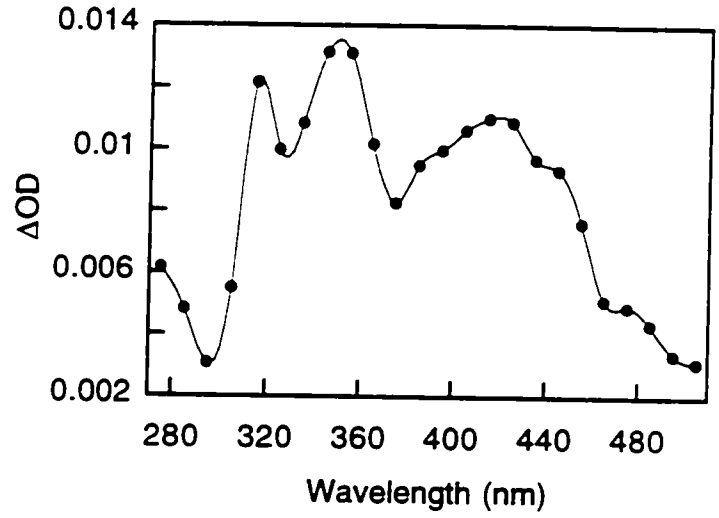

Figure 2.12 Transient absorption spectrum recorded 272 ns after 266 nm laser excitation of **27** (0.5 mM) in deoxygenated acetonitrile.

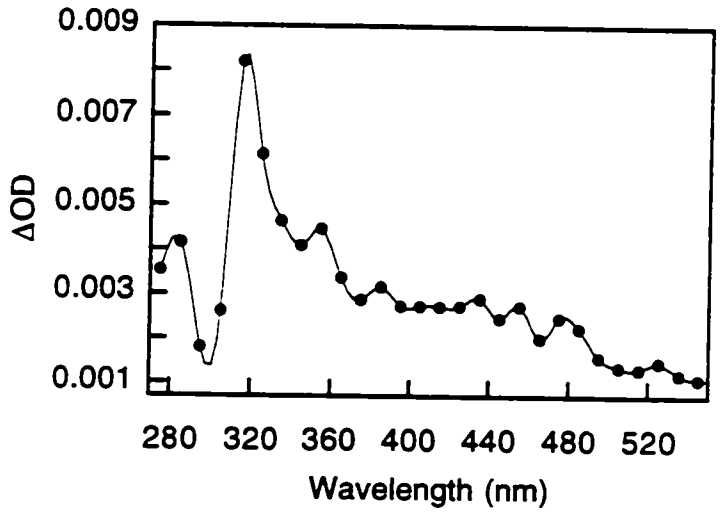

Figure 2.13 Transient absorption spectrum recorded 184 ns after 266 nm laser excitation of **27** (0.5 mM) in oxygen saturated acetonitrile.

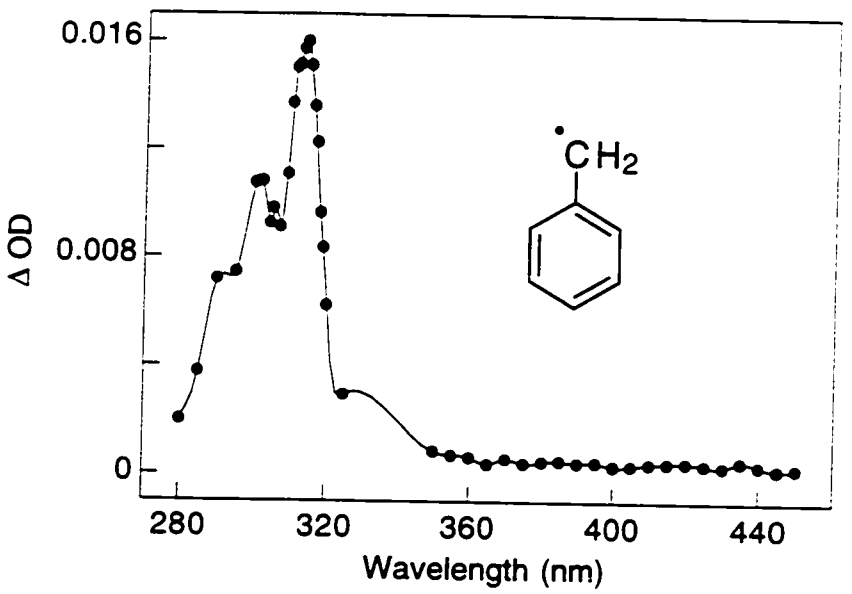

Figure 2.14 Transient absorption spectrum of the benzyl radical.[21]

The experimental conditions were therefore set for a solvent that would prevent such heterolytic cleavage, i.e. pentane. Figure 2.15 corresponds to the spectral data obtained from the photolysis of compound **27** in pentane under nitrogen. Based on this new information, a new concern was added: were we debrominating and forming the desired benzylic radical or not?

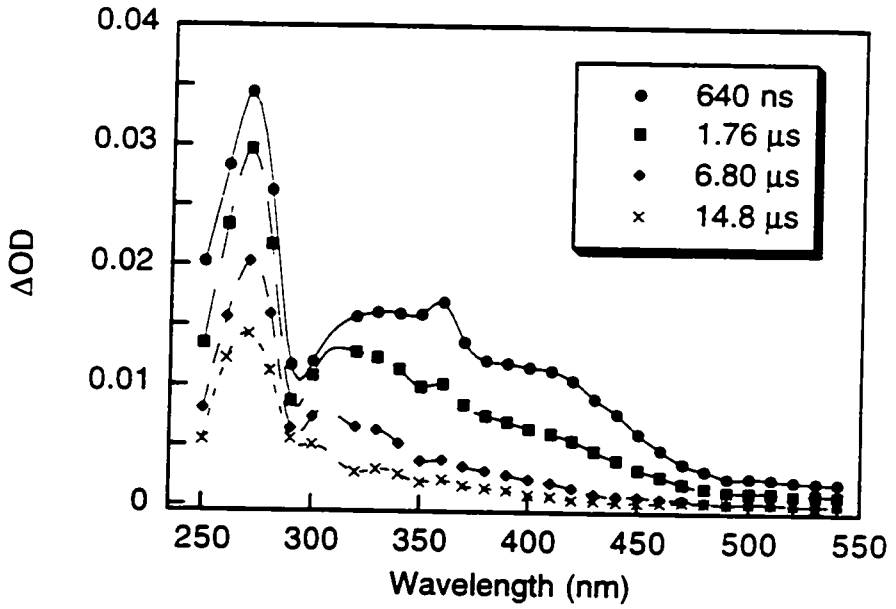

Figure 2.15 Transient absorption spectrum recorded following 308 nm laser excitation of **27** (0.5 mM) in deoxygenated pentane. Inset: delay times for data collection after laser pulse.

A series of experiments were undertaken in order to verify if compound **27** was debrominating upon direct photolysis. It has been shown earlier that while bromine atoms do not have a convenient absorption in the spectral region accessible, they can be monitored readily by addition of either bromide ions or benzene.[22-24] As a matter of convenience, bromide ions are usually added to organic solvents as their tetrabutylammonium salt. It is known that bromine atoms readily form the intermediate $Br_2^{-\bullet}$ by complexation with bromide (rate constant of complexation = 1.6×10^{10} M^{-1} s^{-1}).[23] This newly formed intermediate has an intense absorption band at 370 nm, and a weak but very characteristic band in the 600 nm region that can be monitored with our laser flash systems.[25, 26]

Equation 3.

$$Br^{\bullet} + Br^{-} \rightleftharpoons Br_2^{-\bullet}$$

Scheme 2.5 summarizes the approach employed in the complexation experiments using bromide as a trapping agent. Figure 2.16 shows the results obtained upon laser excitation. The anticipated formation of a strong signal at 370 nm is not observed.

Scheme 2.5 Laser flash photolysis approach for the bromine atom trapping experiment done in the presence of bromide ions.

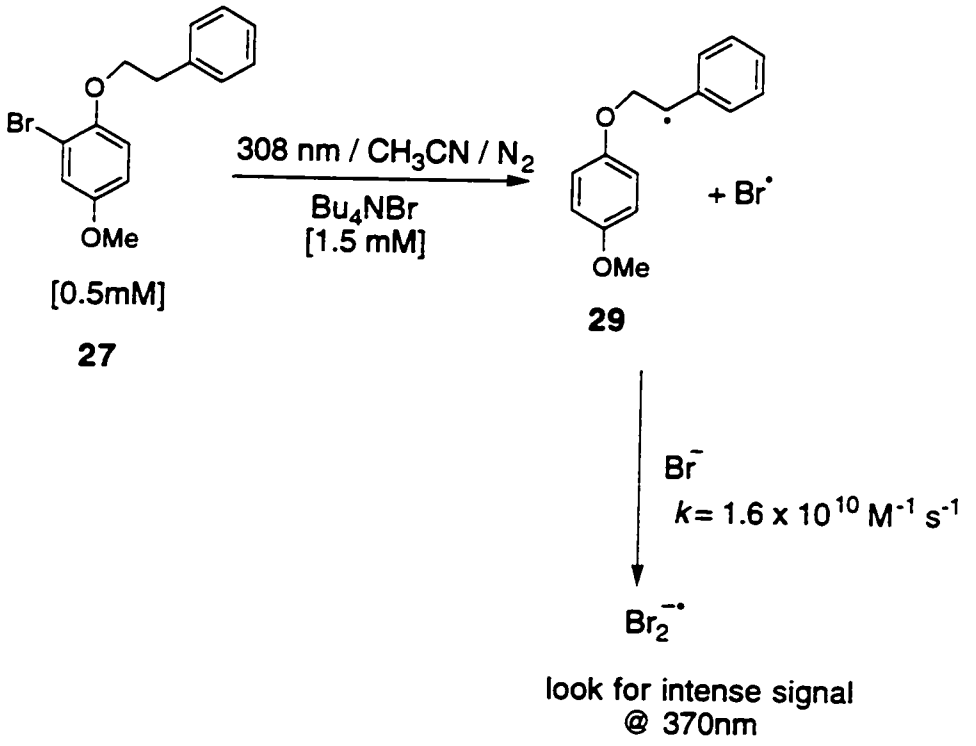

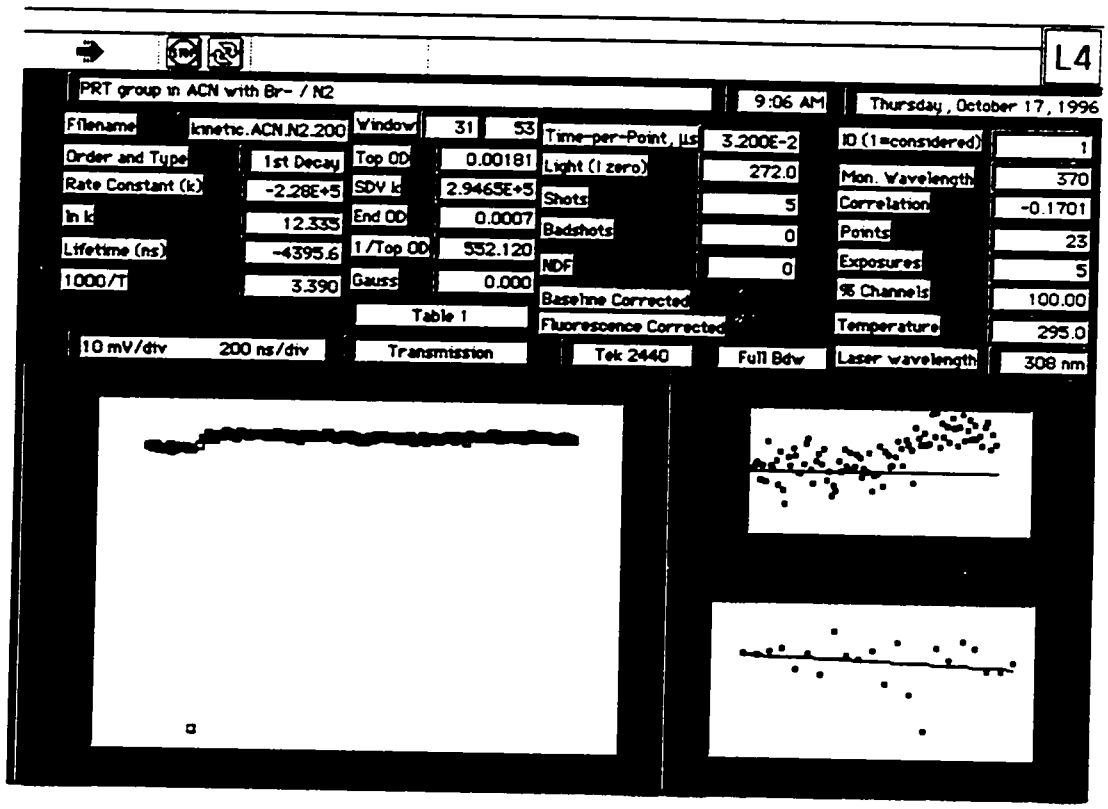

Figure 2.16 Transient kinetic trace recorded following 308 nm laser excitation of **27** (0.5 mM) in the presence of 1.5 mM Bu_4NBr in deoxygenated acetonitrile monitored at 370 nm.

The formation of charge-transfer complexes between halogen atoms (Cl, Br and I) and aromatics in solution and in matrices has been well established in the literature. For benzene, the visible absorption maximum complexed with bromine is 540-550 nm.[24] Experiments were done in a 1:9 benzene:pentane solvent mixture in order to further investigate the presence of bromine atoms for our system. Figure 2.17 and Figure 2.18 compare the spectrum of such a complex with that of our own experimental results.

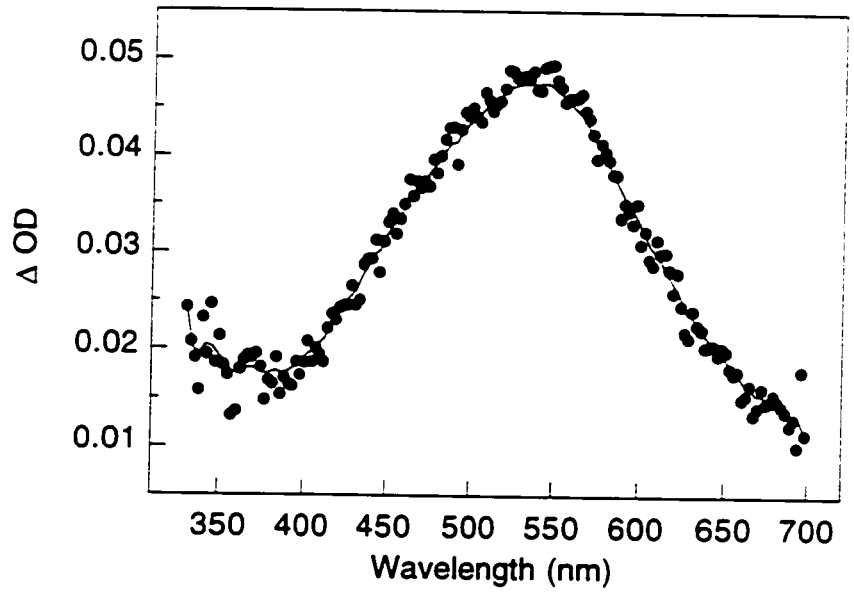

Figure 2.17 Transient absorption spectrum of bromine-benzene complex monitored 1 μs after laser excitation of α-bromoacetophenone (λ_{max} 550 nm) in benzene.[24]

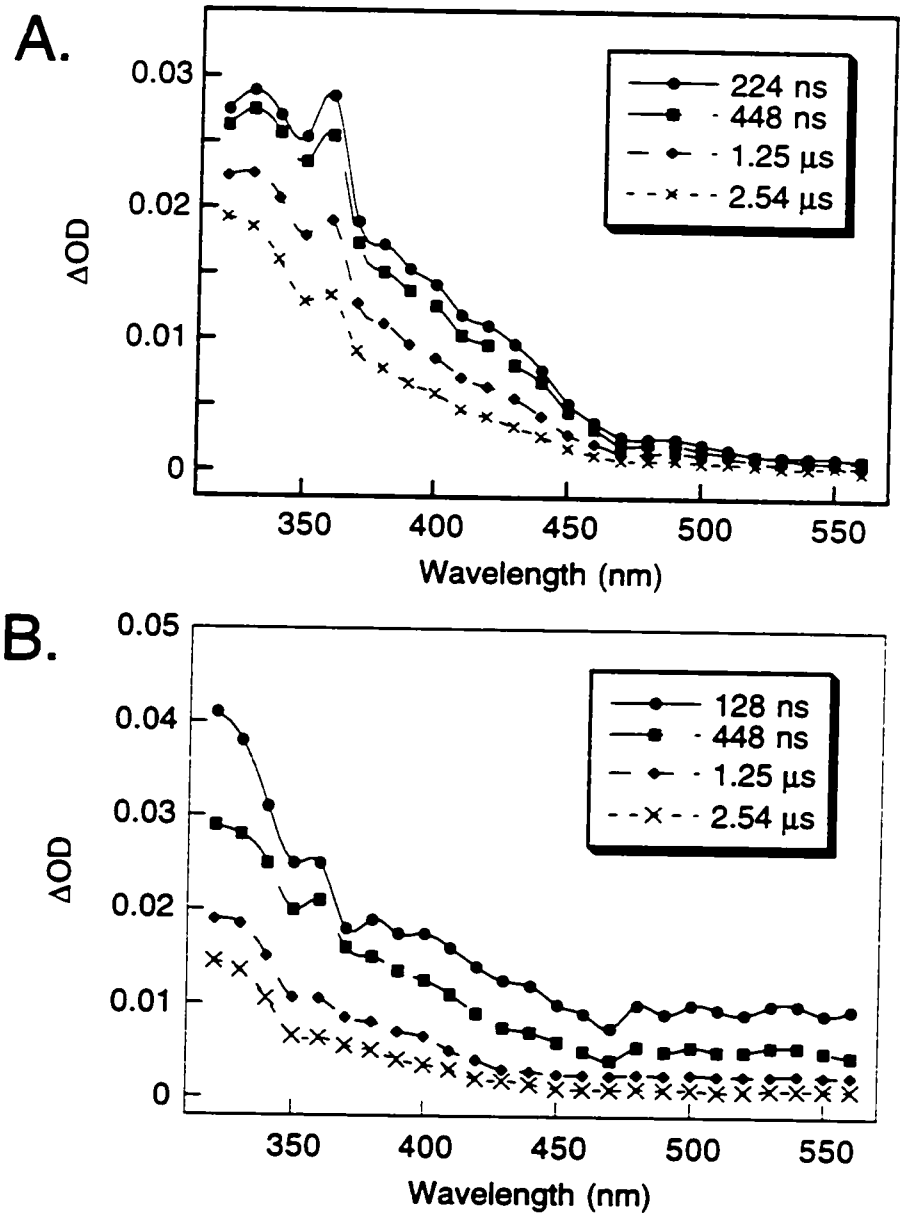

Figure 2.18 Transient absorption spectrum recorded following 308 nm laser excitation of **27** (0.5 mM) in deoxygenated: A-pentane; B-1:9 benzene:pentane solvent mixture. Inset: delay times for data collection after laser pulse.

Both complexation experiments resulted in the failure to detect the generation of bromine atoms upon laser flash photolysis of compound **27**. Clearly a new strategy had to be developed in order to investigate and measure the rate of 1,5-hydrogen atom transfer.

2.2.2. Generation of Benzylic Radicals by the Triethylsilyl Radical Approach

2.2.2.1. Generation of Triethylsilyl Radicals

A method that has known great success over the years for generating trialkylsilyl radicals and that has been widely employed by ESR spectroscopists[27] involves the photodecomposition of di-*tert*-butyl-peroxide in the presence of triethylsilane, Equation 4 and Equation 5.

Equation 4.

$$t\text{-BuO-O-}t\text{-Bu} \xrightarrow{h\nu} 2\ t\text{-BuO}^{\bullet}$$

Equation 5.

$$t\text{-BuO}^{\bullet} + Et_3SiH \xrightarrow{k_1} t\text{-BuOH} + Et_3Si^{\bullet}$$

Transient absorptions due to both *tert*-butoxyl and triethylsilyl radicals are too weak to interfere in laser flash photolysis experiments.[28] Furthermore, with a measured rate constant for the hydrogen abstraction reaction (Equation 5) of $5.7 \times 10^6\ M^{-1}\ s^{-1}$,[29] a system containing 80% triethylsilane as the solvent system results in a 35 ns lifetime for silicon radical formation. For all practical purposes, at such a high triethylsilane concentration the formation of the triethylsilyl radical is considered to be a sufficiently "instantaneous" process and time-resolved studies of the reactions that follow are made possible.

2.2.2.2. Dehalogenation by Silicon-Centered Radicals

Many heteroatom-centered radicals are capable of removing a halogen atom from suitable organic halides. A heteroatom such as silicon has been identified to undergo this type of process.[30, 31] There exist an extensive amount of qualitative and quantitative information regarding the reactivities of various organic halides towards silicon-centered radicals.[32] However, the system under study was not documented in the literature and therefore a first approximation had to be made. The bimolecular rate constant (k_2 in Scheme 2.6) for halogen abstraction between triethylsilyl radicals and phenylbromide was taken as our starting point and has been reported as 1.1×10^8 M^{-1} s^{-1}.[32] As an example, a system having a concentration of 10 mM for the starting material (compound **27**) would yield a lifetime of ~ 1 μs for the growth of the phenyl radical. On the basis of this new strategy, dehalogenation of compound **27** by the silicon-centered radical permitted the generation of the desired carbon-centered radicals as depicted in Scheme 2.6.

Scheme 2.6 Dehalogenation of compound **27** by a silicon-centered radical.

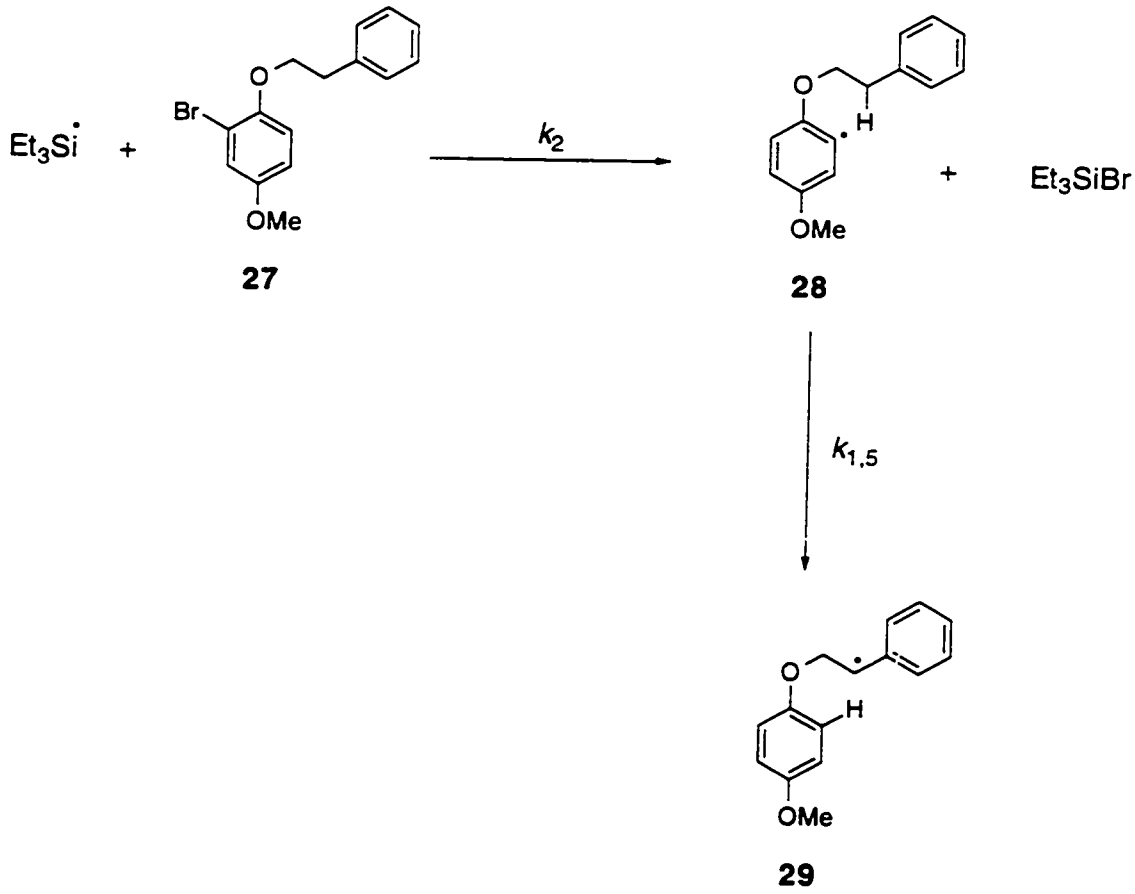

Figure 2.19 shows the spectral data obtained upon laser flash excitation of compound **27** in a 4:1 mixture of triethylsilane and di-*tert*-butyl-peroxide. Figure 2.20 shows a typical kinetic trace for such a system. The outcome of these results demonstrated that under our new experimental conditions we were indeed generating the desired benzylic radical. This conclusion was supported by analogy to the very similar transient spectrum observed in Figure 2.14 for the benzyl radical.

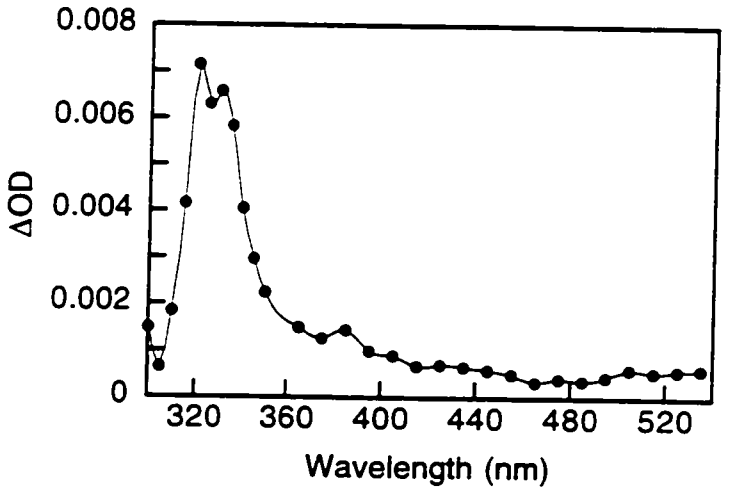

Figure 2.19 Transient absorption spectrum recorded 2.4 μs after 355 nm laser excitation of **27** (10 mM) in a deoxygenated 4:1 triethylsilane:di-*tert*-butyl-peroxide solvent mixture.

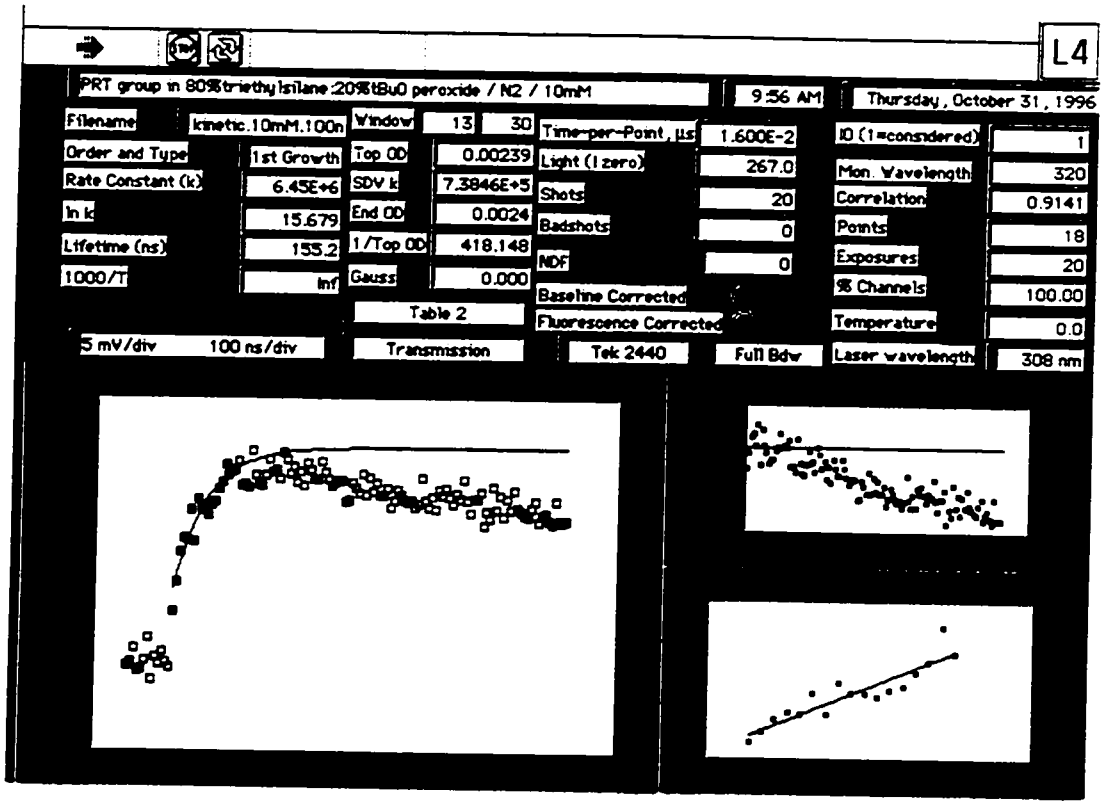

Figure 2.20 Transient kinetic trace recorded following 355 nm laser excitation of **27** (10 mM) in a deoxygenated 4:1 triethylsilane:di-*tert*-butyl-peroxide solvent mixture monitored at 320 nm.

In order to further confirm the identity of the benzylic radical resulting from the photolysis of compound **27**, we decided to verify that no growth could be measured with a similar system that was deprived of a benzylic moiety. A side-by-side experiment was therefore undertaken where compounds **27** and **31** were photolyzed and monitored at 320 nm. It was predicted that compound **31** should be devoid of any significant signal at the wavelength of interest. Such negative results would confirm that the signal observed from the photolysis of compound **27** is undeniably coming from the generation of the benzylic radical. The results obtained are shown with the help of Figure 2.22 and Figure 2.24 and are in perfect agreement with our predictions, therefore permitting us to further explore the desired rate of 1,5-hydrogen atom transfer reaction.

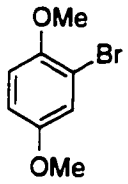

31

Figure 2.21 Structure of 1-bromo-2,5-dimethoxy benzene (**31**).

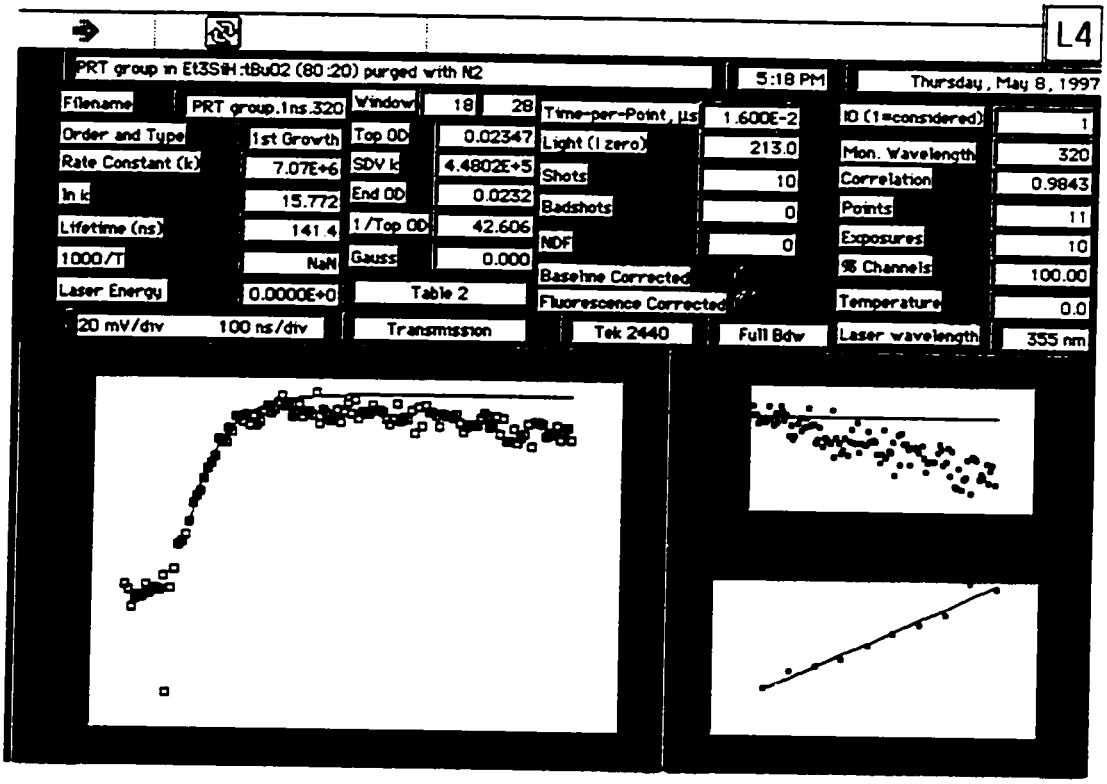

Figure 2.22 Transient kinetic trace recorded following 355 nm laser excitation of **27** (60 mM) in a deoxygenated 4:1 triethylsilane:di-*tert*-butyl-peroxide solvent mixture monitored at 320 nm.

Note that the kinetic fits shown in Figure 2.20 and Figure 2.22, as well as in some other figures in this chapter are a first approximation obtained during the laser work. When needed these fits can be improved by taking into consideration the decay of the long lived transient. For example, this is illustrated in Figure 2.23 where the trace obtained from Figure 2.22 has been refitted with a series of two exponentials with an A→B→C type of mechanism. A refitted value of $6.4 \times 10^6\ s^{-1}$ for the growth signal instead of $7.1 \times 10^6\ s^{-1}$ for the approximated fit has been calculated with such an approach. In addition, a value of $1.3 \times 10^5\ s^{-1}$ has been calculated for the decay of the longer lived transient.

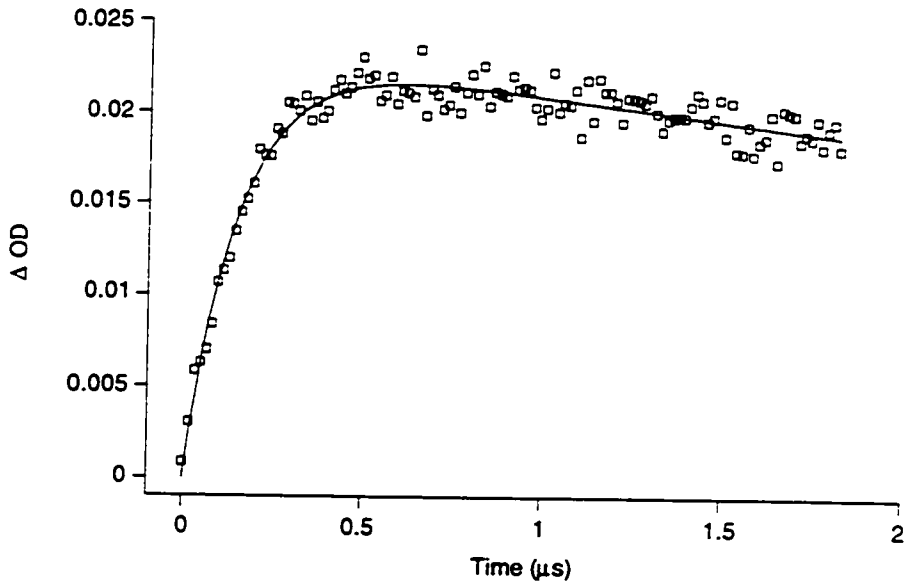

Figure 2.23 Refit of the trace obtained from Figure 2.22 using a series of two exponentials with an A→B→C type of mechanism.

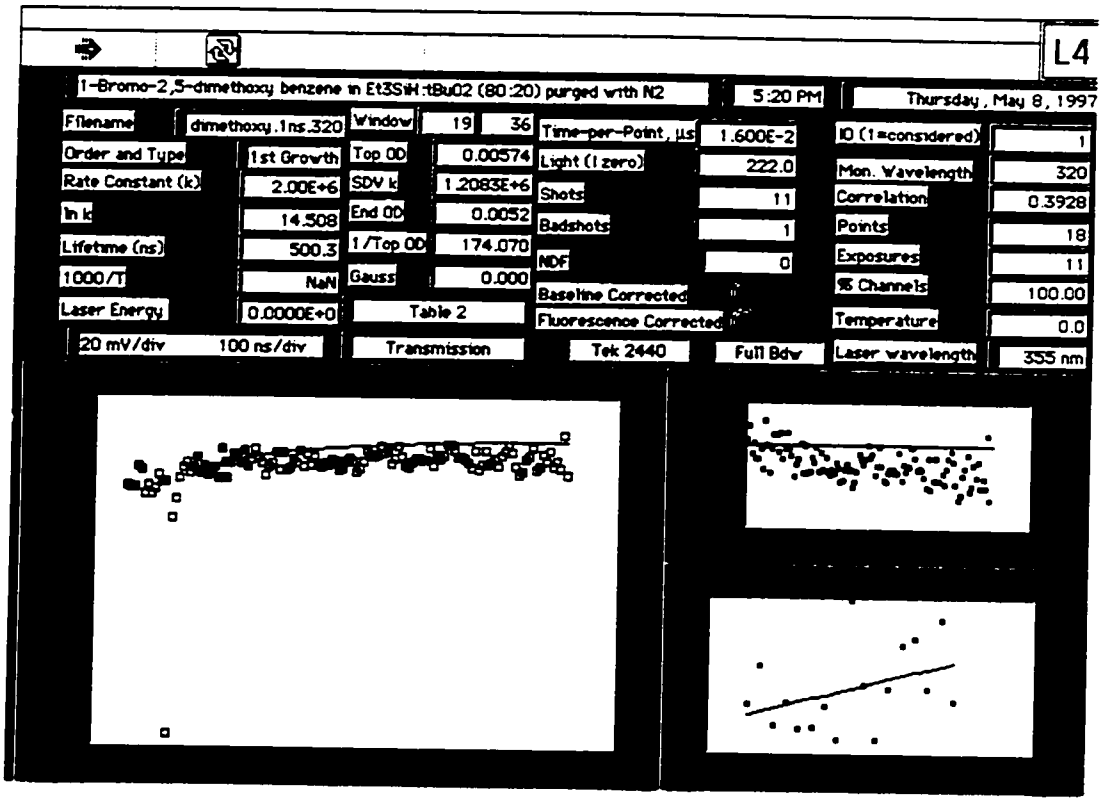

Figure 2.24 Transient kinetic trace recorded following 355 nm laser excitation of **31** (60 mM) in a deoxygenated 4:1 triethylsilane:di-*tert*-butyl-peroxide solvent mixture monitored at 320 nm.

2.2.2.3. Concentration Dependence Studies

In order to study the rate of hydrogen transfer, a series of laser flash photolysis experiments were conducted were the concentration of starting material (compound **27**) was varied over a wide range (10 mM to 200 mM). Referring to Scheme 2.6 and if one still considers the generation of the silyl radical to be "instantaneous", then at relatively low concentrations of compound **27**, the rate limiting step will be k_2[**27**] and therefore $k_{obs} = k_2$[**27**] (since k_2[**27**] < $k_{1,5}$). As the concentration increases, k_{obs} will be expected to plateau at a value equal to the rate of hydrogen transfer ($k_{1,5}$) since it will become the rate limiting phenomenon in the overall reaction scheme. Therefore, at high enough concentrations $k_{obs} = k_{1,5}$ since $k_{1,5} < k_2$[**27**]. The expected graphical behavior of the observed rates can be visualized with the help of Figure 2.25.

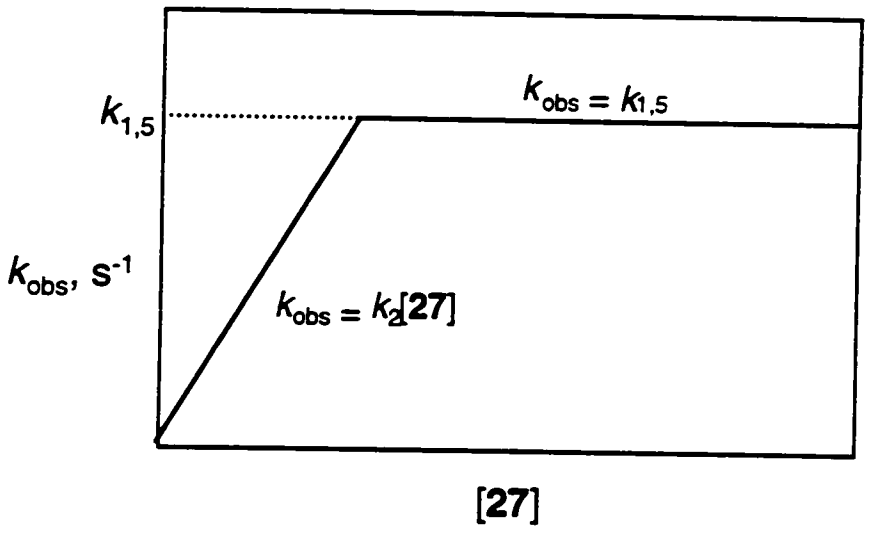

Figure 2.25 Schematic representation of the "expected" behavior for the observed rates of the benzylic radical (**29**) as a function of [**27**].

LFP of compound **27** at different concentrations in a deoxygenated 4:1 triethylsilane:di-*tert*-butyl-peroxide solvent mixture was monitored at 320 nm. The results obtained are shown in Figure 2.26.

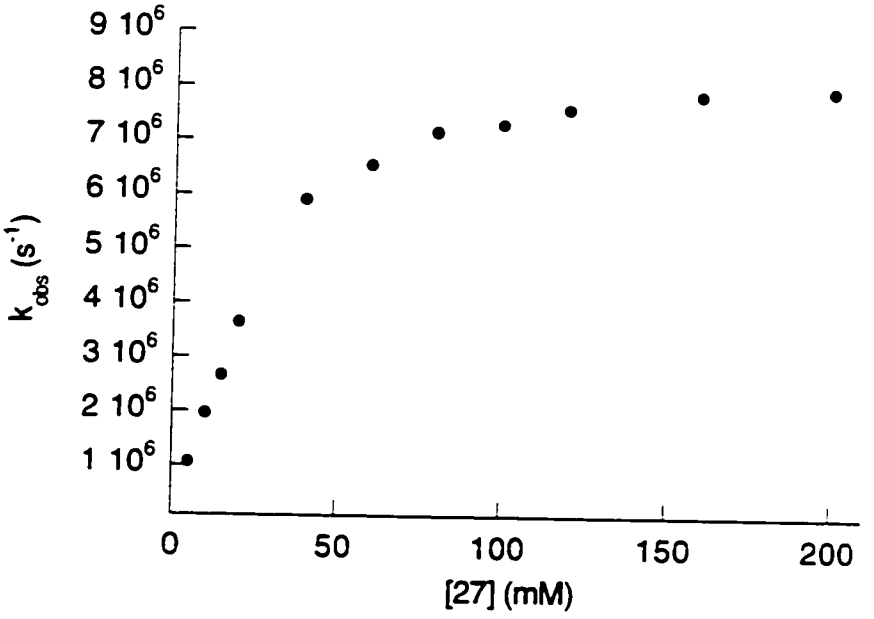

Figure 2.26 k_{obs} for the growth of the benzylic radical (**29**) as a function of [**27**] in a deoxygenated 4:1 triethylsilane:di-*tert*-butyl-peroxide solvent mixture monitored at 320 nm.

From the data obtained in Figure 2.26 a plot of $1/k_{obs}$ versus 1/[**27**] is predicted and found to be linear (Figure 2.27). The slope of such a plot is found to be equal to the reciprocal of the rate of debromination. A value of 2.4×10^8 M^{-1} s^{-1} was therefore calculated for this step. Division of the intercept by the slope gives the reciprocal of the desired 1,5-hydrogen atom transfer reaction. A value of 1.1×10^7 s^{-1} was calculated.

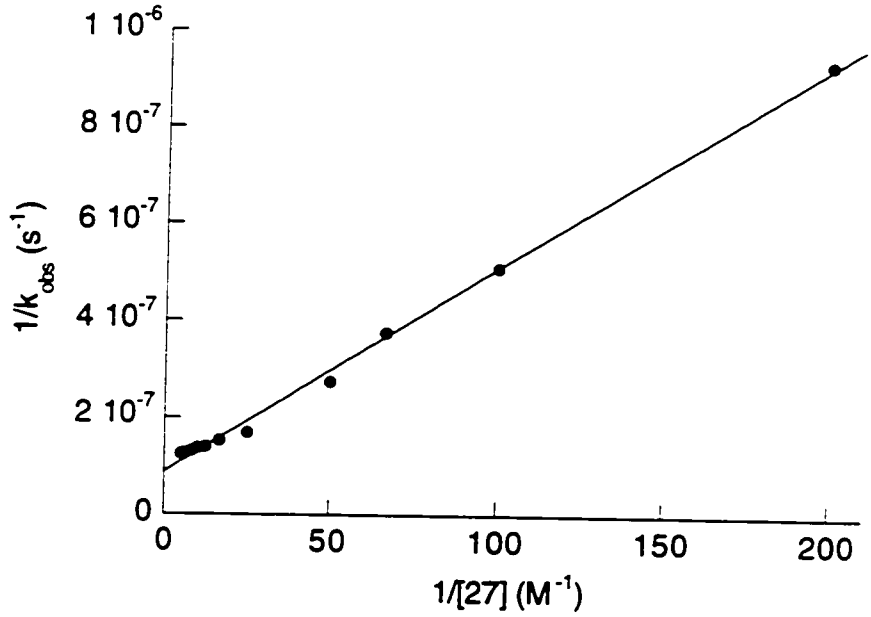

Figure 2.27 Double reciprocal treatment of the data obtained from Figure 2.26.

2.2.2.4. Determination of the Rate of Dehalogenation of 31 by Silicon-Centered Radicals using the "Probe Technique"

As previously mentioned, the rate of debromination by a silicon-centered radical for the present system was not available from the numerous investigations in the literature. In order to isolate and investigate our specific debromination step (step 2 from Scheme 2.6), laser flash photolysis experiments on the related compound **31** were undertaken in the presence of silyl radicals (Equation 6) generated by the aforementioned method. This allowed us to eliminate the 1,5-hydrogen atom transfer step from our mechanism and focus our attention solely on the rate of debromination.

Equation 6.

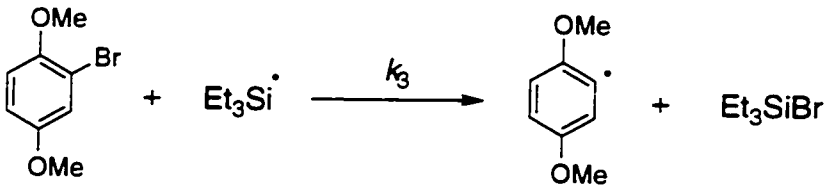

31 **32**

For organic halides which do not yield radicals that are readily detectable by optical means, it is still possible to study the kinetic of the halogen abstraction by triethylsilyl radicals if one refers to a competing reaction serving as a probe. In our case, the 2,5-dimethoxyphenyl radical (**32**) generated via Equation 6 lacks adequate absorptions for direct detection and therefore the "probe technique" was the method of choice in order to overcome this drawback. This technique was originally introduced about 20 years ago and has been very useful in the study of a number of radicals and other intermediates.[33, 34] Using this technique, one needs to identify a substrate that when reacting with the intermediate of interest can generate a product with desirable spectroscopic properties. The product of this trapping reaction should be a transient with a sufficiently long lifetime in the timescale of interest.

The "probe technique" has already been used in the study of phenyl radicals. Earlier work used diphenylmethanol (yielding diphenyl ketyl radicals) or β-methylstyrene (yielding readily detectable benzylic radicals) as probes for the phenyl radicals.[35, 36] In the present study, benzil proved to be well suited as a probe because of its known kinetic and spectroscopic properties for the addition of triethylsilyl radicals to the carbonyl moiety of benzil (Equation 7). The relatively weak but known absorptions for the adduct radical **34** were therefore available from the literature.[37] Photolysis of a deoxygenated 4:1 triethylsilane:di-*tert*-butyl-peroxide solvent mixture containing benzil led to the transient spectrum strongly resembling that of $PhC^{\bullet}(OH)C(O)Ph$,[38] with a

strong maximum at 380 nm and a weak one at 490 nm (Figure 2.28). The growth of the radical adduct **34** after laser pulse (Figure 2.29) followed clean pseudo-first order kinetics according to Equation 8, where k_0 includes all pseudo-first order modes of decay other than reaction with benzil. A value of $3.3 \times 10^8\ M^{-1}\ s^{-1}$ for the addition process (k_4) was determined previously at 300K.[27]

Equation 7.

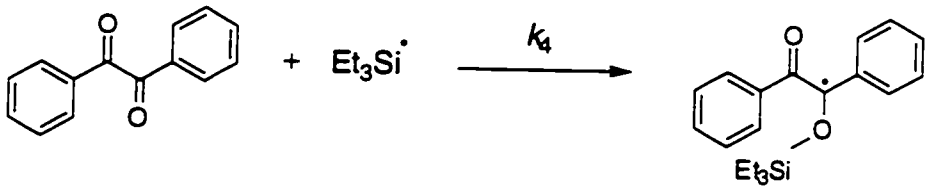

33 **34**

Equation 8.

$$k_{obs} = k_0 + k_4\,[PhC(O)C(O)Ph]$$

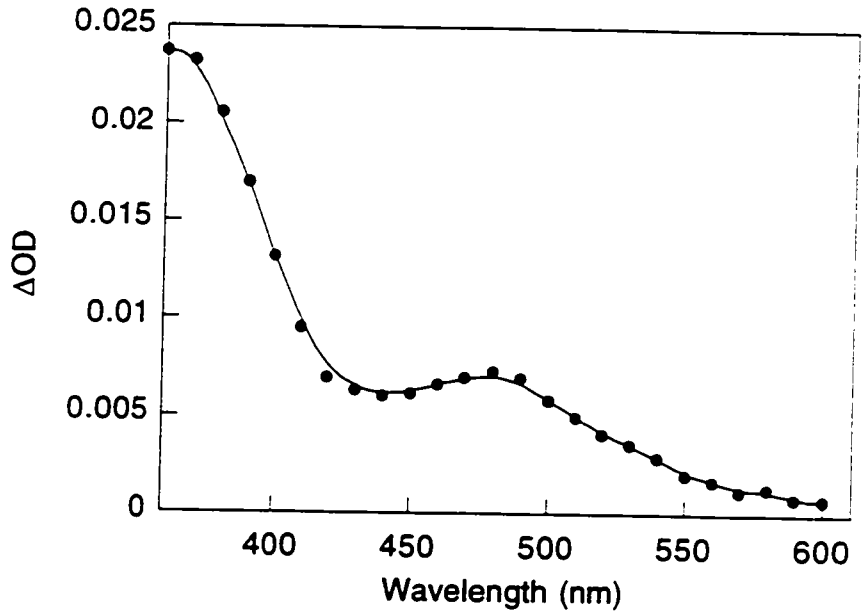

Figure 2.28 Transient absorption spectrum of benzil (6.7×10^{-4} M) in a deoxygenated 4:1 triethylsilane:di-*tert*-butyl-peroxide solvent mixture 5 μs after 355 nm laser excitation.

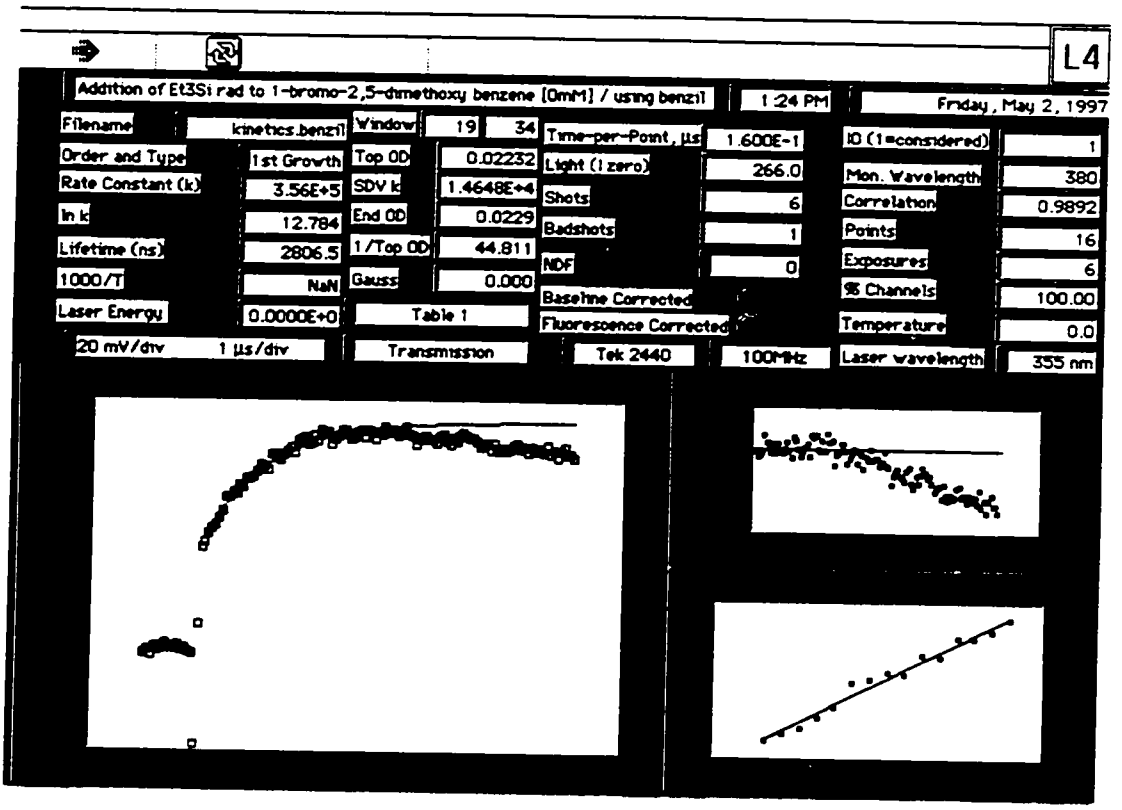

Figure 2.29 Kinetic trace recorded following 355 nm laser excitation of benzil (6.7×10^{-4} M) in a deoxygenated 4:1 triethylsilane:di-*tert*-butyl-peroxide solvent mixture monitored at 380 nm.

When the organic halide of interest competes with benzil for the silicon-centered radicals, the signal corresponding to the adduct radical **34** is modified in two ways: 1) the "plateau" signal (maximum) is reduced and 2) the rate constant k_{obs}, associated with the growth of radical **34** increases and is now given by Equation 9.

Equation 9.

$$k_{obs} = k_0 + k_3\,[\text{1-bromo-2,5-dimethoxy benzene}] + k_4\,[\text{PhC(O)C(O)Ph}]$$

Therefore, experiments where the concentration of benzil is kept constant and that of the aryl halide is varied will allow the determination of the rate

constant of debromination (k_3) to be determined even if this reaction is considered "invisible" to our spectroscopic technique. The concentration of benzil was kept at 6.7×10^{-4} M throughout these experiments. At such a low value, its own absorptions are relatively weak at the exciting wavelength and thereby allows for a selective excitation of the di-*tert*-butyl-peroxide which is essential for the generation of silicon-centered radicals.

The corresponding quenching plot according to Equation 9 is shown in Figure 2.30. A linear regression analysis of the data yielded a rate constant for the debromination (k_3) of compound **31** of 4.6×10^8 M^{-1} s^{-1}. This value is in fair agreement with both the literature value for the rate of debromination of bromobenzene ($k = 1.1 \times 10^8$ M^{-1} s^{-1})[32] and our previously determined rate constant ($k_2 = 2.4 \times 10^8$ M^{-1} s^{-1}) for compound **27**. Having two electron donating substituents present in the aromatic systems of compounds **27** and **31** enables us to expect faster rate constants for debromination compared to the parent compound (bromobenzene). It should be noted here that the likely side chain reaction involving aryl radicals and triethylsilane generating silicon-centered radicals would only contribute to sample depletion and therefore would not interfere with the measurements involved.

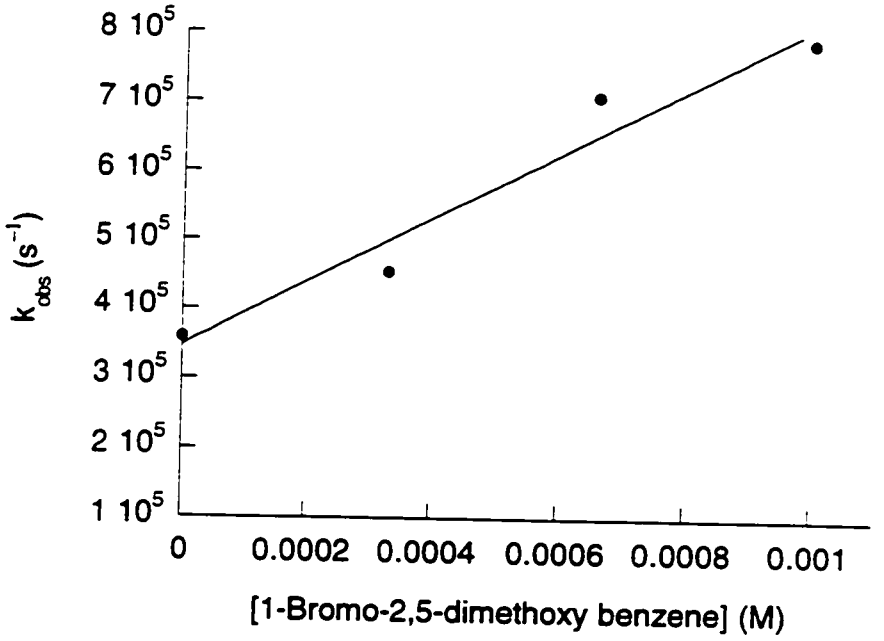

Figure 2.30 Concentration dependence of the growth rate constant observed, k_{obs}, for the reaction of **31** with triethylsilyl radical in a deoxygenated 4:1 triethylsilane:di-*tert*-butyl-peroxide solvent mixture. Probed with 6.7×10^{-4} M benzil and monitored at 380 nm.

2.3. Conclusion

In conclusion, generation of the benzylic radical resulting from dehalogenation of compound **27** by triethylsilyl radicals enabled us to determine the rate of the 1,5-hydrogen atom transfer reaction. A value of $1.1 \times 10^7\ s^{-1}$ was calculated with the help of concentration dependence studies. The rate of dehalogenation of compounds **27** and **31** were measured to be $2.4 \times 10^8\ M^{-1}\ s^{-1}$ and $4.6 \times 10^8\ M^{-1}\ s^{-1}$, respectively, and were in fair agreement with the rate of dehalogenation of the parent compound, bromobenzene, having a value of $1.1 \times 10^8\ M^{-1}\ s^{-1}$.[32] Direct photolysis of compound **27** did not generate the anticipated aryl radical destined to undergo the desired 1,5-hydrogen atom transfer reaction. Based on spectral evidence, the signals obtained did not correspond to the growth of a benzylic radical. Trapping experiments were also unsuccessful in detecting the formation of bromine atom complexes upon direct laser flash photolysis.

2.4. Experimental

2.4.1. Materials and General Techniques

Solvents used for laser flash photolysis (acetonitrile, benzene, pentane) and synthesis (methanol) were OmniSolv grade from BDH and were used without any further purification. Anhydrous tetrahydrofuran (BDH) was distilled from sodium/benzophenone under argon. *p*-Methoxyphenol, 1-bromo-2,5-dimethoxy benzene, diethyl azodicarboxylate, phenethyl alcohol, triphenyl phosphine, bromine and triethylsilane were purchased from the Aldrich Chemical Company and used as received. Di-*tert*-butyl-peroxide (Aldrich) was passed through an alumina column immediately before use to eliminate traces of hydroperoxide. Benzil (Aldrich) was recrystallized twice from ether.

Melting points were obtained in capillary tubes using Mel-Temp II melting point apparatus and are uncorrected. Proton magnetic resonance spectra (^{1}H NMR) were recorded at 500 MHz with a Bruker AMX500 spectrometer. Carbon magnetic resonance spectra (^{13}C NMR) were measured at 125 MHz with a Bruker AMX500 spectrometer. All spectra were taken in chloroform-d_1 and the chemical shift values are in parts per million (ppm) and reported downfield from tetramethylsilane (TMS) using the solvent peaks (^{1}H: δ 7.24 ppm; ^{13}C: δ 77.0 ppm) as references. A V.G. micromass 7070 HS instrument at an ionization energy of 70 eV was used to determine mass spectra. Commercial aluminum sheets coated (0.2 mm layer thickness) with silica gel 60 F_{254} (E. Merck) were used for analytical thin layer chromatography (TLC). Developing of the plates was done by either UV irradiation and/or by dipping in a solution of ceric sulfate (1%) ammonium molybdate (2.5%) in a 10% aqueous sulfuric acid solution and then heated. Silica gel (E. Merck, 230-400 mesh) was used for all column chromatography.

Anhydrous sodium sulfate was used as a drying agent for organic solutions. A Buchi rotatory evaporator connected to a water aspirator was used to remove organic solvents.

2.4.2. Synthesis

2.4.2.1. Bromination with Br_2[13]

Preparation of 2-bromo-4-methoxyphenol (26)

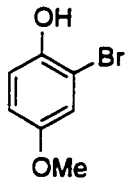

26

Br_2 (5.5 mL, 10.6 mmol) was added dropwise to a solution of *p*-methoxyphenol (11.9 g, 9.6 mmol) in methanol (50 mL) at 0 °C under argon. After stirring at 0 °C for 2 h, the ice bath was removed and the solution was allowed to further react at room temperature. The solution was left overnight. The blue-green solution was diluted with dichloromethane and washed four times with a 50% solution of $Na_2S_2O_3$ (until the gray-white cloudiness in the organic phase disappeared). The organic phase was washed two times with a saturated solution of bicarbonate and then rotovaped to yield a brownish residue. This residue was passed through a silica plug and then concentrated under vacuo to give brownish crystals. Purification was made by flash chromatography using silica gel (pentane:EtOAc = 20:1). The orange-white crystals obtained were then sublimed to give pure compound **26** as a white crystalline solid: mp 40-42 °C; ^{1}H NMR δ 6.99 (d, *J*= 2.9 Hz, 1H), 6.92 (d, *J*= 8.9 Hz, 1H), 6.78 (d of d, J= 2.9, 8.9 Hz, 1H), 5.10 (s, 1H), 3.73 (s, 3H); ^{13}C NMR δ 153.8, 146.5, 116.9, 116.3, 115.4, 109.9, 56.0; HRMS calcd for $C_7H_7O_2Br$

201.9627, found 201.9646. A mass-spectral analysis was done in order to verify that no dibromination had occurred during synthesis. The characterization of the ortho positionning of bromine substitution within the aromatic ring had already been established by the literature cited.

2.4.2.2. Mitsunobu Reaction[39]

Preparation of 2-Bromo-4-methoxy-1-(2-phenylethoxy)benzene (27)

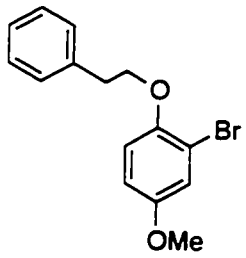

27

Diethyl azodicarboxylate (DEAD) (2.30 mL, 11.8 mmol) was added dropwise to a solution of compound **26** (2.00 g, 9.7 mmol), phenethyl alcohol (1.16 mL, 9.7 mmol) and triphenyl phosphine (2.98 g, 11.5 mmol) in dry THF (125 mL) at 23 °C. After stirring at room temperature for 18 h under argon, the solvent was removed. The residue was purified by chromatography (pentane:EtOAc = 60:1) to give **27** as a clear oil. Unsuccessful sublimation was attempted. Compound **27** crystallized out overnight to yield a pure white crystalline solid (1.95 g, 64%): mp 47-49 °C; ^{1}H NMR δ 7.27 (m, 5H), 7.09 (d, *J* =2.7 Hz, 1H), 6.78 (d, *J* = 8.9 Hz, 1H), 6.75 (d of d, *J* = 2.8, 8.9 Hz, 1H), 4.14 (t, *J* = 7.0 Hz, 2H), 3.76 (s, 3H), 3.11 (t, *J* = 7.0 Hz, 2H); ^{13}C NMR δ 154.2, 149.7, 138.2, 129.2, 128.4, 126.5, 118.9, 114.8, 113.7, 112.9, 71.0, 55.9, 35.9; HRMS calcd for $C_{15}H_{15}O_2Br$ 306.0251, found 306.0268.

2.4.3. Laser Flash Photolysis

Nanosecond laser flash photolysis experiments were carried out using a Lumonics EX-530 excimer laser for excitation (Xe-HCl-He mixtures, 308 nm, ~6 ns, ~60 mJ/pulse) or were excited with either the third harmonic (355 nm, ~6 ns pulse width, ~25 mJ/pulse) or the fourth harmonic (266 nm, ~6 ns pulse width, ~15 mJ/pulse) of a Continuum Surelite Nd-YAG laser. The signals from a monochromator-photomultiplier detector system were initially captured by a Tektronix 2440 digital oscilloscope interfaced (GPIB) to a PowerMacintosh computer. Software for the laser system was written in the LabVIEW 3.1.1 programming environment from National Instruments. The basic components of our instrument are similar to those described earlier.[38, 40]

The time-resolved studies were carried out on static samples of approximately 2 mL of solution contained in Suprasil quartz cells with a 7-mm^2 optical path. These samples were prepared at concentrations that did not exceed an optical density of 0.4 at the laser wavelength to avoid either shock waves or concentration gradients from the transient species. Special care was taken to shake each samples after every laser shot in order to avoid product buildup or sample depletion. Unless otherwise stated, samples were deoxygenated by bubbling with oxygen-free nitrogen for at least 15 minutes prior to the experiments. All measurements were performed at room temperature.

2.5. References

[1] J. K. Kochi, *Free Radicals*. New York: John Wiley & Sons, **1973**.

[2] B. Giese, "Formation of C-C Bonds by Addition of Free Radicals to Alkenes," *Angew. Chem. Int. Ed. Engl.*, **22** , 753-764, **1983**.

[3] B. Giese, "Synthesis with Radicals-C-C Bond Formation via Organotin and Organomercury Compounds," *Angew. Chem. Int. Ed. Engl.*, **24** , 553-565, **1985**.

[4] W. P. Neumann, "Tri-*n*-butyltin Hydride as Reagents in Organic Synthesis," *Synthesis* , 665-683, **1987**.

[5] D. P. Curran, D. Kim, H. T. Liu, and W. Shen, "Translocation of Radical Sites by Intramolecular 1,5-Hydrogen Atom Transfer," *J. Am. Chem. Soc.*, **110**, 5900-5902, **1988**.

[6] D. P. Curran, "The Design and Application of Free Radical Chain Reactions in Organic Synthesis. Part 1.," *Synthesis* , 417-439, **1988**.

[7] D. P. Curran and W. Shen, "Radical Translocation Reactions of Vinyl Radicals: Substituent Effects on 1,5-Hydrogen Transfer Reactions," *J. Am. Chem. Soc.*, **115** , 6051-6059, **1993**.

[8] B. Giese, *Radicals in Organic Synthesis*. Oxford: Pergamon Press, **1986**.

[9] E. I. Heiba and R. M. Dessau, "Free-Radical Isomerization. I. A Novel Rearrangement of Vinyl Radicals," *J. Am. Chem. Soc.*, **89** , 3772-3777, **1967**.

[10] D. P. Curran, A. C. Abraham, and H. T. Liu, "Radical Translocation Reactions of *o*-Iodoanilides: The Use of Carbon-Hydrogen Bonds as Precursors of Radicals Adjacent to Carbonyl Groups," *J. Org. Chem.*, **56** (14) , 4335-4337, **1991**.

[11] D. P. Curran and H. S. Yu, "New Applications of 1,5-Hydrogen Atom Transfer Reactions: Self-Oxidizing Protecting Groups," *Synthesis* , 123-127, **1992**.

[12] D. P. Curran, K. V. Somayajula, and H. S. Yu, "Intramolecular Hydrogen Transfer Reactions of *o*-(Bromophenyl)dialkylsilyl Ethers. Preparation of Rapamycin-d_1," *Tetrahedron Lett.*, **33** (17) , 2295-2298, **1992**.

[13] D. P. Curran and J. Xu, "*o*-Bromo-*p*-methoxyphenyl Ethers. Protecting / Radical Translocating (PRT) Groups That Generate Radicals from C-H Bonds β to Oxygen Atoms," *J.Am.Chem.Soc.*, **118** , 3142-3147, **1996**.

[14] V. C. Snieckus, J.-C., C. P. Sloan, H. Liu, and D. P. Curran, "Intramolecular α-Amidoyl to Aryl 1,5-Hydrogen Atom Transfer Reactions. Heteroannulation and α-Nitrogen Functionalization by Radical Translocation," *J. Am. Chem. Soc.*, **112** , 896-898, **1990**.

[15] G. Stork and P. M. Sher, "A Catalytic Tin System for Trapping of Radicals from Cyclization Reactions. Regio- and Stereocontrolled Formation of Two Adjacent Chiral Centers," *J. Am. Chem. Soc.*, **108** , 303-304, **1986**.

[16] A. L. J. Beckwith and W. B. Gara, "Mechanism of Cyclization of Aryl Radicals containing Unsaturated ortho-Substituents," *J. Chem. Soc., Perkin Trans 2* , 795-802, **1975**.

[17] A. N. Abeywickrema and A. L. J. Beckwith, "Rate Constants for the Cyclization of some Aryl Radicals bearing Unsaturated ortho-Substituents," *J. Chem. Soc., Chem. Commun.* , 464-465, **1986**.

[18] A. L. J. Beckwith and G. F. Meijs, "Iododediazoniation of Arenediazonium Salts Accompanied by Aryl Radical Ring Closure," *J. Org. Chem.*, **52** , 1922-1930, **1987**.

[19] A. N. Abeywickrema, A. L. J. Beckwith, and S. Gerba, "Consecutive Ring Closure and Neophyl Rearrangement of Some Alkenylaryl Radicals," *J. Org. Chem.*, **52** , 4072-4078, **1987**.

[20] Z. B. Alfassi, G. I. Khaikin, and P. Neta, "Arylperoxyl Radicals. Formation, Absorption Spectra, and Reactivity in Aqueous Alcohol Solutions," *J. Phys. Chem.*, **99** , 265-268, **1995**.

[21] C. Chatgilialoglu, "Electronic Absorption Spectra of Free Radicals," in *CRC Handbook of Organic Photochemistry*, vol. 2, J. C. Scaiano, Ed. Boca Raton, Florida: CRC Press, **1989**, pp. 3-11.

[22] J. C. Scaiano, M. Barra, M. Krzywinski, R. Sinta, and G. Calabrese, "Laser Flash Photolysis Determination of Absolute Rate Constants for Reactions of Bromine Atoms in Solution," *J. Am. Chem. Soc.*, **115** , 8340-8344, **1993**.

[23] J. C. Scaiano, M. Barra, G. Calabrese, and R. Sinta, "Photochemistry of 1,2-Dibromoethane in Solution. A Model for the Generation of Hydrogen Bromide," *J. Chem. Soc., Chem. Commun.* (19) , 1418-1419, **1992**.

[24] W. G. McGimpsey and J. C. Scaiano, "Photochemistry of α-Chloro and α–Bromoacetophenone. Determination of Extinction Coefficients for Halogen Benzene Complexes," *Can. J. Chem.*, **66** , 1474-1478, **1988**.

[25] D. Zehavi and J. Rabani, "The Oxidation of Aqueous Bromide Ions by Hydroxyl Radicals. A pulse Radiolytic Investigation," *J. Phys. Chem.*, **76** , 312-319, **1972**.

[26] G. L. Hug, *Optical Spectra of Nonmetallic Inorganic Transient Species in Aqueous Solution*, vol. NSRDS-NBS 69. Washington: National Bureau of Standards, **1981**.

[27] C. Chatgilialoglu, J. C. Scaiano, and K. U. Ingold, "Absolute Rate Constants for the Addition of Triethylsilyl Radicals to the Carbonyl Group," *J.Am.Chem.Soc.*, **104** , 5119-5123, **1982**.

[28] C. Chatgilialoglu, K. U. Ingold, J. C. Scaiano, and H. Woynar, "Absolute Rate Constants for Some Reactions Involving Triethylsilyl Radicals in Solution," *J. Am. Chem. Soc.*, **103** , 3231-3232, **1981**.

[29] C. Chatgilialoglu, J. C. Scaiano, and K. U. Ingold, "Absolute Rate Constants for the Reactions of tert-Butoxyl Radicals and some Ketone Triplets with Silanes," *Organometallics*, **1** (3) , 466-469, **1982**.

[30] L. H. Sommer and L. A. Ulland, "Silicon Radicals. Relative Rates and Selectivity Ratios in the Radical Reactions of Silicon-Hydrogen Bonds with Carbon-Halogen Bonds," *J. Am. Chem. Soc.*, **94** , 3803-3806, **1972.**

[31] R. A. Jackson and F. Malek, "Radical-initiated Reduction of Chloroformates to Alkanes by Tri-*n*-propylsilane. A Method for Removal of Unwanted Hydroxy- Groups from Organic Molecules," *J. Chem. Soc., Perkin Trans. 1* , 1207-1211, **1980.**

[32] C. Chatgilialoglu, K. U. Ingold, and J. C. Scaiano, "Absolute Rate Constants for the Reaction of Triethylsilyl Radicals with Organic Halides," *J.Am.Chem.Soc.*, **104** (19) , 5123-5127, **1982.**

[33] R. D. Small and J. C. Scaiano, "Absolute Rates of Hydrogen Abstraction by *tert*-Butoxy Radicals," *J. Am. Chem. Soc.*, **100** (1) , 296-298, **1978.**

[34] H. Paul, R. D. Small, and J. C. Scaiano, "Hydrogen Abstraction by *tert*-Butoxy Radicals. A Laser Photolysis and Electron Spin Resonance Study," *J. Am. Chem. Soc.*, **100** (14) , 4520-4527, **1978.**

[35] D. Weldon, S. Holland, and J. C. Scaiano, "Temperature Dependence of the Reactions of Phenyl Radicals with 1,1-Diphenylethylene, Carbon Tetrachloride, and Cyclohexene," *J. Org. Chem.*, **61** , 8544-8546, **1996.**

[36] J. C. Scaiano and L. C. Stewart, "Phenyl Radical Kinetics," *J. Am. Chem. Soc.*, **105** , 3609-3614, **1983.**

[37] A. Alberti and A. Hudson, "Dynamic Migration of Organometallic Groups in Free Radical Adducts of Benzil," *Chem. Phys. Lett.*, **48** , 331-333, **1977.**

[38] J. C. Scaiano, "Solvent Effects in the Photochemistry of Xanthone," *J. Am. Chem. Soc.*, **102** , 7747-7753, **1980.**

[39] O. Mitsunobu, "The Use of Diethyl Azodicarboxylates and Triphenylphosphine in Synthesis and Transformation of Natural Products," *Synthesis* , 1-28, **1981.**

[40] J. C. Scaiano, M. Tanner, and D. Weir, "Exploratory Study of the Intermolecular Reactivity of Excited Diphenylmethyl Radicals," *J. Am. Chem. Soc.*, **107** , 4396-4403, **1985**.

3. Claims to Original Research

1) Establishing that ring-substituted α-bromoacetophenones react with alcohols in a chain reaction pathway. Demonstrating that two different mechanisms, involving hydrogen or electron transfer by ketyl radicals, are available for the photodecomposition leading to the corresponding acetophenones, HBr, and the carbonyl compound from oxidation of the alcohol.

2) Demonstrating from isotope incorporation using deuterated alcohols, that in the chain transfer process above, electron transfer dominates in the case of 2-propanol, while hydrogen transfer is more important for methanol. Establishing that the only parameter playing a major role as a discriminating factor between both mechanisms is the reducing strength of the ketyl radicals.

3) Establishing the first example of an absolute rate constant for a protecting/radical translocating group involving 1,5-hydrogen atom transfer reactions as a means of generating radicals from C-H bonds β to oxygen atoms. The rate of 1,5-hydrogen atom transfer ($1.1 \times 10^7\ s^{-1}$) and the rate of dehalogenation ($2.4 \times 10^8\ M^{-1}\ s^{-1}$) of 2-bromo-4-methoxy-1-(2-phenylethoxy) benzene (**27**) using the triethylsilyl radical approach was measured with the help of laser flash photolysis techniques.

4) Establishing the rate of dehalogenation ($4.6 \times 10^8\ M^{-1}\ s^{-1}$) of 1-bromo-2,5-dimethoxy benzene (**31**) by silicon-centered radicals using the "probe technique".

Publications resulting from the work presented in this thesis

[1] S. V. Jovanovic, J. Renaud, A. B. Berinstain, and J. C. Scaiano, "Kinetic Study of the Reactions of Methoxy-Substituted Phenacyl Radicals," *Can. J. Chem.*, **73** (2), 223-231, **1995**.

[2] J. Renaud, and J. C. Scaiano, "Chain Mechanisms for the Dehydrobromination of Ring-Substituted α-Bromoacetophenones in Alcohols," *Res. Chem. Intermed.*, **21**, 457-465, **1995**.

[3] J. Renaud, and J. C. Scaiano, "Hydrogen vs. Electron Transfer Mechanisms in the Chain Decomposition of Phenacyl Bromides. Use of Isotopic Labeling as a Mechanistic Probe," *Can. J. Chem.*, **74**, 1724-1730, **1996**.

[4] J. Renaud, and J. C. Scaiano, "First Absolute Rate Constant Measurement for the 1,5-Hydrogen Atom Translocation Reaction of an *o*-Bromo-*p*-methoxy Ether. A Protecting/Radical Translocating (PRT) Group that Generates Radicals from C-H Bonds β to Oxygen Atoms," in preparation.

Other publications

[1] S. Monahan, J. Renaud, and J. C. Scaiano, "Dramatic Effect of Magnetite Particles on the Dynamics of Photogenerated Free Radicals," *Photochem. Photobiol.*, **65** (4), 759-762, **1997**.

IMAGE EVALUATION
TEST TARGET (QA-3)

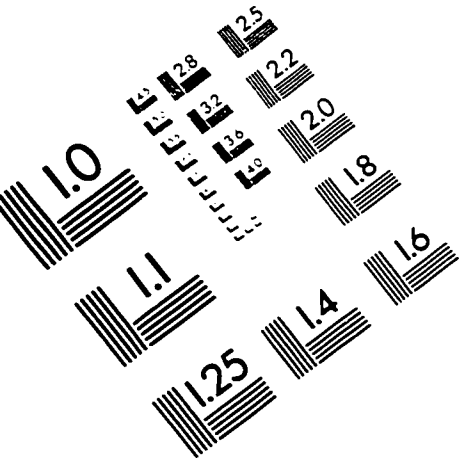

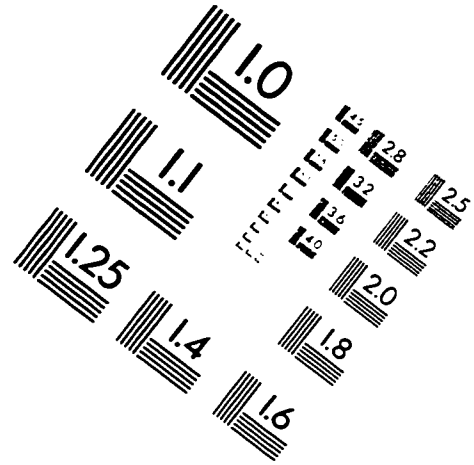

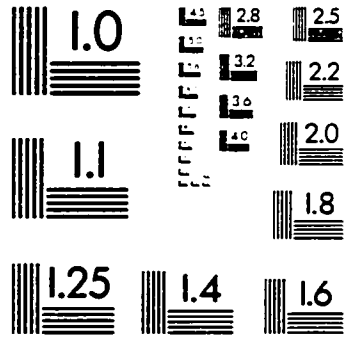

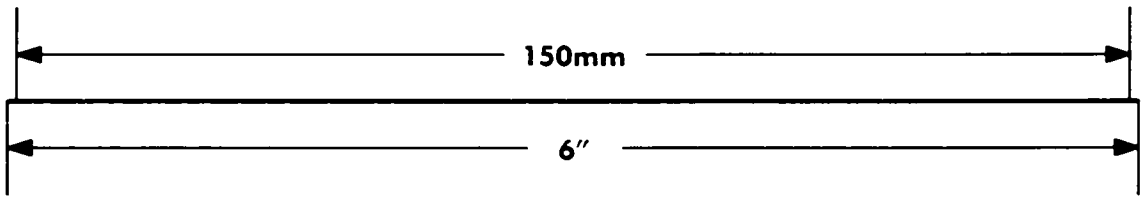

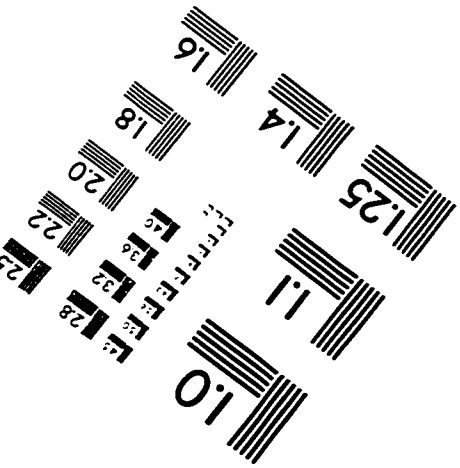

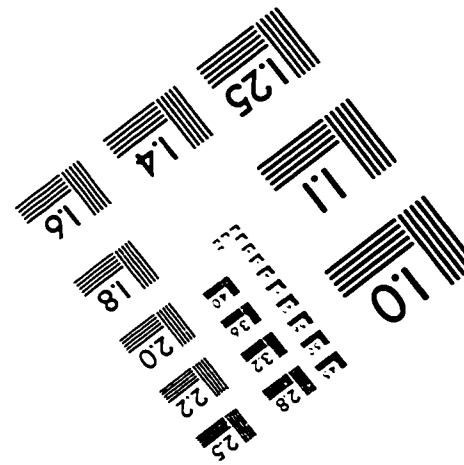

APPLIED IMAGE, Inc
1653 East Main Street
Rochester, NY 14609 USA
Phone: 716/482-0300
Fax: 716/288-5989